PLANT POLYSACCHARIDES AS POTENTIAL BIOACTIVE THERAPEUTICS: NOVEL APPROACHES TOWARDS PRODUCTION, STRUCTURAL CHARACTERIZATION, IMMUNOMODULATION AND QUALITY CONTROL

by

Rajarshi Ghosh

A Dissertation Submitted in Partial Fulfillment
of the Requirements for the Degree of
Doctor of Philosophy in Molecular Biosciences

Middle Tennessee State University
August 2019

Dissertation Committee:

Dr. Anthony L. Farone, Chair

Dr. Paul C. Kline

Dr. Elliot C. Altman

Dr. Mary B. Farone

Dr. Kevin L. Bicker

DECLARATION

All contents presented in this dissertation are my original works performed in collaboration with colleagues at the Departments of Biology and Chemistry, Middle Tennessee State University. I was the main contributor to the works presented in Chapters II, III, IV, and V. The plant tissue culture samples used in this study were provided by Shannon Smith from the laboratory of Dr. Elliot Altman at MTSU. The live cell assays reported in Chapter IV were performed by Logan Bowling and Devyn Hayes in the laboratory of Dr. David Nelson at MTSU. The multiplex cytokine panels were completed at Eve Technologies, Canada. The glycosyl linkage analyses and 1D NMR spectroscopy were performed at the Complex Carbohydrate Research Center, University of Georgia.

Some of the contents of Chapters I and II are part of my dissertation proposal submitted at MTSU. Some of the methods reported in Chapter II are from an article published in *International Journal of Biological Macromolecules*, for which I was the second author (cited below).

Hosain, N. A.; **Ghosh, R**.; Bryant, D. L.; Arivett, B. A.; Farone, A. L.; Kline, P. C. Isolation, structure elucidation, and immunostimulatory activity of polysaccharide fractions from *Boswellia carterii* frankincense resin. *Int. J. Biol. Macromol.* **2019,** *133*, 76-85.

Results presented in Chapters III and IV are currently under review in the *International Journal of Biological Macromolecules*. Chapter V is a published article in *BMC Research Notes* (cited below).

Ghosh, R.; Kline, P. HPLC with charged aerosol detector (CAD) as a quality control platform for analysis of carbohydrate polymers. *BMC Res. Notes* **2019** *12*(1), 268.

Dedicated to the pioneers of botanical medicine and natural products research

ACKNOWLEDGEMENTS

First and foremost, I would like to thank my advisor Dr. Anthony Farone for patiently mentoring me throughout the course of my PhD studies. I always appreciated the freedom with which he let me explore multidisciplinary fields of science outside the boundaries of our lab. Thanks to his approach, I was able to learn and incorporate a diverse range of techniques in my research. I am equally thankful to Dr. Paul Kline, my co-mentor for letting me work in his biochemistry research lab throughout my stay at MTSU. It would not have been possible to learn different aspects of biochemistry and analytical chemistry without his guidance. This work would also be incomplete without the intellectual input and funding from Dr. Elliot Altman and the Tennessee Center for Botanical Medicine Research. I was able to receive hands on training from some of the best carbohydrate chemists in the world due to Elliot's encouragement and funding support. Additionally, I would like to thank my other committee members Dr. Mary Farone and Dr. Kevin Bicker for their time, availability, and guidance.

I would like to credit a large part of my intellectual and professional development to the members of the Farone lab. I would specially like to thank Brock Arivett, with whom I was able to co-author multiple publications. This dissertation as well as my stay at MTSU would not have been complete without the help and friendship of Dan Bryant and Desta Kidane of the Farone lab. I am also thankful to the many collaborators with whom I have successfully completed projects at MTSU.

Finally, I am eternally grateful to my parents and other members of my family for constantly supporting me in every aspect of my life.

ABSTRACT

Historically, plants have been a tremendous source of novel bioactive small molecules or secondary metabolites. However, botanical macromolecules have not been as thoroughly studied. Among the different types of macromolecules, plant polysaccharides have shown potential in the biomedical field due to their immunomodulatory properties along with minimal toxicity. Novel immunomodulatory polysaccharides may be important for immunotherapies and discovery of adjuvants. Additionally, the use of polysaccharides as nutraceuticals and functional foods is becoming popular. Despite the interest in bioactive polysaccharides there are challenges to overcome. Purification costs, structural variability, bacterial endotoxin contamination, and laborious quality control procedures have hindered commercialization. In this study, novel methodologies have been employed in an attempt to address some of these challenges. A plant tissue culture-based system was used to produce polysaccharides with consistent structural characteristics and reduced endotoxin content. The structural features of four immunomodulatory polysaccharide fractions from *Panax quinquefolius* (American ginseng) suspension cultures were analyzed to begin to elucidate structure-function relationships. Structural analyses revealed the presence of arabinogalactan type II polysaccharides in three fractions and a pectic (rhamnogalacturonan I) polysaccharide in one fraction. The fractions activated RAW 264.7 murine macrophage cells and primary murine splenocytes by enhancing the production of several proinflammatory mediators such as nitric oxide, IL-6, TNF-α, MCP-1, and GM-CSF *in vitro* and *ex vivo.* Macrophage activation signaling pathways stimulated by treatment with purified polysaccharides were: iNOS, NF-κB (p65/RelA),

and MAPK (p38). The polysaccharides also stimulated mouse splenocyte proliferation, another major indicator of immunostimulation. Finally, this study not only explored novel strategies for production of bioactive polysaccharides using tissue culture, but also developed methods for rapid quality control of carbohydrate polymers using HPLC coupled with charged aerosol detector (CAD). Overall, these studies have shown that American ginseng suspension culture polysaccharides have the potential to be developed into potent immunomodulatory therapeutics.

TABLE OF CONTENTS

LIST OF TABLES

CHAPTER III

LIST OF FIGURES

CHAPTER III

CHAPTER IV

LIST OF APPENDICES

LIST OF ABBREVIATIONS

ACN	Acetonitrile
ANOVA	Analysis of variance
Ara	Arabinose
ATCC	American Type Culture Collection
BCA	Bicinchoninic acid
CAD	Charged aerosol detector
CCRC	Complex Carbohydrate Research Center
ConA	ConcanavalinA
CR	Complement receptor
CRD	Carbohydrate recognition domain
DEAE	Diethylaminoethyl
EdU	5-ethynyl-2´-deoxyuridine
ELISA	Enzyme-linked immunosorbent assay
ELSD	Evaporative light scattering detector
ERK	Extracellular signal-regulated kinase
FDA	Food and Drug Administration
FBS	Fetal bovine serum
FPLC	Fast protein liquid chromatography
Fuc	Fucose
Gal	Galactose
GalA	Galacturonic acid
GalN	Galactosamine
G-CSF	Granulocyte-colony stimulating factor
GC-MS	Gas chromatography-mass spectrometry
Glc	Glucose
GlcA	Glucuronic acid
GlcN	Glucosamine
GlcNAc	N-Acetylglucosamine
GM-CSF	Granulocyte macrophage-colony stimulating factor
GPC	Gel permeation chromatography
HA	Hyaluronic acid
HILIC	Hydrophilic interaction liquid chromatography
HPLC	High performance liquid chromatography
HPAEC-PAD	High performance anion exchange chromatography with pulsed amphoteric detection
HPSEC	High performance size exclusion chromatography
IdoA	Iduronic acid
IFN	Interferon
IL	Interleukin
iNOS	Inducible nitric oxide synthase
JNK	c-Jun N-terminal kinase
LAL	Limulus amoebocyte lysate
LOD	Limit of detection

LPS	Lipopolysaccharide
LOQ	Limit of quantification
Man	Mannose
MAPK	Mitogen activated protein kinase
MCP-1	Monocyte chemoattractant protein-1
MS	Mass spectrometer
MTSU	Middle Tennessee State University
MTT	3-(4,5-dimethylthiazol-2-yl)-2,5-diphenyltetrazolium bromide
NAG	North American ginseng
NF-κB	Nuclear factor kappa B
NO	Nitric oxide
NMR	Nuclear magnetic resonance
Neu5Ac	N-Acetylneuraminic acid
PBS	Phosphate-buffered saline
PI3K	Phosphoinositide 3-kinase
PMAA	Partially methylated alditol acetate
PMP	1-phenyl-3-methyl-5-pyrazolone
QC	Quality control
Rha	Rhamnose
RID	Refractive index detector
RIPA	Radio-immunoprecipitation assay
ROS	Reactive oxygen species
RSD	Relative standard deviation
RSP	Relative splenocyte proliferation
SEC	Size exclusion chromatography
SEM	Standard error of the mean
SR	Scavenger receptor
TCBMR	Tennessee Center for Botanical Medicine Research
TEA	Triethylamine
TFA	Trifluoroacetic acid
TLR	Toll-like receptors
TMS	Trimethylsilyl
TNF	Tumor necrosis factor
WHO	World Health Organization
Xyl	Xylose

CHAPTER I

INTRODUCTION

1.1. Botanical Polysaccharides as Potential Therapeutics

Traditional botanical medicine has been historically popular for disease prevention and treatment around the world. According to the World Health Organization (WHO), about three quarters of the world still relies on traditional medicine for its healthcare, especially in developing countries (Kumar et al., 2012). The botanical medicine market is worth more than $60 billion worldwide (Licciardi and Underwood, 2011). The use of plant medicines has reached unparalleled levels in western society in recent years. Scientific research on traditional medicine has led to the purification of numerous bioactive compounds. Plant derived compounds currently contribute to more than 40% of all US Food and Drug Administration (FDA) approved pharmaceuticals (Newman and Cragg, 2016). However, the majority of botanical medicine research has been concentrated on secondary metabolites or small molecules such as alkaloids, terpenoids, saponins, and flavonoids. Among the different types of macromolecules, carbohydrates as therapeutics has been relatively under researched. Although, carbohydrates, such as oligosaccharides, polysaccharides, and glycoconjugates, make up a large percentage of plant biomass, the biological effects of these compounds are largely unknown. Research over the last two decades has shed light on to the possible roles of plant polysaccharides in cellular function, metabolism, and disease (Li et al., 2013). It has also been reported that complex carbohydrates present in common fruits and vegetables contribute to their functional properties (Yamada and Kiyohara, 2007). Overall, these

high molecular weight compounds have shown potential to be developed into novel natural health products and nutraceuticals for the treatment of various diseases and metabolic disorders (Li et al., 2013).

Recent studies have shown that certain botanical polysaccharides have anticancer (Zong et al. 2012), immunomodulatory (Schepetkin and Quinn, 2006), and antimicrobial properties (Yoo et al., 2012) as well as minimal toxicity (Schepetkin and Quinn, 2006). The immunomodulatory properties of polysaccharides have been the major focus of worldwide research due to an increasingly promising body of accumulated scientific evidence over the last two decades. Immunomodulators offer many advantages, such as stimulation or suppression of beneficial or deleterious immune responses. These modulators are helpful in improving the overall resistance of the body against pathogens. One of the most promising recent alternatives to classical antibiotic treatment is the use of immunomodulators. The development of preventive strategies to resist disease could be a more efficient and effective long-term healthcare strategy (Schepetkin and Quinn, 2006). Identification of novel immunomodulatory complexes can also be crucial for existing immunotherapy and vaccination practices (Licciardi and Underwood, 2011). Polysaccharides have the potential to be developed into adjuvants and wound healing agents due to their potent immunostimulatory properties. Additionally, the use of complex carbohydrates as prebiotics and functional food in our diet is becoming popular as consumer demand for healthy food rises (Thakur et al., 2012). A better understanding of the structure-function relationship of botanical polysaccharides and their putative mechanisms of immunomodulation will further aid in the design and formulation of safe and effective commercial carbohydrate-based therapeutics. Different sections of this

chapter will introduce key concepts, major challenges, and novel approaches towards development of plant polysaccharides as therapeutic agents.

1.2 Plant Polysaccharides as Exogenous Immunomodulators

Immunomodulators have become increasingly popular in recent years for the treatment of several neurodegenerative diseases such as cancer. Since, the immune system plays a critical role in the maintenance of homeostasis, compounds having immunomodulatory properties can be beneficial in the recovery from many diseases (Yamada and Kiyohara, 2007). Activation immunotherapy, a subset of immunotherapy, focuses on the administration of endogenous immune system enhancing factors such as interferon-γ (IFN-γ), interleukin-2 (IL-2), IL-12, granulocyte-colony stimulating factor (G-CSF), and granulocyte macrophage-colony stimulating factor (GM-CSF) to boost the host immune system (Getsch et al., 2011). The stimulation of host immune response by these immune system enhancing factors is commonly used for cancer treatments in western medicine. In complementary and alternative medicine, exogenous immunostimulants from plants are historically used to elicit a host immune response. Among the botanical immunostimulants, plant polysaccharides have the ability to mediate immunomodulatory effects through non-targeted and targeted modulation of key cellular and molecular interactions (Licciardi and Underwood, 2011). Several botanical polysaccharides bind to Toll-like receptors (e.g. TLR-2 and TLR-4), scavenger receptor (SR), complement receptor 3 (CR3), and the carbohydrate recognition domain (CRD) of lectin receptors (e.g. Dectin 1) to activate innate immune system cells such as macrophages (Loh et al., 2017; Schepetkin and Quinn, 2006). This activation triggers

several interconnected processes such as increased phagocytic activity, chemokinesis, chemotaxis, degranulation followed by increased expression of adhesion molecules on the macrophage surface, interaction with the endothelium, and migration of macrophages to the tissues (Vetvicka, 2011). Important markers of polysaccharide stimulation of macrophages include formation of reactive oxygen species (ROS), increasing content of hydrolytic and metabolic enzymes, and secretion of cytokines and chemokines (Vetvicka and Vetvickova, 2017). Polysaccharides are also known to induce macrophage hematopoiesis by increasing the levels of GM-CSF (Schepetkin and Quinn, 2006). The immunostimulatory process is thought to be regulated by inducible nitric oxide synthase (iNOS), nuclear factor kappa B (NF-κB), and mitogen-activated protein kinases (MAPK) such as p38, extracellular signal-regulated kinase 1/2 (ERK1/2), and phosphoinositide 3-kinase (PI3K) (Loh et al., 2017). Some studies have also shown that certain plant polysaccharides affect both Th1 and Th2 branches of adaptive immune response (Khajuria et al., 2007). However, such studies are preliminary and effects of polysaccharides on adaptive immunity is a continuing topic of interest worldwide. Plant polysaccharides have the potential to be utilized as a low-cost alternative to endogenous immunomodulators and antibiotics, especially in developing countries, where the burden of disease is high and access to medical care is limited (Licciardi and Underwood, 2011).

1.3 Importance of Polysaccharide Structure in Eliciting an Immune Response

Historically, polysaccharides have been thought to induce a non-specific immune response determined by size rather than chemical structure (Li et al., 2013). Inadequate structural characterization of immunomodulatory polysaccharides in many studies over

the years have hindered broad structure-activity relationship analysis. A closer look into their overall structure is revealing important information about specific structure-function relationships. Structural properties such as monosaccharide composition, glycosyl linkages, and degree of branching all potentially have important roles in their biological activities. Physicochemical properties of molecules such as solubility, osmotic effect, and surface properties are dependent on both their composition and architecture (Zong et al., 2012). Several reports have demonstrated that polysaccharides with higher uronic acid content are more bioactive than neutral polysaccharides (Azike at al., 2015; Yu et al., 2017). However, there have been conflicting reports concerning immunomodulatory neutral polysaccharides (Wang et al., 2015). Among the different types of plant polysaccharides: glucans, mannans, pectins, arabinogalactans, galactans, fructans, and xylans have all been reported to possess immunomodulatory properties *in vitro* and *in vivo* (Ferreira et al., 2015). Detailed structural analysis of polysaccharides is necessary to determine the interactions of specific moieties with immunocompetent cells.

1.4 Challenges towards Commercialization of Carbohydrate-Based Therapeutics

Despite the interest in carbohydrate-based therapeutics, nutraceuticals, and functional food, there have been several challenges in the commercialization of these products. Elucidation of structure-activity relationship remains a significant hurdle in the field of carbohydrates due to limitations in characterization techniques. High purification costs and erratic yields are some of the key obstacles towards commercialization (Giavasis, 2014). The heterogeneity and diversity of plant polysaccharides as well as extraction methodologies can lead to undesirable batch-to-batch structural variability

(e.g. size, molecular weight, monosaccharide composition, linkage, degree of branching etc.) in commercial products (Giavasis, 2014). Lipopolysaccharide (LPS) contamination, originating from gram-negative bacteria in polysaccharide preparations has also been a cause for concern (Gertsch et al., 2011; Pugh et al. 2008). Only a few polysaccharides (e.g. β-glucan from various fungi) that have gone through clinical trials as immunomodulators and anticancer agents have found commercial success in some countries (Vetvicka, 2011). Most polysaccharide extracts and nutraceuticals currently sold worldwide lack stringent quality control (QC) due to limitations in QC methodologies and lack of regulations by federal agencies. Commercial success of carbohydrate-based therapeutics is only possible after solving some of the key issues discussed here.

1.5 *Panax quinquefolius* (North American Ginseng) as a Source of Bioactive Polysaccharides

Panax quinquefolius or North American ginseng (NAG), one of the two most prominent species of ginseng, is a well-known medicinal herb widely used in traditional medicine. Biological activities of NAG include antioxidant, immunomodulatory, and anti-tumor properties (Azike et al., 2015; Biondo et al., 2008; Lemmon et al., 2012; Luo et al., 2008; Luo and Fang, 2008). These health-promoting properties have been largely attributed to two classes of compounds namely ginsenosides and polysaccharides (Lemmon et al., 2012). The vast majority of scientific literature indicates that complex polysaccharides are responsible for the immune stimulating properties of NAG (Azike et al., 2015; Biondo et al., 2008, Lemmon et al., 2012; Yu et al., 2017). Commercial

products such as CVT-E002 (commonly available as Cold-FX), a poly-furanosyl-pyranosyl polysaccharide-rich extract from NAG, which claims to have beneficial effects on influenza and the common cold, are widely available worldwide (Biondo et al., 2008). Other partially fractionated NAG root polysaccharide extracts isolated by Azike et al., (2015) have also shown promising immunomodulatory effects *in vitro*, *ex vivo,* and *in vivo.* There are also several reports of purified polysaccharides from NAG that have demonstrated immunomodulatory properties. A glucogalactan isolated from NAG root has stimulated cytokines such as IFN-γ, IL-2, and IL-10 and inhibited growth of lung tumors in the murine Lewis lung carcinoma model (Zhu et al., 2012). Glucogalactans from NAG root have also demonstrated desensitization of mouse macrophages by inhibiting proinflammatory mediators such as tumor necrosis factor-α (TNF-α), IL-1β, and IL-6 (Wang et al., 2015). This seemingly paradoxical behavior of immunostimulation and potential anti-inflammation by some NAG polysaccharides is currently being investigated by some researchers (Azike et al., 2015). Other neutral as well as acidic heteropolysaccharides isolated by Wang et al., (2015) and Yu et al., (2017) enhanced lymphocyte proliferation, macrophage phagocytosis, and production of proinflammatory mediators such as nitric oxide (NO), TNF-α, and IL-6 *in vitro.* Overall, these studies indicate that NAG is a rich source of bioactive polysaccharides which can be potentially commercialized into immunomodulatory therapeutics. Unfortunately, ginseng takes 5-7 years to become commercially viable, which is detrimental to commercialization. The popularity of NAG as a medicinal plant has also resulted in the dwindling of the plant's natural habitat (Burkhart et al., 2012). Due to overuse, NAG has been listed as "economically threatened" in the United States (US Fish and Wildlife Services) and a

"species at risk" in Canada (Species at Risk Public Registry). Alternate methods for the production of NAG tissues using biotechnology are necessary to extract bioactive metabolites for commercial purposes without compromising the plant population in the wild. Plant tissue culture offers a viable alternative wherein a large biomass of NAG tissue can be produced for extraction and study. Research on bioactive polysaccharides isolated from tissue culture-derived NAG can provide new avenues for the production of commercial carbohydrate-based therapeutics.

1.6 Novel Approaches

1.6.1 Plant Tissue Culture as a Viable Platform for the Production of Bioactive Polysaccharides

Plant tissue culture has been successfully used for many years for the production of valuable plant-specific secondary metabolites (Wang et al., 2012). However, the technique has not been extensively used for the production of primary metabolites such as polysaccharides. It has been shown that tissue culture techniques can be used to produce similar compounds that whole plants produce in a controlled environment (Vanisree et al., 2004). Metabolites can be produced *in vitro* without regard to season, environmental conditions or climate change, and cultured cells will be pathogen-free making processing easier (Murthy et al., 2014). Polysaccharides isolated from plants in nature are often contaminated with bacterial endotoxin (LPS) leading to false positives in immunostimulatory studies (Pugh et al., 2008). The production of endotoxin-free polysaccharides using tissue culture can be an important step in their validation as immunostimulatory agents. In addition, structural variability of botanical polysaccharides

from one batch to another has been a major challenge in commercialization efforts for many years. This platform can potentially eliminate the problem of structural variability as compounds are produced in a controlled environment for a definite amount of time. The plant tissue culture-based platform is not only suitable for large-scale production of standardized NAG polysaccharides but also promotes conservation efforts.

1.6.2 High Performance Liquid Chromatography-Charged Aerosol Detector (HPLC-CAD) as a QC Platform

Adequate QC methods are essential to ensure the safety and efficacy of commercial carbohydrate-based therapeutics. However, the QC process has been historically challenging due to the heterogeneity of polysaccharides, the presence of epimers, formation of anomers, and lack of a chromophore. The QC of commercial complex carbohydrates is often time-consuming due to the lack of a single platform capable of analyzing purity, homogeneity, molecular weight, and monosaccharide composition. Laborious derivatization techniques required for composition analysis of carbohydrates is a major bottleneck in the pipeline for rapid QC of commercial products. Hence, direct analysis of sugars without derivatization has become popular in recent years. Hydrophilic interaction liquid chromatography (HILIC), a variant of normal phase chromatography, coupled with semi-universal detectors such as CAD or evaporative light scattering detector (ELSD) offers alternative methods for direct analysis of sugars (Karlson et al., 2005; Yan et al., 2016). The CAD offers several advantages compared to other similar detectors used in the direct monosaccharide composition analysis. It offers greater sensitivity than ELSD and refractive index detector (RID), a broad dynamic range

of up to 4 orders of magnitude, and consistent response (Hu et al., 2013). The response of CAD does not depend on the structural properties of the analyte, and hence it is suitable for the detection of non-UV and weakly UV active compounds. It is compatible with gradient elution unlike RID and allows detection of all non-volatile and most semi-volatile analytes (Ligor et al., 2013). It is relatively inexpensive and easy to use with few controllable parameters compared to a mass spectrometer (MS). As a semi-universal detector, CAD has the potential to be used as a multipurpose QC analytical tool for i) underivatized monosaccharide composition analysis in conjunction with HILIC and ii) determination of homogeneity and molecular weight of polysaccharide samples using size exclusion chromatography (SEC).

1.7 Research Aims

The primary aim of this dissertation is the elucidation of structural features and immunomodulatory properties of polysaccharides isolated from *Panax quinquefolius* (NAG) suspension cultures. The Tennessee Center for Botanical Medicine Research (TCBMR) at Middle Tennessee State University (MTSU) has an initiative to develop methods to rapidly grow NAG via tissue culture and to assess the potency of the bioactive compounds as immunomodulators. The tissue culture platform was used to extract and isolate polysaccharide fractions to fulfill the objectives of this study. The structural features of four polysaccharides fractions have been reported in Chapter III. The immunomodulatory effects along with putative mechanisms of action of two polysaccharide fractions have been reported in Chapter IV. These studies are intended to

demonstrate the commercial applicability of the tissue culture platform as a source of standardized bioactive polysaccharides.

The secondary aim of this dissertation involved development of a novel QC platform for analysis of commercial complex carbohydrate polymers. Methods were developed to analyze purity, homogeneity, molecular weight, and monosaccharide composition of polysaccharides using HPLC-CAD. The results of this study have been reported in Chapter V.

CHAPTER II

MATERIAL AND METHODS

2.1 *Panax quinquefolius* Suspension Culture Generation and Maintenance

Panax quinquefolius (NAG) seeds were purchased from Wisconsin farmers through National Ginseng LLC. Shannon Smith and Dr. John DuBois at the TCBMR verified the seeds for authenticity. Sterilized (Murashige and Skoog, 1962; Wang, 1990) and scarified seeds were germinated on MS salts medium (Wang, 1990) under the following conditions: - temperature: 27±3°C; humidity: 100%; light conditions: none. Gibberellic acid concentrations of 0.433 μM, 0.577 μM, and 1.15 μM were used in an array to stimulate germination of seeds on Murashige and Skoog medium. Tissues were allowed to grow on the medium for two months to achieve proper size for explant selection. Explants were excised and plated on a callus induction medium that was experimentally optimized for growth (Abrahamian and Kantharajah, 2011; Wang 1990). The callus tissues were maintained and passaged for two years before stable cell lines of actively growing calli were developed. Appendix A shows the image of NAG callus tissue along with the growth rate of NAG callus per passage.

The stable callus cell lines were used to generate NAG suspension cultures. Ten g of callus tissue was used to inoculate liquid medium cell suspensions. Formulation of the liquid medium cell suspension was based on the recipe described above along with 0.57 mM L-ascorbic acid and 0.78 mM citric acid added to the medium (Abrahamian and Kantharajah, 2011). The medium was refreshed every 30 days. Once the tissues achieved 500 cc volume, they were filter separated, dried and analyzed. Suspension cultures were

generated and maintained by Shannon Smith at the TCBMR throughout the duration of the experiments.

2.2 Extraction and Purification of Polysaccharides

Dried NAG suspension culture tissues (10 g) were extracted in 500 mL of 95% (v/v) ethanol at 80°C for 4 h. The ethanol extract was discarded to eliminate secondary metabolites and the residue was further extracted in 500 mL of diH_2O at 80°C for 16 h. The aqueous extract was filtered and concentrated to 100 mL and divided into four tubes for ease of handling. Five mL of Sevag reagent (1:4 n-butanol:chloroform) was added to each tube containing 25 mL of aqueous extract to deproteinate the sample (Sevag et al., 1938). The mixture was sonicated for 20 min and centrifuged at 1000xg for 10 min. The upper aqueous layer was collected and the deproteination process was repeated three times. Polysaccharides were then precipitated from the deproteinated extracts by the addition of four volumes of 95% (v/v) ethanol. The precipitated crude polysaccharides were pooled together and solubilized in diH_2O.

The crude polysaccharide extract was applied to a DEAE-Sepharose Fast Flow 16/10 anion exchange fast protein liquid chromatography (FPLC) column (GE Healthcare Life Sciences, USA). A stepwise gradient of NaCl (0 M, 0.1 M, 0.2 M, 0.3 M, 0.4 M and 1 M) at a flow rate of 3 mL/min was used to elute out the polysaccharides. Each gradient step consisted of four column volumes (column volume = 20.1 mL). The eluate was collected at 5 mL/tube. The presence of sugar in the tubes was assayed using a phenol sulfuric acid assay (Dubois et al., 1936) and a chromatogram was constructed. Based on the resulting elution profile, four major fractions were identified, pooled and concentrated

under reduced pressure. The fractions were named AGC1 (water eluate), AGC2 (0.1 M NaCl eluate), AGC3 (0.2 M NaCl eluate), AGC4 (0.3 M NaCl eluate), AGC5 (0.4 M NaCl eluate), and AGC6 (1 M NaCl eluate). Based on preliminary immunostimulatory assays *in vitro* (Section 3.2.1), AGC1, one of the most active fractions, was further purified using a preparatory grade HiLoad 26/60 Superdex-200 size exclusion FPLC column (GE Healthcare Life Sciences, USA). A buffer of 0.5 M NaCl and 0.3 M $NaPO_4$ at a flow rate of 1 mL/min was used as the eluent. Fractions (10 mL/tube) were collected and analyzed for the presence of sugars using the phenol sulfuric acid assay (Dubois et al., 1936). Further structural analyses were carried out on purified AGC1, AGC2, AGC3 and AGC4. The yields of AGC5 and AGC6 were insufficient to conduct further analysis.

2.3 Structural Analysis of Polysaccharide Fractions

2.3.1 Molecular Weight Determination

The homogeneity and molecular weight of the fractions were determined by high performance size exclusion chromatography (HPSEC) on a TOSOH HLC-8320GPC EcoSEC instrument equipped with RID. Chromatographic analysis was carried out using a TSK Gel PwXL G4000 (7.8 X 300 mm) analytical size exclusion column with 0.5 M NaCl and 0.3 M $NaPO_4$ as eluent at a flow rate of 0.5 mL/min. The average molecular weight of the polysaccharides was calculated based on a calibration curve (log molecular weight versus retention times) of dextran standards of known molecular weights (5 kDa, 25 kDa, 50 kDa, 150 kDa, and 410 kDa).

2.3.2 Monosaccharide Composition Analysis by HPLC

Preliminary monosaccharide composition analysis was carried out by HPLC using a Dionex Ultimate 3000 HPLC coupled to a UV detector. Polysaccharides (2-5 mg) were hydrolyzed in 2 M trifluoroacetic acid (TFA) at 120°C for 6 h. TFA was then removed by evaporation under a stream of air and the residue was resuspended in 200 µL of DiH_2O. The sample was neutralized by the addition of NaOH. The resulting hydrolysate was mixed with 50 µL of 0.5 M 1-phenyl-3-methyl-5-pyrazolone (PMP) reagent in methanol and heated at 80°C for 1 h. The sample was then extracted with 500 µL of chloroform three times and the upper aqueous layer was collected and filtered (0.2 µm). The PMP derivatives were then analyzed using the following method reported by Hosain et al., 2019. Separation was carried out on a Phenomenox Hyperclone (4.6 X 150 mm; 5µm) ODS C-18 column. The mobile phase consisted of (A) 15% acetonitrile (ACN) with 50 mM sodium phosphate (pH 6.9) and (B) 40% ACN with 50 mM sodium phosphate (pH 6.9). The following gradient elution at a flow rate of 0.6 mL/min was used: 0% B at 0-5 min, 0-8% B at 5-15 min, 8-20% B at 15-50 min, 20% B at 50-55 min, 20-0% B at 55-58 min, and 0% B at 58-65 min. A wavelength of 254 nm was used to monitor the PMP derivatized sugars. Retention times of PMP derivatives of authentic monosaccharide standards were used for identification purposes. Relative amounts of different monosaccharides (mol%) in the samples were determined based on respective peak areas.

2.3.3 Monosaccharide Composition Analysis by Gas Chromatography-Mass Spectrometry (GC-MS)

An alternative and more sensitive method using GC-MS was used to verify the HPLC monosaccharide composition results of AGC1. AGC1 (1-2 mg) was hydrolyzed in 1 M methanolic HCl at 80°C for 16 h. The methanolysis products were heated at 80°C for 30 min with Tri-Sil HTP (HDMS:TMCS:Pyridine) reagent. The resultant trimethylsilyl (TMS) methyl glycosides were analyzed using a GCMS-QP2010S instrument (Shimadzu Corp., Japan). The derivatized sample was analyzed on a RTX-5SilMS column (30 m X 0.32 mm X 0.25 μm). The GC operation was performed using the method reported by Hosain et al., 2019. An initial column temperature of 80°C was held for 2 min, then increased to 140°C at a rate of 20°C/min, temperature was again held for 2 min, then increased to 200°C at a rate of 2°C/min and finally increased to 250°C at a rate of 30°C/min, which was held for 5 min. Retention times and mass spectra of TMS methyl glycosides of authentic monosaccharide standards were used for identification purposes. Relative amounts of monosaccharides in the fractions were determined based on respective peak areas.

2.3.4 Glycosyl Linkage Analysis by GC-MS

Glycosyl linkage analysis of AGC1, AGC2, AGC3, and AGC4 was carried out at the Complex Carbohydrate Research Center (CCRC), University of Georgia. The polysaccharides (1 mg) were permethylated using iodomethane, followed by hydrolysis with TFA, reduction with sodium borodeuteride, and acetylation by acetic anhydride following a method reported by Heiss et al., 2009. The resultant partially methylated

alditol acetate (PMAA) derivatives were analyzed by GC-MS. Approximately, 1 μL of the PMAA derivatives were analyzed on a 30 m Supelco 2330 bonded-phase fused-silica capillary column. The GC operation was performed under the following conditions: initial column temperature of 80°C for 2 min, then increased to 170°C at a rate of 30°C/min, and finally increased to 240°C at a rate of 4°C/min, which was held for 20 min. The glycosyl linkages were determined based on retention times and mass spectra. The CCRC spectral database for PMAAs was used for interpretation of mass spectra.

2.3.5 1D-NMR Spectroscopy

A one dimensional proton NMR spectra was obtained to analyze the anomeric conformations (α and β) of sugars present in AGC1. AGC1 (<10 mg) was deuterium exchanged by lyophilization in D_2O, re-dissolved in 0.5 mL D_2O, transferred to a 3 mm OD NMR-tube and analyzed on a Varian Inova-600 MHz spectrometer at 25°C. The chemical shifts were measured relative an internal acetone peak (δ_H =2.22 ppm). The analysis was performed at the CCRC, UGA.

2.4. Determination of Protein Concentration

The protein content in the samples was determined using a Pierce™ bicinchoninic acid (BCA) assay (Smith et al., 1985) kit following manufacturer's protocol (ThermoFisher Scientific, USA). UV absorbance of the samples at 280 nm was also indicative of protein presence. Absorbance at 220-995 nm was measured using a Molecular Devices SpectraMax plate reader.

2.5 Determination of Endotoxin Concentration

The polysaccharide fractions were processed through a Pierce™ high capacity endotoxin removal resin (ThermoFisher Scientific, USA) following manufacturer's protocol to remove bacterial endotoxin or LPS contaminants. Prior to immunostimulatory assays, endotoxin levels in the samples were quantified using a Wako limulus amoebocyte lysate (LAL) Pyrostar™ kit according to manufacturer's protocol.

2.6 Mammalian Cell Culture

2.6.1 RAW 264.7 Murine Macrophage Cell Line

RAW 264.7 murine macrophage cells were (ATCC TIB 71) purchased from American Type Culture Collection, USA. The cells were grown in DMEM medium supplemented with 10% heat-inactivated fetal bovine serum (FBS) and 1% penicillin/streptomycin and maintained at 37°C in a humidified 5% CO_2 incubator. The cells were passaged every 3-4 days throughout the duration of the experiments.

2.6.2 Primary Murine Splenocytes

Male ICR mice (<200 g) were purchased from Charles River Laboratories, USA. The mice were sacrificed following a protocol approved by the Institutional Animal Care and Use Committee (Appendix B). The mice were initially asphyxiated by CO_2 followed by cervical dislocation. Splenocytes were harvested according to a method reported by Wang et al., (2013). The spleens were aseptically removed, homogenized, and placed in phosphate-buffered saline (PBS). A lysis buffer solution (0.15 M NH_4Cl, 10 mM $KHCO_3$, 1 mM EDTA-Na2, pH 7.2) was added to the cell suspension and vortexed for 2

min to lyse the red blood cells. Two mL of calf serum was added to the cell suspension followed by centrifugation at 500xg for 5 min. The bottom layer containing splenocytes were collected and washed with PBS buffer three times. The splenocytes were resuspended in RPMI 1640 medium with 10% heat-inactivated FBS and 1% penicillin/streptomycin. The splenocyte cell suspension was maintained at 37°C in a humidified 5% CO_2 incubator until further treatments with polysaccharides.

2.7 Cell Treatments

The RAW 264.7 murine macrophage cells were counted using a hemacytometer, adjusted to a desired concentration, seeded onto 96-well or 6-well plates, and incubated overnight at 37°C in a humidified 5% CO_2 incubator. Detailed seeding densities for each assay are mentioned in subsequent sections. After overnight incubation, cells were washed with 1X PBS and treated with different concentrations of polysaccharides and controls in DMEM medium with 5% FBS for 24 h. Culture supernatants and cell lysates were collected after 24 h treatments and stored at -80°C until further analysis.

Primary murine splenocytes were counted using a hemacytometer, adjusted to a concentration of 5 X 10^6 cells/mL, seeded onto 96-well plates (5 X 10^5 cells/well), and incubated at 37°C in a humidified 5% CO_2 incubator for 1 h. Splenocytes were then treated with different concentrations of polysaccharides and controls in complete RPMI medium for 48 h. After 48 h treatments, culture supernatants were collected and stored at -80°C until further analysis.

2.8 Cell Viability Assay

The relative cell viability of RAW 264.7 cells in response to polysaccharide and control treatments was determined by the 3-(4,5-Dimethylthiazol-2-yl)-2,5-diphenyltetrazolium bromide (MTT) assay. Cells (5 X 10^4 cells/well in a 96-well plate) were treated with different doses (1, 12.5, 25, and 50 µg/mL) of polysaccharide fractions (AGC1, AGC2, AGC3, and AGC4), LPS (1 µg/mL) and culture medium for 24 h. The relative cell viability of the treated cells was measured by a MTT cell proliferation assay kit (Cayman Chemical Company, USA) according to manufacturer's instructions.

2.9 Assessment of Cytokine Production

The production of mouse proinflammatory cytokines, chemokines, and growth factors (IFN-γ; IL-1β; IL-2; IL-4; IL-6; IL-10; IL-12 p70; GM-CSF; monocyte chemoattractant protein-1, MCP-1; and TNF-α) in response to polysaccharide (12.5 µg/mL) or LPS (1 µg/mL) treatments in culture supernatants was analyzed by Eve Technologies, Canada. RAW 264.7 cells (5 X 10^4 cells/well in a 96-well plate) and primary murine splenocytes (5 X 10^5 cells/well in a 96-well plate) were treated with polysaccharides and controls for 24 h and 48 h respectively, supernatants collected, frozen, and shipped to Eve Technologies for a multiplex bead-based analysis of cytokines.

Dose-dependent production of proinflammatory cytokines such as IL-6 and TNF-α in culture supernatants was also measured by ELISA following manufacturer's protocol (R&D Systems, USA). RAW 264.7 cell densities of 5 X 10^4 cells/well and 1 X 10^5 cells/well in a 96-well plate were used for the dose-dependent TNF-α and IL-6 ELISA

experiments, respectively. The cell density for primary murine splenocytes was the same as before.

2.10 NO (Griess) Assay

Nitrite concentration in culture medium of cells (RAW 264.7 macrophages and primary murine splenocytes) exposed to different doses of polysaccharides (1, 12.5, 25, and 50 μg/mL) or controls were determined as an estimate of NO production using the Griess assay. RAW 264.7 cells (1 X 10^5 cells/well in a 96-well plate) and primary murine splenocytes (5 X 10^5 cells/well in a 96-well plate) were treated with polysaccharides and controls for 24 h and 48 h respectively. Culture supernatants and 1X modified Griess reagent (Sigma Aldrich, USA) were mixed together in equal ratios and incubated at room temperature for 15 min. Absorbance was measured at 540 nm using a Molecular Devices SpectraMax microplate reader and NO concentration was calculated based on a nitrite standard curve (1 – 100 μM).

2.11 *NOS2* Gene Expression Kinetics

A novel RAW 264.7 *NOS2*-mCherry reporter cell line was generated by the Nelson laboratory at MTSU. The reporter cell line was used to study the kinetics of *NOS2* gene expression in response to AGC1 (25 μg/mL) and LPS (1 μg/mL) treatments by live cell imaging. The mCherry expression in live cells following polysaccharide/control treatments was measured at 30 min intervals by fluorescence microscopy using a Nikon Ti-Eclipse wide-field microscope (Nikon, USA), equipped with a CoolSNAP Myo camera (Photometrics, AZ, USA), and computer-controlled stage. The cells were maintained at 37°C with 5% CO_2 using a stage incubator and full environmental

enclosure (InVivo Scientific, MO, USA) throughout the duration of the kinetic measurements. The reporter expression after 24 h treatments was also quantified using a Zeiss LSM700 confocal microscope with mCherry fluorescence excited using a 555 nm laser. The acquisition of images was performed using Zen software (Zeiss, USA). The images were analyzed using Fiji (Schindelin et al., 2012). These experiments were a collaborative effort between the Nelson and Farone laboratories.

2.12 Role of NF-κB (p65) and MAPK (p38) in Immunostimulation

The putative mechanisms of action of immunostimulation due to polysaccharide treatments were investigated in RAW 264.7 murine macrophage cells. RAW 264.7 cells (5 X 10^4 cells/well) seeded onto 96-well plates were pre-treated either with a known inhibitor of the NF-κB (p65) signaling pathway, BAY11-7082 (concentration: 5 μM) (Pierce et al., 1997) or with a known inhibitor of the MAPK (p38) pathway, SB202190 (concentration: 30 μM) (Bain et al., 2007) for 1 h. The pre-treated cells were then stimulated with either LPS (1 μg/mL) or polysaccharide fractions (12.5 μg/mL) for 4 h. After 4 h, the culture supernatants were collected and analyzed for the presence of TNF-α. The production of TNF-α due to inhibitor (BAY11-7082 or SB202190) pre-treatments were compared to controls (only polysaccharide or LPS stimulation). A significant (p<0.5) reduction of TNF-α production due to the inhibitor pre-treatments were indicators of the potential roles of NF-κB (p65) and MAPK (p38) signaling pathways in the immunostimulatory process triggered by polysaccharides. TNF-α quantification was performed using ELISA following manufacturer's protocol (R&D Systems, USA).

2.13 Western Blot Analysis

RAW 264.7 cells (1.8 X 10^6 cells/well) seeded onto 6-well plates were treated with polysaccharides, LPS (1 µg/mL), or culture medium for 24 h. The cells were lysed using a radio-immunoprecipitation assay (RIPA) buffer containing protease inhibitor cocktails and the resultant cell lysates were used to analyze the expression of inducible nitric oxide synthase (iNOS). The total protein concentration in the lysates were quantified using a BCA assay kit (ThermoFisher Scientific, USA). The protein content in the samples was normalized by dilution with RIPA buffer. The western blot analysis was carried out following the method reported by Park et al. (2017). The expression of iNOS in the polysaccharide-treated cells versus untreated control cells were measured qualitatively.

2.14 Splenocyte Proliferation

Proliferation of primary murine splenocytes in response to polysaccharide and control treatments was determined using the i) MTT cell proliferation assay (Cayman Chemical Company, USA) and ii) Click-iT™ Plus 5-ethynyl-2´-deoxyuridine (EdU) flow cytometry assay (Invitrogen, USA).

2.14.1 MTT Cell Proliferation Assay

Primary murine splenocytes were harvested, seeded onto 96-well plates (5 X 10^5 cells/well), and treated with different concentrations of polysaccharides (1, 12.5, 25 and 50 µg/mL), concanavalin A (ConA) (0.5 µg/mL), or RPMI 1640 complete medium for 48 h. After 48 h treatment, splenocyte proliferation was measured by the MTT cell

proliferation assay kit (Cayman Chemical Company, USA) according to the manufacturer's protocol. Relative splenocyte proliferation was calculated using the following equation: RSP= [($Abs_{sample}/Abs_{untreated\ control}$) X 100] – 100.

2.14.2 Click-iT™ Plus EdU Flow Cytometry Assay

Murine splenocytes were harvested and treated as described in section 2.14.1. Following treatment, splenocytes were accessed for replicating DNA using Click-iT™ Plus EdU Flow Cytometry Assay, which relies on the incorporation of 5-ethynyl-2'-deoxyuridine in place of thymine during DNA synthesis and subsequent detection by conjugation of Alexa Fluor™ 488 picolyl azide by click reaction as per manufacturer's instructions. (Invitrogen, USA) The number of EdU positive cells was then determined using 488 nm laser of the Guava® easyCyte™ HCT flow cytometer. (Luminex Corp., Austin, TX USA) Cells were considered positive if the green fluorescence was greater than 10^3 and the forward scatter exceeded 360.

2.15 Development of QC Methodologies for the Analysis of Carbohydrate Polymers by HPLC-CAD

A novel HILIC-CAD gradient method was developed for simultaneous analysis of amino, acidic and select neutral monosaccharides without derivatization. This method can be potentially used for the direct (without derivatization) analysis of monosaccharide composition in complex carbohydrates. A separate SEC-CAD method that can analyze homogeneity and molecular weight of carbohydrate polymers was also reported. Overall, HPLC-CAD was demonstrated as a QC platform for the analysis of commercial

carbohydrate-based polymers. Detailed chromatographic methods along with optimization and validation results have been reported in Chapter V.

2.16 Statistical Analysis

Stable NAG cell culture (callus culture) lines were used to initiate liquid suspension cultures at least three separate times independently. Crude polysaccharides were isolated independently from different batches of dried suspension culture cells and purified. Purified fractions from multiple batches were pooled together for structural analyses and biological assays. All structural and biological analyses were performed at least in triplicate. The results of the immunoassays were reported as mean ± SEM (n = 9). Statistical significance ($p<0.05$) was determined using one-way analysis of variance (ANOVA) followed by Dunnett's/Dunn's multiple comparison test or student's t-test (GraphPad Prism 7, USA) unless otherwise stated.

CHAPTER III

STRUCTURAL ANALYSIS OF NAG SUSPENSION CULTURE POLYSACCHARIDES

3.1. Background

Carbohydrates, one of the most abundunt natural products, have been used as food or structural building blocks for many years. However, recent research has revealed that complex carbohydrates from plants not only contain nutrinonal benefits but also possess therapeutic functionality (Yamada and Kiyohara, 2007; Li et al., 2013). These biopolymers have been touted by some researchers as potential immunomodulatory, anticancer, tissue engineering, and wound-healing therapeutic candidates (Schepetkin and Quinn, 2006). Unlike other biomacromolecules, the diversity of carbohydrates is unique and the possible combinations and ratios of monosaccharide units and glycosidic linkages are huge. Biological properties of complex carbohydrates are possibly correlated to their physicochemical properties such as size, monosaccharide composition, glycosidic linkages, and monsaccharide sequences (Li et al., 2013). Hence, structural characterization of polysaccharides is necessary to develop safe and effective bioactive carbohydrate-based therapeutics.

Polysaccharides from *Panax quiquefolius* (North American ginseng; NAG), a well-known medicinal herb in traditional medicine, have been identfied as major bioactive compounds in recent years (Azike et al., 2015). Several crude, partially purified, and homogeneous polysaccharides from mature NAG have shown promise as immunomodulatory and antitumor agents (Azike et al., 2015). Due to overuse of the plant

and dwindling natural habitats, some researchers have turned to tissue culture as an alternative method for producing NAG for research and medicinal use. Additionally, tissue culture is convenient as large quantities of tissue can be produced in a short period of time in a sterile and controlled environment. Also, the production of metabolites in a controlled and sterile environment can potentially eliminate batch-to-batch structural variability and bacterial endotoxin contamination, which are major issues hindering the commercialization of bioactive polysaccharides. NAG tissue culture is commonly used for the production of bioactive triterpenoid saponins known as ginsenosides (Wang et al., 2012). Polysaccharides have not been previously isolated from NAG tissue culture system. The TCBMR at MTSU initiated a project to grow NAG tissues via suspension culture for isolation and characterization of polysaccharides. The structural features of four polysaccharide fractions have been reported in this chapter. The structural analyses of NAG suspension culture polysaccharide fractions will provide a foundation for structure-function relationship studies and development of safe and effective carbohydrate-based NAG nutraceuticals.

3.2. Results and Discussion

3.2.1. Extraction and Purification of Polysaccharides

Dried NAG suspension culture tissues were ground to a fine powder before extraction of polysaccharides. The presence of large aggregates of tissues during extraction may decrease the final yield of polysaccharides. The classical method of hot ethanol extraction followed by hot water extraction was used to extract crude polysaccharides from the powdered suspension culture tissues. The hot ethanol extraction

is essential to remove plant secondary metabolites, essential oils, lipids, and other low molecular weight compounds (Cui et al., 2014). Additionally, the aqueous extract was thoroughly deproteinated by treatment with Sevag reagent (Sevag et al., 1938). The yield of the crude polysaccharide obtained after precipitation with ethanol of the deproteinated aqueous extract was 3-5% (w/w) of the total dry weight. We compared the polysaccharide yields between suspension culture tissues and mature NAG root tissues. The polysaccharide yield of mature NAG roots was found to be variable between 5-10% (w/w). Other publications have also reported an average polysaccharide yield of 10% (w/w) in mature NAG root tissues (Azike et al., 2015). We are currently optimizing our tissue culture system to enhance polysacchaide yields. It has been reported that the presence of different sugar substrates such as sucrose, glucose, galactose, and arabinose in tissue culture medium affect polysaccharide yield and productivity (Gunter and Ovodov, 2002). Enhancing polysaccharide yields will be critical for the future commercial appplication of the NAG tissue culture system.

The crude polysaccharide was chromatographed on a DEAE-Sepharose anion exchange column with an increasing gradient of NaCl as the mobile phase. The initial fractionation produced six fractions by 0 M, 0.1 M, 0.2 M, 0.3 M, 0.4 M, and 1 M NaCl elution in a stepwise gradient (Fig. 3.1). The complete extraction and purification scheme is depicted in fig. 3.1. The fractions eluted by 0 M, 0.1 M, 0.2 M, and 0.3 M NaCl had sufficient yields for further structural analyses and preliminary biological activity assessment *in vitro*. These four fractions were named AGC1 (0 M fraction), AGC2 (0.1 M fraction), AGC3 (0.2 M fraction), and AGC4 (0.3 M fraction). Prior to preliminary bioassays, all fractions were treated to remove any potential bacterial endotoxin

contamination by passing through an endotoxin removal resin. All four fractions demonstarted some degree of immunostimulatory activity in RAW 264.7 murine macrophage cells *in vitro*. Among the four fractions, the water eluted neutral fraction AGC1 showed the greatest immunostimulation at a dose of 12.5 µg/mL. TNF-α production in 12.5 µg/mL AGC1-treated RAW 264.7 cells was 1618 pg/mL, 438 pg/mL, and 607 pg/mL higher compared to AGC2, AGC3, and AGC4-treated cells. After preliminary bioassays, it was decided to further purify AGC1 using a Superdex-200 size exclusion column. The size exclusion chromatogram revealed the presence of one major peak in AGC1. Further strcuture elucidation of AGC1 including molecular weight analysis, monosaccharide composition analysis, glycosyl linkage analysis, and determination of anomeric conformations was conducted in this study. Although, AGC2, AGC3, and AGC4 were not purified further, structural features (molecular weight, monosaccharide composition, and linkage) of the three fractions were also analyzed. Prior to structural analysis, biochemical tests were conducted to evaluate the presence of proteins in the four fractions. A BCA assay showed that the protein concentration in the samples was <1%. A wavelength scan (200-800 nm) of the samples showed no peaks at 280 nm confirming the absence of protein. Appendix C shows a representative wavelength scan graph of sample AGC1.

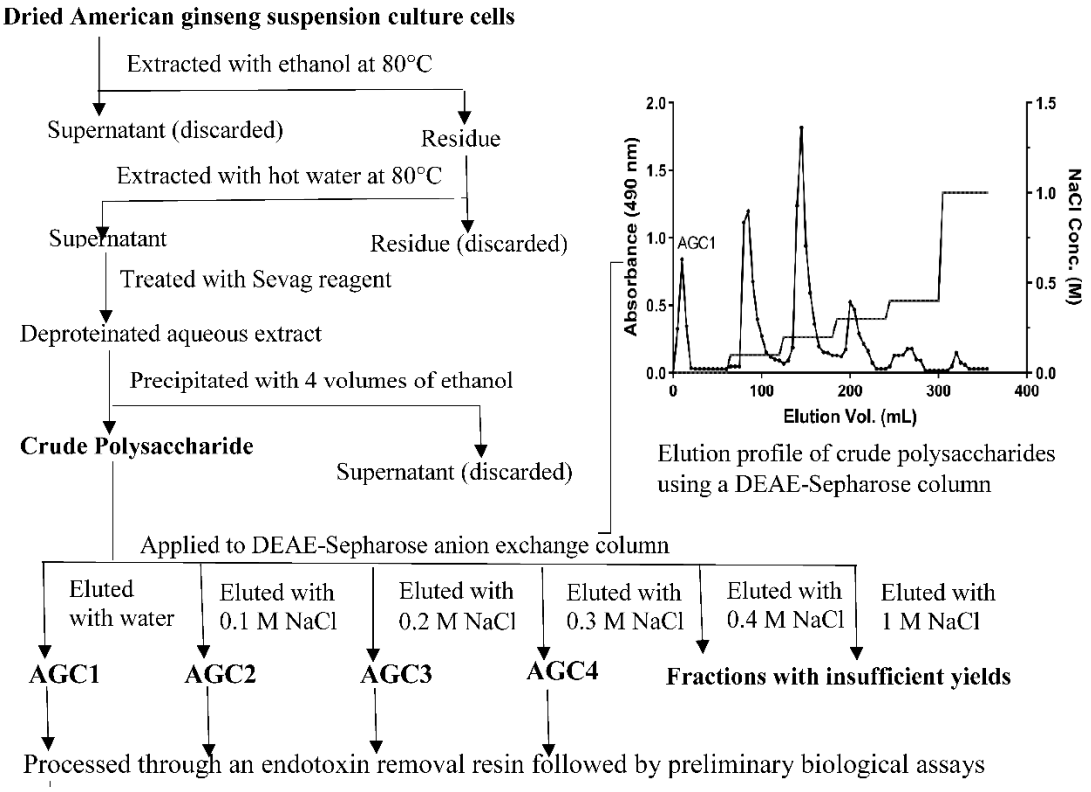

Figure 3.1. Extraction and fractionation scheme of NAG suspension culture polysaccharides. Crude polysaccharides were extracted from dried NAG suspension culture cells using hot ethanol extraction followed by hot water extraction. The aqueous extract was deproteinated by Sevag reagent followed by precipitation of polysaccharides by the addition of four volumes of ethanol. The crude polysaccharide was chromatographed on a DEAE-Sepharose anion exchange column using a stepwise gradient of NaCl. The four major fractions (eluted by 0 M, 0.1 M, 0.2 M, and 0.3 M NaCl) were further processed through an endotoxin removal resin prior to preliminary bioassays. Structural analyses were carried out on all four major fractions.

3.2.2. Molecular Weight Determination

The homogeneity and molecular weight of the four fractions were determined by HPSEC-RID. The HPSEC-RID chromatogram of AGC1 after sequential anion exchange and size exclusion chromatography shows the presence of one major peak (Fig. 3.2). The average molecular weight of the peak was determined to be 5.2 kDa (Table 3.1). The presence of one peak in HPSEC does not necessarily mean that the fraction is homogeneous. However, the amount of impurities in AGC1, if any, is negligible. It should also be noted that the primary commercial application of these polysaccharides would be as a nutraceutical. The purity of AGC1 as determined by HPSEC is suitable for use as a nutraceutical or dietary supplement. The HPSEC-RID chromatograms also revealed that AGC2, AGC3, and AGC4 are heterogeneous fractions (Appendix D). AGC2 has two distinct peaks with average molecular weights of 56.49 kDa and 3.18 kDa. Similarly, AGC3 has two peaks with average molecular weights of 32.14 kDa and 4.81 kDa. AGC4 has one major non-symmetrical broad peak with an average molecular weight of 34.12 kDa. A non-symmetrical broad peak is generally indicative of a heterogeneous fraction. The molecular weights of the major peaks present in the fractions are summarized in Table 3.1.

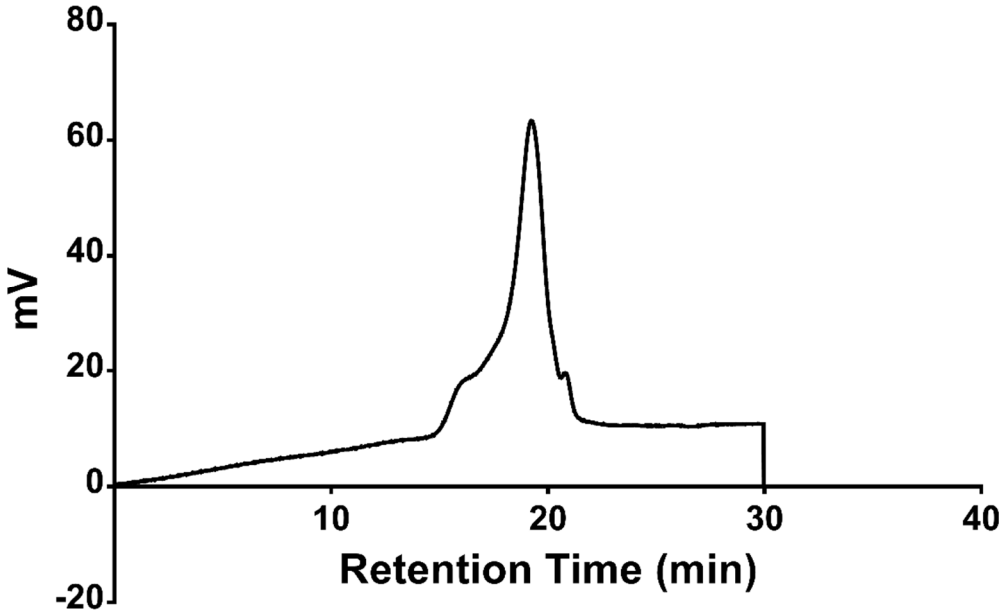

Figure 3.2. HPSEC-RID chromatogram of AGC1. The chromatogram indicates the presence of one major peak with an average molecular weight of 5.2 kDa.

Table 3.1 Average molecular weight of major peaks in AGC1, AGC2, AGC3, and AGC4.

Fraction	Average Molecular Weight of Major Peaks (kDa)
AGC1	5.20
AGC2	56.49 3.18
AGC3	32.14 4.81
AGC4	34.12

3.2.3. Monosaccharide Composition Analysis

Analysis of monosaccharide composition is an important step in the structural characterization of polysaccharides. Several techniques involving derivatization have been proposed over the years to determine the monosaccharide composition of polysaccharides. The most commonly used methods involve acid hydrolysis of the glycosidic bonds, derivatization of the monosaccharide units using PMP (for HPLC analysis) or TMS (for GC-MS analysis), and subsequent identification and quantification of sugars by HPLC or GC-MS. The advantage of PMP derivatization is that the cyclic ring structures of monosaccharides are opened up and the sugars can be identified as single peaks in a HPLC analysis (Hosain et al., 2019). Although, the single peaks of PMP derivatized sugars lead to a simpler analysis, certain PMP monosaccharide derivatives

such as the aldopentoses, arabinose and xylose, are difficult to separate in reverse phase chromatography. Fig. 3.3A shows the separation of nine PMP derivatives of monosaccharide standards by reverse phase (C18) chromatography. It is evident from the chromatogram that arabinose and xylose co-elute and as a result, it is difficult to identify and quantify these two sugars with certainty. However, due to ease of analysis, this method was used to analyze the monosaccharide composition of AGC1, AGC2, AGC3, and AGC4. Fig. 3.3B shows a representative chromatogram of PMP derivatives of monosaccharides present in AGC1. AGC1 is predominantly composed of galactose (58.49%) and arabinose/xylose (27.1%) along with the presence of minor amounts of neutral sugar residues such as mannose, rhamnose, and glucose. The monosaccharide composition of all four fractions is summarized in table 3.2. The representative chromatograms of PMP derivatives of monosaccharides present in AGC2, AGC3, and AGC4 are also shown (Appendix E). It is noticeable that the composition of AGC2 is relatively similar to AGC1. The difference between AGC1 and AGC2 is the presence of minor amounts of uronic acids such as glucuronic acid and galacturonic acid in the sample. Since AGC2, AGC3, and AGC4 are eluted with an increasing gradient of NaCl in anion exchange chromatography, it is expected that these fractions would contain acidic sugar residues or other anionic species. AGC3 also predominantly contains galactose (43.36%) and arabinose/xylose (37.2%) along with other minor neutral sugars. The major difference between AGC3 and the other fractions is the higher percentage of rhamnose (8.1%) and galacturonic acid (6.8%) in the sample. This might indicate the presence of a different type of polysaccharide in fraction AGC3. AGC4 contains the highest percentage of galactose (82.83%) along with minor amounts of other sugars. The

amount of uronic acids in AGC4 is also comparatively higher compared to the rest of the fractions.

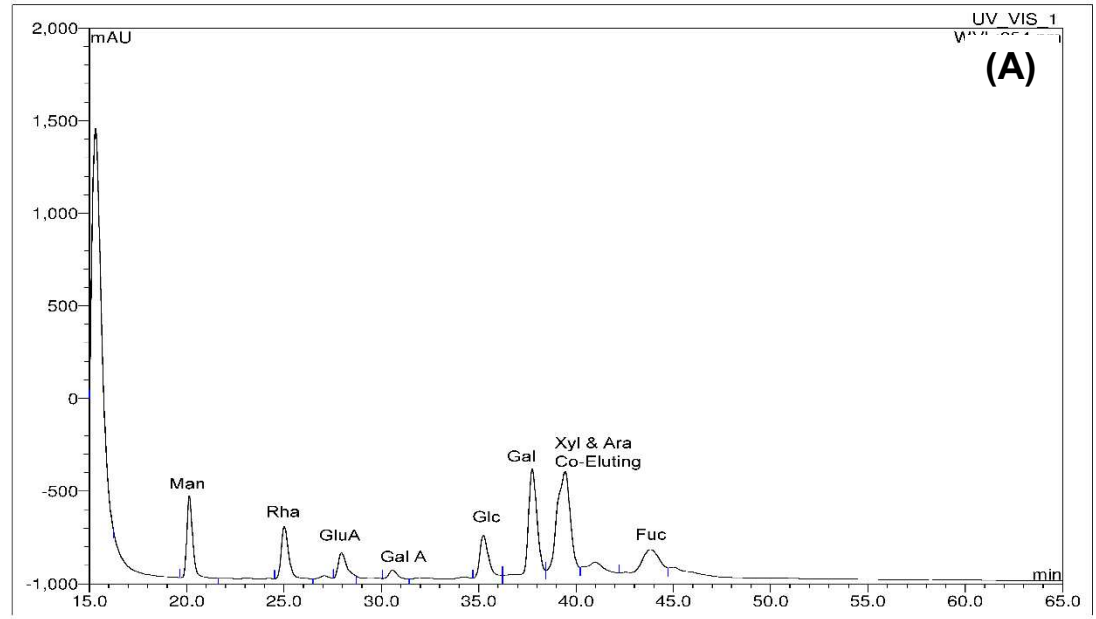

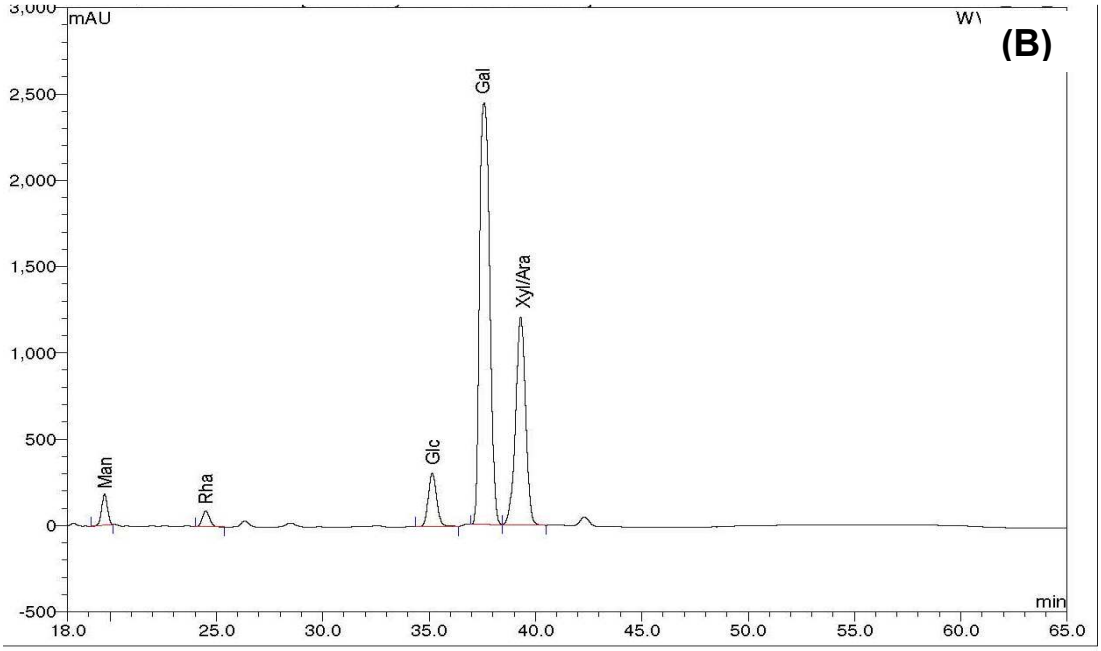

Figure 3.3. Monosaccharide composition analysis by HPLC. The samples (monosaccharide standards or polysaccharides) were acid hydrolyzed followed by derivatization using PMP. The PMP derivatives of monosaccharides were separated and detected by reverse phase HPLC at 254 nm. (A) shows the separation of nine PMP derivatives of monosaccharide standards (Man, Rha, GlcA, GalA, Glc, Gal, Xyl, Ara, and Fuc). (B) is a representative HPLC chromatogram showing the presence of Man, Rha, Glc, Gal and Xyl/Ara residues in AGC1.

Table 3.2. Monosaccharide composition of NAG polysaccharide fractions based on HPLC analysis of PMP derivatives

Monosaccharide	AGC1 (Mol %)	AGC2 (Mol %)	AGC3 (Mol %)	AGC4 (Mol %)
Man	3.243	1.288	2.265	2.697
Rha	1.710	2.845	6.020	2.730
Glc A	ND*	2.063	3.585	6.123
GalA	ND*	1.962	1.963	6.830
Glc	9.447	2.020	1.490	1.220
Gal	58.493	56.813	43.355	82.833
Ara/Xyl	27.103	33.298	37.195	5.713

*Not Detected

Since, AGC1 is one of the most active immunostimulatory fractions with future potential commercial application as a nutraceutical, it was decided to further analyze and

confirm the HPLC composition results of AGC1 by GC-MS. In this method, most common monosaccharides including arabinose and xylose can be properly separated. The major disadvantage of this method is that the TMS methyl glycosides of monosaccharides exist in multiple cyclic forms representative of their population in solution. As a result, each monosaccharide appears as multiple peaks in a total ion chromatogram. The presence of multiple peaks for each monosaccharide can result in a chromatogram that can be difficult to interpret. Appendix F shows the total ion chromatograms of eight common monosaccharides that are usually found in plant polysaccharides. Fig. 3.4 shows the GC-MS total ion chromatogram of TMS methyl glycosides obtained from sample AGC1. Based on the GC-MS analysis, AGC1 contains galactose (60.093%), arabinose (19.165%), xylose (11.363%), and glucose (6.298%) with minor amounts of rhamnose (1.548%) and mannose (0.790%). These results are fairly consistent with the HPLC composition results reported earlier.

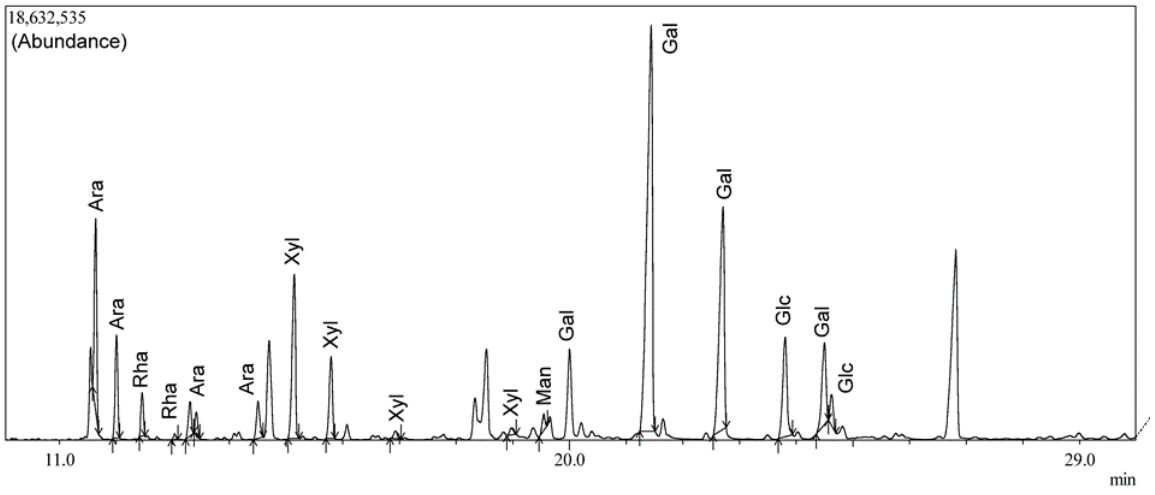

Figure 3.4. Monosaccharide composition analysis of AGC1 by GC-MS. The sample was hydrolyzed followed by TMS derivatization. The total ion chromatogram of the TMS methyl glycosides indicate the presence of arabinose (19.165%), rhamnose (1.548%), xylose (11.363%), mannose (0.79%), galactose (60.093%) and glucose (6.298%) in the sample.

3.2.4. Glycosyl Linkage Analysis

The glycosyl linkage analysis of the four fractions was conducted by GC-MS. Analysis of PMAA derivatives of AGC1 showed that the predominant linkages present in the fraction were 3-substituted galactopyranosyl (48.5%), 3,6-linked galactopyranosyl (10.2%), terminal galactopyranosyl (5.2%), 6-linked galactopyranosyl (4.4%), 4-linked arabinopyranosyl or 5-linked arabinofuranosyl (4%), and terminal arabinofuranosyl (4.5%) residues. The total ion chromatogram of PMAA derivatives of AGC1 and the respective mass spectra of the glycosyl residues have been shown in fig. 3.5 and appendix H, respectively. The presence of low percentages of terminal residues indicate that AGC1 is likely composed of high molecular weight compounds. The results also revealed that most of the glycosyl residues are in the pyranose form. The linkages strongly indicate the presence of arabinogalactan type II polysaccharides in AGC1. Type II arabinogalactans are comprised of a branched galactan core made up of 3-linked, 6-linked, and 3,6-distributed galactopyranosyl residues (Yamada and Kiyohara, 2007). Short side chains of 6-galactopyranose residues are also commonly found along with terminal arabinofuranosyl units (Yamada and Kiyohara, 2007). Along with type II

arabinogalactans, glucans are also speculated to be present in AGC1 due to the presence of 4-linked glucopyranosyl residues (5.7%). Other minor linkages such as 2-Xylp/4-Xylp and 2-Araf/3-Araf might indicate the presence of small amounts of arabinoxylans in the sample. The predominant glycosyl linkages found in AGC2 are also similar to AGC1 with notable differences in the relative amounts (mol%) of the residues (Table 3.4+Appendix G). This suggested that AGC2 is predominantly composed of type II acidic arabinogalactans along with minor amounts of glucans and arabinoxylans. The higher percentage of terminal residues (>45%) in AGC2 indicate the presence of low molecular weight compounds. Similarly, AGC4 also contains a high percentage of terminal residues (>60%) (Table 3.6+Appendix G). Linkage analysis of AGC4 suggests the presence of the galactan core and the terminal arabinofuranosyl residues of type II arabinogalactans. Interestingly, contrary to the results of the monosaccharide composition analysis, no uronic acid residues were detected in AGC4 in the linkage analysis. Also, there are notable differences in the relative mol% values obtained from monosaccharide composition and linkage analysis of all the samples. These discrepancies might have been caused due to differences in hydrolysis conditions as well as evaporation of the derivatized volatile residues. Overall, we can conclude that AGC1, AGC2, and AGC4 predominantly contain glycosyl residues belonging to type II arabinogalactan polysaccharides. This is the first study on the structural characterization of polysaccharide fractions isolated from NAG suspension cultures. Although, a number of polysaccharides have been previously isolated from mature NAG tissues, the majority of published reports lack important structural information such as glycosyl linkages. Thus far, none of the previously isolated polysaccharides from mature NAG have been

reported to be type II arabinogalactans. However, acidic arabinogalactans (type II) and arabinogalactan proteins have been previously isolated from the suspension culture and tissue culture medium of higher plants such as Echinacea, sycamore, and tobacco (Clarke et al., 1979; Gunter and Ovodov, 2002; Komalavilas et al., 1991; Luettig et al., 1989; Popov et al., 1999). Some of these tissue culture-derived acidic arabinogalactans have shown promising macrophage activating properties in preliminary studies (Luettig et al., 1989; Popov et al., 1999). It will be interesting to see if the fractions isolated in this study have similar immunostimulatory properties.

The glycosyl linkages found in AGC3 were different from the other three fractions. AGC3 contains 2,4-substituted rhamnopyranosyl (8.1%) and 4-substituted galacturonopyranosyl residues (6.8%). These linkages are commonly found in a type of pectic polysaccharide called rhamnogalacturonan I (Table 3.5+Appendix G). Rhamnogalacturonan I is comprised of a backbone made up of alternating 2-linked rhamnose and 4-linked galacturonic acid residues (Yamada and Kiyohara, 2007). The 4-position of the rhamnose is often substituted with a range of neutral and acidic side chains such as arabinogalactans, arabinans, and galactans (Yamada and Kiyohara, 2007). Interestingly, AGC3 contains 4-linked galactans (15.6%) and the core residues of type II arabinogalactans (Table 3.5). A high percentage of terminal-galactopyranosyl residues (47.7%) also indicate the presence of low molecular weight compounds in AGC3. Guo et al., (2015) has previously isolated a pectic polysaccharide fraction containing rhamnogalacturonan I from mature NAG roots. These type of pectic polysaccharides have also been isolated and well-characterized in tissue culture systems of higher plants

such as sycamore (McNeil et al., 1980). Our study is the first to isolate a polysaccharide fraction composed of rhamnogalacturonan I pectins in NAG suspension cultures.

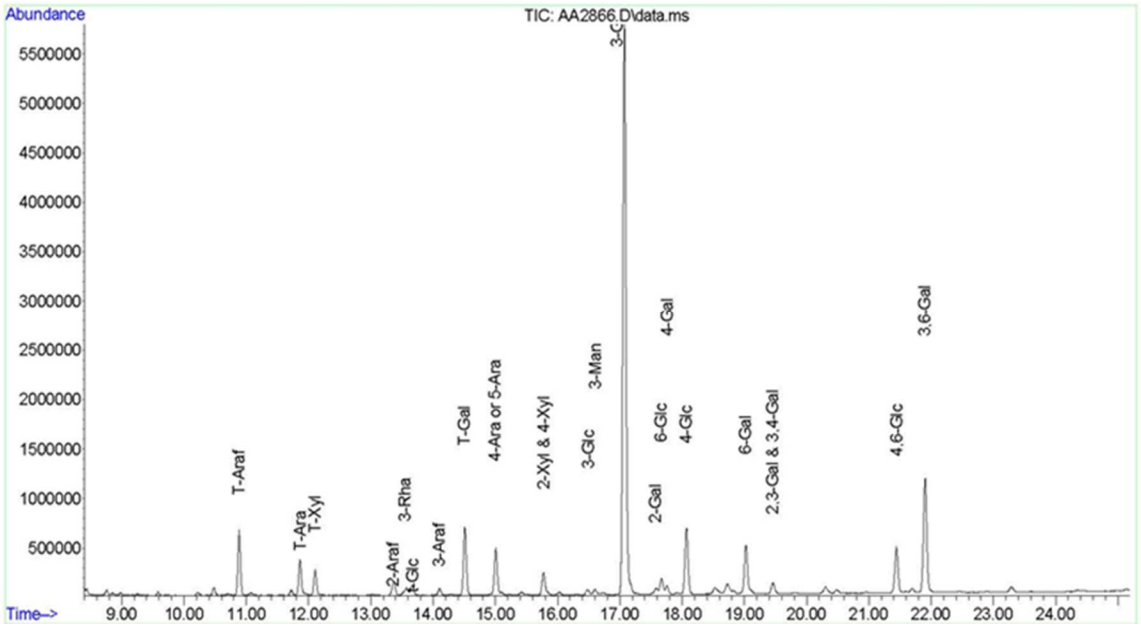

Figure 3.5. Total ion chromatogram of PMAA derivatives of AGC1. The TIC indicates the presence of t-Araf, t-Ara, t-Xyl, 2-Araf, 3-Rha, t-Glc, 3-Araf, t-Gal, 4-Ara or 5-Araf, 2-Xyl or 4-Xyl, 3-Glc, 3-Man, 3-Gal, 2-Gal, 6-Glc, 4-Gal, 4-Glc, 6-Gal, 2,3-Gal or 3,4-Gal, 4,6-Glc and 3,6-Gal residues in AGC1. Residues were identified based on retention times and mass spectra.

Table 3.3. Glycosyl linkages present in AGC1

Monosaccharide	Glycosyl Linkage	Mol %
Ara	Terminal Arabinofuranosyl residue (t-Araf)	4.5
	Terminal Arabinopyranosyl residue (t-Arap)	2.7
	2 linked Arabinofuranosyl residue (2-Araf)	1.2
	3 linked Arabinopyranosyl residue (3-Araf)	0.5
	4 linked Arabinopyranosyl residue (4-Arap) or 5 linked Arabinofuranosyl residue (5-Araf)	4.0
Xyl	Terminal Xylopyranosyl residue (t-Xylp)	1.7
	2 linked Xylopyranosyl residue & 4 Xylopyranosyl residue (2-Xylp & 4-Xylp)	1.9
Rha	3 linked Rhamnopyranosyl residue (3-Rhap)	0.7
Glc	Terminal Glucopyranosyl residue (t-Glcp)	0.7
	3 linked Glucopyranosyl residue (3-Glcp)	0.3
	4 linked Glucopyranosyl residue (4-Glcp)	5.7
	6 linked Glucopyranosyl residue (6-Glcp)	1.3
	4,6 linked Glucopyranosyl residue (4,6-Glcp)	3.8
Gal	Terminal Galactopyranosyl residue (t-Galp)	5.2
	2 linked Galactopyranosyl residue (2-Galp)	0.5
	3 linked Galactopyranosyl residue (3-Galp)	48.5
	4 linked Galactopyranosyl residue (4-Galp)	0.7
	6 linked Galactopyranosyl residue (6-Galp)	4.4
	2,3 linked Galactopyranosyl residue & 3,4 Galactopyranosyl residue (2,3-Galp & 3,4-Galp)	1.0
	3,6 linked Galactopyranosyl residue (3,6-Galp)	10.2
Man	3 linked Mannopyranosyl residue (3-Manp)	0.3

Table 3.4. Glycosyl linkages present in AGC2

Monosaccharides	Glycosyl Linkage	Mol %
Ara	Terminal Arabinofuranosyl residue (t-Araf)	3.6
	Terminal Arabinopyranosyl residue (t-Arap)	1.2
	4 linked Arabinopyranosyl residue (4-Arap) or 5 linked Arabinofuranosyl residue (5-Araf)	1.5
Xyl	Terminal Xylopyranosyl residue (t-Xylp)	1.1
	2 linked Xylopyranosyl residue & 4 Xylopyranosyl residue (2-Xylp & 4-Xylp)	2.2
Rha	2 linked Rhamnopyranosyl residue (2-Rhap)	0.3
	Terminal Rhamnopyranosyl residue (t-Rhap)	0.8
	2, 4 linked Rhamnopyranosyl residue (2,4-Rhap)	0.2
	2, 3,4 linked Rhamnopyranosyl residue (2,3,4-Rhap)	0.1
Glc	Terminal linked Glucopyranosyl residue (t-Glcp)	0.4
	4 linked Glucopyranosyl residue (4-Glcp)	2.3
Gal	Terminal Galactofuranosyl residue (t-Galf)	0.4
	Terminal Galactopyranosyl residue (t-Galp)	41.4
	3 linked Galactopyranosyl residue (3-Galp)	7.0
	4 linked Galactopyranosyl residue (4-Galp)	2.7
	6 linked Galactopyranosyl residue (6-Galp)	22.6
	2,3 linked Galactopyranosyl residue (2,3-Galp)	0.4
	4,6 linked Galactopyranosyl residue (4,6-Galp)	0.4
	3,6 linked Galactopyranosyl residue (3,6-Galp)	8.5
Man	4,6 linked Mannopyranosyl residue (4,6-Manp)	1.6
GlcA	Terminal linked Glucuronopyranosyl residue (t-GlcAp)	1.0
Api	3 linked Apiopyranosyl residue (3-Apiose)	0.2

Table 3.5. Glycosyl linkages present in AGC3

Monosaccharides	**Glycosyl Linkage**	**Mol %**
Ara	Terminal Arabinofuranosyl residue (t-Araf)	3.4
	Terminal Arabinopyranosyl residue (t-Arap)	3.5
	3 linked Arabinofuranosyl residue (3-Araf)	0.2
	4 linked Arabinopyranosyl residue (4-Arap) or 5 linked Arabinofuranosyl residue (5-Araf)	0.7
Xyl	Terminal Xylopyranosyl residue (t-Xylp)	0.1
Rha	2, 4 linked Rhamnopyranosyl residue (2,4-Rhap)	8.1
Glc	Terminal linked Glucopyranosyl residue (t-Glcp)	0.6
	4 linked Glucopyranosyl residue (4-Glcp)	1.4
Gal	Terminal Galactofuranosyl residue (t-Galf)	0.1
	Terminal Galactopyranosyl residue (t-Galp)	47.7
	3 linked Galactopyranosyl residue (3-Galp)	1.1
	4 linked Galactopyranosyl residue (4-Galp)	15.6
	6 linked Galactopyranosyl residue (6-Galp)	8.1
	3,4 linked Galactopyranosyl residue (3,4-Galp)	1.5
	3,6 linked Galactopyranosyl residue (3,6-Gal)	0.2
GalA	4 linked Galacturonopyranosyl residue (4-GalA)	6.8
GlcA	Terminal linked Glucuronopyranosyl residue (t-GlcA)	0.8
	4 linked Glucuronopyranosyl residue (4-GlcA)	0.2

Table 3.6. Glycosyl linkages present in AGC4

Monosaccharides	**Glycosyl Linkage**	**Mol %**
Ara	Terminal Arabinofuranosyl residue (t-Araf)	1.1
	Terminal Arabinopyranosyl residue (t-Arap)	2.1
Xyl	Terminal Xylopyranosyl residue (t-Xylp)	1.1
	4 linked Xylopyranosyl residue (4-Xylp)	1.0
Rha	2 linked Rhamnopyranosyl residue (2-Rhap)	2.7
Glc	Terminal Glucopyranosyl residue (t-Glcp)	2.6
	4 linked Glucopyranosyl residue (4-Glcp)	1.5
Gal	Terminal Galactofuranosyl residue (t-Galf)	9.2
	Terminal Galactopyranosyl residue (t-Galp)	51.9
	3 linked Galactopyranosyl residue (3-Galp)	9.1
	2 linked Galactopyranosyl residue (2-Galp)	3.8
	4 linked Galactopyranosyl residue (4-Galp)	6.8
	6 linked Galactopyranosyl residue (6-Galp)	3.1
	2,3 linked Galactopyranosyl residue & 3,4 linked Galactopyranosyl residue (2,3-Galp & 3,4-Galp)	1.5
	4,6 linked Galactopyranosyl residue (4,6-Galp)	1.7
	3,6 linked Galactopyranosyl residue (3,6-Galp)	0.9

3.2.5. 1D-NMR Spectroscopy

The anomeric conformations of AGC1, one of the most active and pure immunostimulatory fractions, was further determined by 1D-H NMR (Fig. 3.6). The broad nature of the peaks in the spectrum indicates the presence of high molecular weight compounds in the sample. This was consistent with our results of HPSEC and linkage analysis. However, due to the broad peak shapes and the presence of many low abundance sugar residues that have similar chemical shifts, it was not possible to definitely assign and annotate the peaks of the spectrum. Tentative assignments were made based on the linkage analysis results. According to the linkage analysis, almost half (48.5%) of the sample is composed of 3-Galp residues. The two largest peaks in the anomeric region of the spectrum at 5.14 and 4.55 ppm were tentatively assigned to the α- and β-anomeric protons of 3-Galp, respectively. The peaks at 4.95 and 4.48 ppm were tentatively assigned to the α- and β-anomeric protons of the next most abundant residue 3,6-Galp, respectively. The integration of the peaks corresponding to the anomeric protons showed that AGC1 contained 45% α-anomers and 55% β-anomers. Future 2D NMR experiments are necessary to further characterize AGC1 and unambiguously assign the peaks of the 1D spectrum.

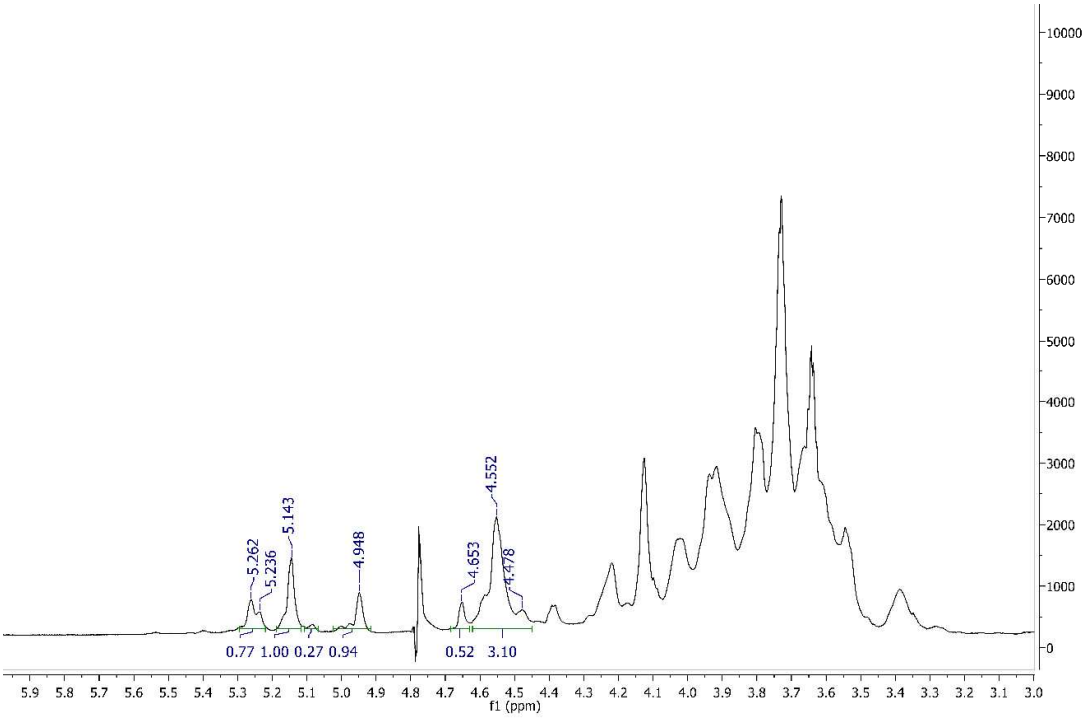

Figure 3.6. 1D-H NMR spectrum of AGC1. The broad nature of the peaks indicates the presence of high molecular weight compounds in AGC1. The group of signals from 4.40-4.6 ppm have been tentatively assigned to the β-anomeric protons of the most abundant residues present in AGC1. The group of signals from 4.9-5.5 ppm have been tentatively assigned to the α-anomeric protons of the most abundant residues present in AGC1. The integration of the peaks corresponding to the anomeric protons showed that AGC1 contained 45% α-anomers and 55% β-anomers.

3.3. Chapter Conclusions

Four polysaccharide fractions (AGC1, AGC2, AGC3, and AGC4) were isolated via anion exchange chromatography from NAG suspension culture tissues. Out of the four fractions, AGC1 showed the highest immunostimulatory activity in preliminary

assays *in vitro.* Further purification by size exclusion chromatography and subsequent HPSEC-RID analysis indicated that AGC1 is a relatively pure fraction (average molecular weight: 5.2 kDa). AGC2, AGC3, and AGC4 were found to be heterogeneous fractions. Monosaccharide composition and glycosyl linkage analysis of all four fractions revealed that AGC1, AGC2, and AGC4 are predominantly composed of type II arabinogalactan polysaccharides. AGC3 was predominantly composed of rhamnogalacturonan I pectic polysaccharide. Although, a 1D-H NMR analysis was carried out, it failed to further elucidate the structural features of AGC1 due to its complexity. Future 2D NMR and sequencing experiments are necessary to completely characterize the polysaccharides. Based on our preliminary bioactivity assessment, it was decided to conduct further dose-dependent *in vitro* and *ex vivo* immunostimulatory bioassays with AGC1 (type II arabinogalactan) and AGC3 (rhamnogalacturonan I pectin). The results of the bioassays are reported in Chapter IV. This is a first of a kind study on the isolation and structural characterization of NAG suspension culture polysaccharides. This study will provide a foundation for future structure-activity relationship studies on NAG tissue culture polysaccharides and their development as potential nutraceuticals and dietary supplements.

CHAPTER IV

IMMUNOSTIMULATORY EFFECTS OF NAG SUSPENSION CULTURE POLYSACCHARIDES

4.1 Background

Panax quinquefolius (NAG) roots are a well-known source of bioactive polysaccharides. Several crude, partially purified, and pure NAG root polysaccharides have shown promising immunomodulatory effects *in vitro* and *in vivo* (Azike et al., 2015; Lemmon et al., 2012; Yu et al., 2017). Proprietary NAG polysaccharide extracts such as CVT-E002 have also been commercialized in the last decade (Biondo et al., 2008). Additionally, there has been an effort to purify and characterize novel immunostimulatory complexes from plants for use as adjuvant and immunotherapeutic agents (Schepetkin and Quinn, 2006). Immunomodulatory polysaccharides have also emerged as a cheaper alternative for endogenous immune system enhancing factors. In spite of their potential application as therapeutics, a few major challenges persist. Batch-to-batch structural variability and presence of bacterial endotoxin in samples is a cause for concern for both research and commercial applications. Structure-activity relationship and mechanistic studies on immunomodulation are still in its initial stages. In order to address some of these issues, the TCBMR at MTSU initiated a project to grow large quantities of NAG tissues via suspension culture. Growth and maintenance of suspension cultures in a controlled and sterile environment allow for the production of natural polysaccharides with consistent structural features and reduced endotoxin content. In Chapter III, the structural features of four polysaccharide fractions isolated from NAG

suspension cultures were reported. The structural analyses revealed that three fractions (AGC1, AGC2, and AGC4) contained glycosyl residues predominantly belonging to arabinogalactan type II polysaccharides and one fraction (AGC3) contained linkages belonging to rhamnogalacturonan I polysaccharide. In this chapter, the *in vitro* and *ex vivo* immunostimulatory activities of AGC1 (arabinogalactan type II) and AGC3 (rhamnogalacturonan I) have been reported. The potential roles of NF-κB (p65) and MAPK (p38) pathways in the immunostimulatory process are also discussed in this chapter.

4.2 Results and Discussion

4.2.1 Cell Viability Assays

The toxicity of NAG suspension culture polysaccharide fractions was tested in RAW 264.7 murine macrophage cells by the MTT assay. All four fractions displayed no potential cytotoxicity *in vitro* (Fig. 4.1). The percentage cell viability of RAW 264.7 cells was determined to be greater than 95% in response to different doses (1, 12.5, 25, and 50 μg/mL) of NAG suspension culture polysaccharide fractions. These results are consistent with other reports highlighting the non-toxic nature and minimal side-effects of plant polysaccharides. The low toxicity of plant polysaccharides is considered to be a major advantage compared to the highly toxic nature of bacterial immunomodulatory polysaccharides and several synthetic immunomodulators (Schepetkin and Quinn, 2006).

4.2.2 Endotoxin Quantification

After processing through the Pierce™ high capacity endotoxin removal resin, the endotoxin content in the polysaccharide samples was determined by the LAL assay. Although, the LAL assay is a widely accepted method for endotoxin quantification in biological samples, it is not always ideal for analysis of carbohydrates as multiple studies have reported cross-reactivity (Mikami et al., 1982; Pearson et al., 1984). However, due to lack of better alternative methods, the LAL assay was used to quantify endotoxin levels in this study. The LAL-reactive material in AGC1 and AGC3 samples that were used for dose-dependent *in vitro* and *ex vivo* immunostimulatory assays were 0.075 ng/μg and 0.2 ng/μg, respectively.

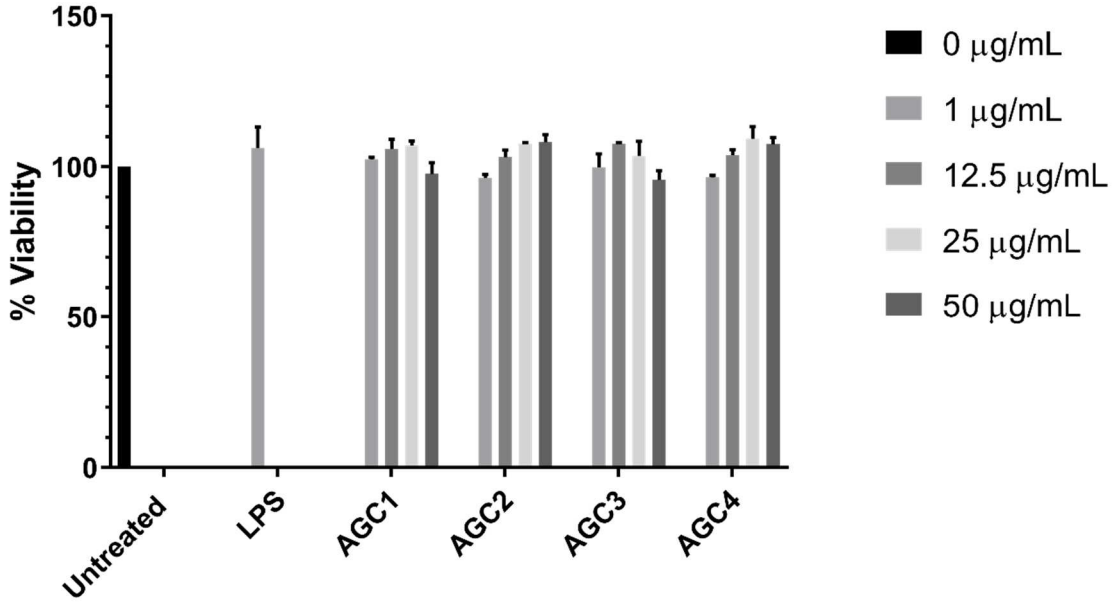

Figure 4.1. Cell viability of RAW 264.7 murine macrophages in response to polysaccharide treatments. Cells were treated with four different concentrations (1, 12.5, 25, and 50 µg/mL) of polysaccharide fractions (AGC1, AGC2, AGC3, and AGC4) for 24 h. Following 24 h treatment, the percentage cell viability was measured using the MTT assay kit (Cayman Chemical Company, USA). Results are expressed as mean ± SEM for three independent experiments.

4.2.3 Comparison of Immunostimulation between Polysaccharides and LPS Treatments in RAW 264.7 Cells

Endotoxin or LPS contamination in polysaccharide samples can lead to false positives in immunostimulatory assays. Hence, it is important to quantify endotoxin levels in samples and determine its potential contribution towards immunostimulation. The approximate endotoxin content in 12.5 µg/mL of AGC1 and AGC3 was estimated to be 0.9375 ng/mL and 2.5 ng/mL, respectively, based on the LAL assay. A comparative immunostimulatory assay was conducted between LPS (1.25 ng/mL or 2.5 ng/mL), AGC1 (12.5 µg/mL), and AGC3 (12.5 µg/mL) in RAW 264.7 cells to assess the contribution of the LPS contaminant in the immunostimulatory bioassays. Proinflammatory cytokines, TNF-α and IL-6, were measured in response to polysaccharide or LPS treatments by ELISA. The production of both TNF-α and IL-6 was significantly higher ($p<0.05$) in AGC1 (12.5 µg/mL) treated cells compared to LPS (1.25 ng/mL) treatments (Fig. 4.2). Similarly, AGC3 (12.5 µg/mL) produced significantly higher amounts of TNF-α compared to LPS (2.5 ng/mL) treatments (Fig. 4.3). The

production of IL-6 was not compared between AGC3 and LPS-treated groups. The significantly higher production of proinflammatory cytokines by the polysaccharides compared to equivalent levels of LPS contaminants suggest that both AGC1 and AGC3 are true immunostimulants.

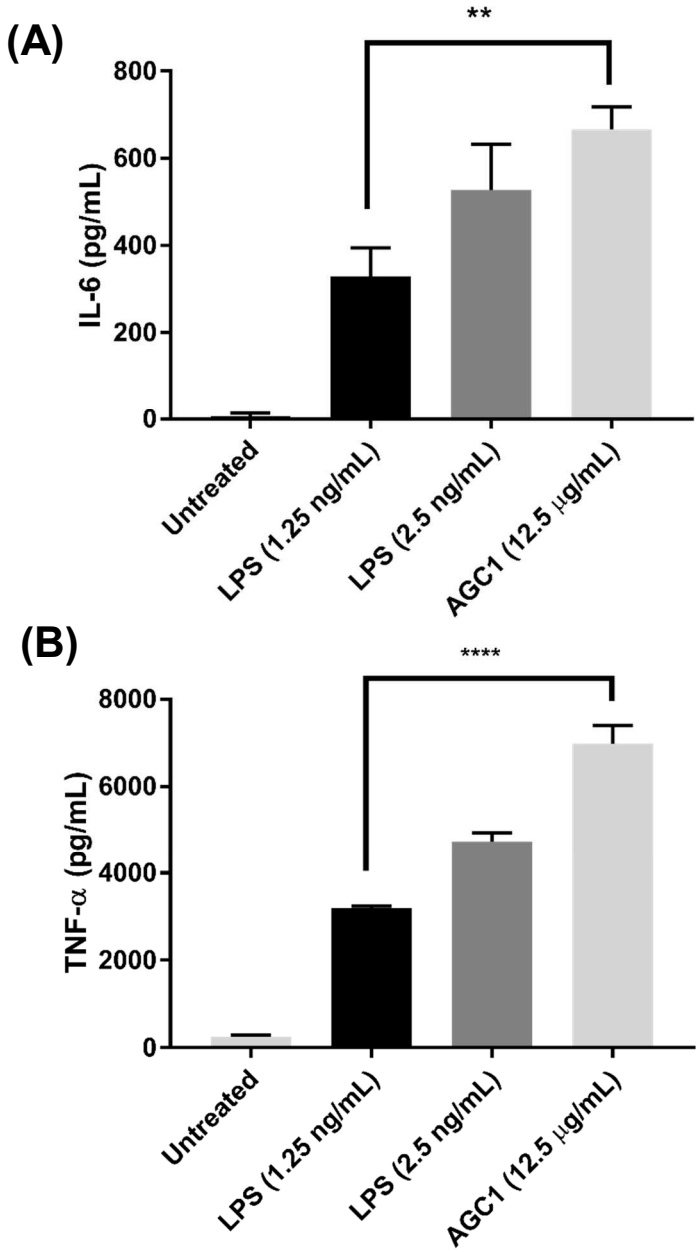

Figure 4.2. Comparative analysis of IL-6 (A) and TNF-α (B) production in response to LPS (1.25 and 2.5 ng/mL) and AGC1 (12.5 µg/mL) treatments in RAW 264.7 cells. Cells were treated with AGC1 or LPS for 24 h. The culture supernatants were then collected and analyzed for the presence of IL-6 and TNF-α by ELISA (R&D Systems, USA). Results are expressed as mean ± SEM for three independent experiments. Statistical significance was reported based on one-way ANOVA followed by Tukey's multiple comparison test (****p<0.000; 1.25 ng/mL of LPS versus AGC1).

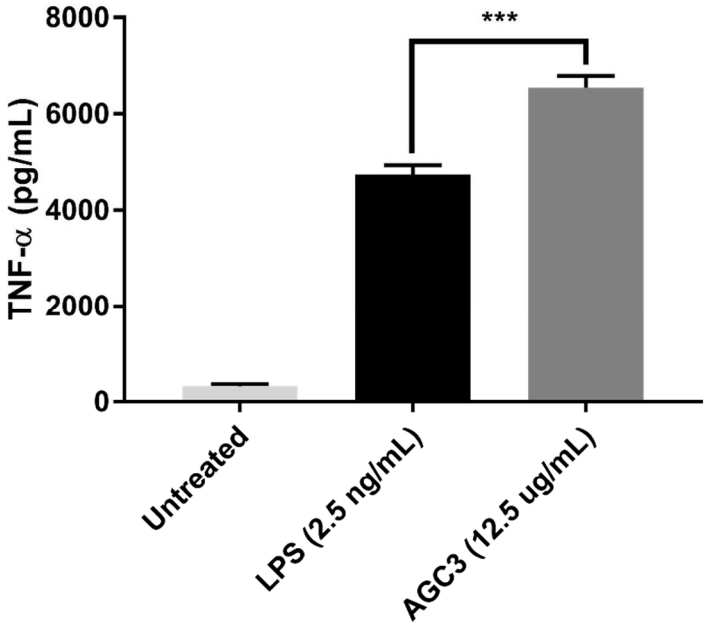

Figure 4.3. Comparative analysis of TNF-α production in response to LPS (2.5 ng/mL) and AGC3 (12.5 µg/mL) treatments in RAW 264.7 cells. Cells were treated with AGC3 or LPS for 24 h. Following 24 h treatments, culture supernatants were collected and analyzed for the presence of TNF-α by ELISA (R&D Systems, USA).

Results are expressed as mean ± SEM for three independent experiments. Statistical significance was reported based on one-way ANOVA followed by Tukey's multiple comparison test (***p<0.001; LPS versus AGC3).

4.2.4 Cytokine Production in RAW 264.7 Cells

Cytokines and chemokines are low molecular weight signaling molecules that serve a variety of functions ranging from regulation of inflammation, cellular proliferation, and tissue repair (Duque and Descoteaux, 2014). Production of proinflammatory cytokines such as TNF-α, IL-1, IL-6, IL-8, and IL-12 in macrophages is considered as a major indicator of an immunostimulatory or inflammatory response (Duque and Descoteaux, 2014). In this study, a panel of mouse cytokines, chemokines and growth factors (IFN-γ, IL-1β, GM-CSF, IL-2, IL-4, IL-6, IL-1β; IL-12 p70, MCP-1, and TNF-α) were analyzed in RAW 264.7 murine macrophages in response to AGC1 and AGC3 treatments. AGC1 (25 μ g/mL) and AGC3 (25 μg/ml) was found to significantly stimulate five (TNF-α, IL-6, MCP-1, GM-CSF, and IL-10) out of the ten cytokine mediators. AGC1 stimulated IL-6 by 150-fold over untreated followed by GM-CSF (64-fold), TNF-α (27-fold), and MCP-1 (9-fold) (Fig. 4.4A). AGC3 stimulated IL-6 by 197-fold over untreated followed by GM-CSF (26-fold), TNF-α (9-fold), and MCP-1 (7-fold) (Fig. 4.5A). The anti-inflammatory cytokine IL-10, which suppresses macrophage activation and proinflammatory response, was also stimulated by 5-fold over untreated in response to both AGC1 and AGC3 treatments (Fig. 4.4A and Fig. 4.5A). The heightened production of IL-10 is important to prevent harmful excessive inflammatory response.

Other cytokines including IL-1β, IFN-γ, IL-2, and IL-4 were either not produced by RAW 264.7 cells or unaffected by polysaccharide treatments. An interesting observation was the difference in trends of cytokine production between polysaccharides and positive control LPS (1 µg/mL) treatments (Fig. 4.4B). The stimulation of IL-6 and GM-CSF by 1 µg/mL of LPS was 1067-fold and 1074-fold over untreated respectively. On the contrary, the increase in the production of IL-6 and GM-CSF by the polysaccharides was <200-fold over untreated. However, the stimulation of TNF-α and MCP-1 by LPS as well as polysaccharides were similar. TNF-α was upregulated 39-fold by LPS and 27-fold by AGC1 at their respective doses. MCP-1 was stimulated 16-fold by LPS and 9-fold over untreated by AGC1. This difference in the trends of cytokine production between polysaccharides and LPS further indicates that the immunostimulatory effects of AGC1 and AGC3 are not due to endotoxin contamination.

The production of TNF-α and IL-6 in response to different doses (1, 12.5, 25, and 50 µg/mL) of polysaccharides was further evaluated *in vitro*. Both AGC1 and AGC3 significantly ($p<0.05$) stimulated TNF-α at doses of 12.5-50 µg/mL (Fig. 4.4C and Fig. 4.5B). TNF-α is a potent pyrogenic cytokine that regulates chemokine release and recruits lymphocytes, neutrophils, and monocytes to the site of inflammation (Duque and Descoteaux, 2014). The stimulation of TNF-α production by the polysaccharides is a major indicator of their immunostimulatory potential. AGC1 also significantly stimulated IL-6 at doses of 25-50 µg/mL (Fig. 4.4D). AGC3 significantly enhanced production of IL-6 only at a higher dose of 50 µg/mL (Fig. 4.5C). IL-6 serves as both proinflammatory and anti-inflammatory cytokine with roles that affect immunity, tissue repair, and

metabolism (Duque and Descoteaux, 2014). Similar to TNF-α, the enhanced IL-6 production is another indicator of the immunomodulatory properties of AGC1 and AGC3.

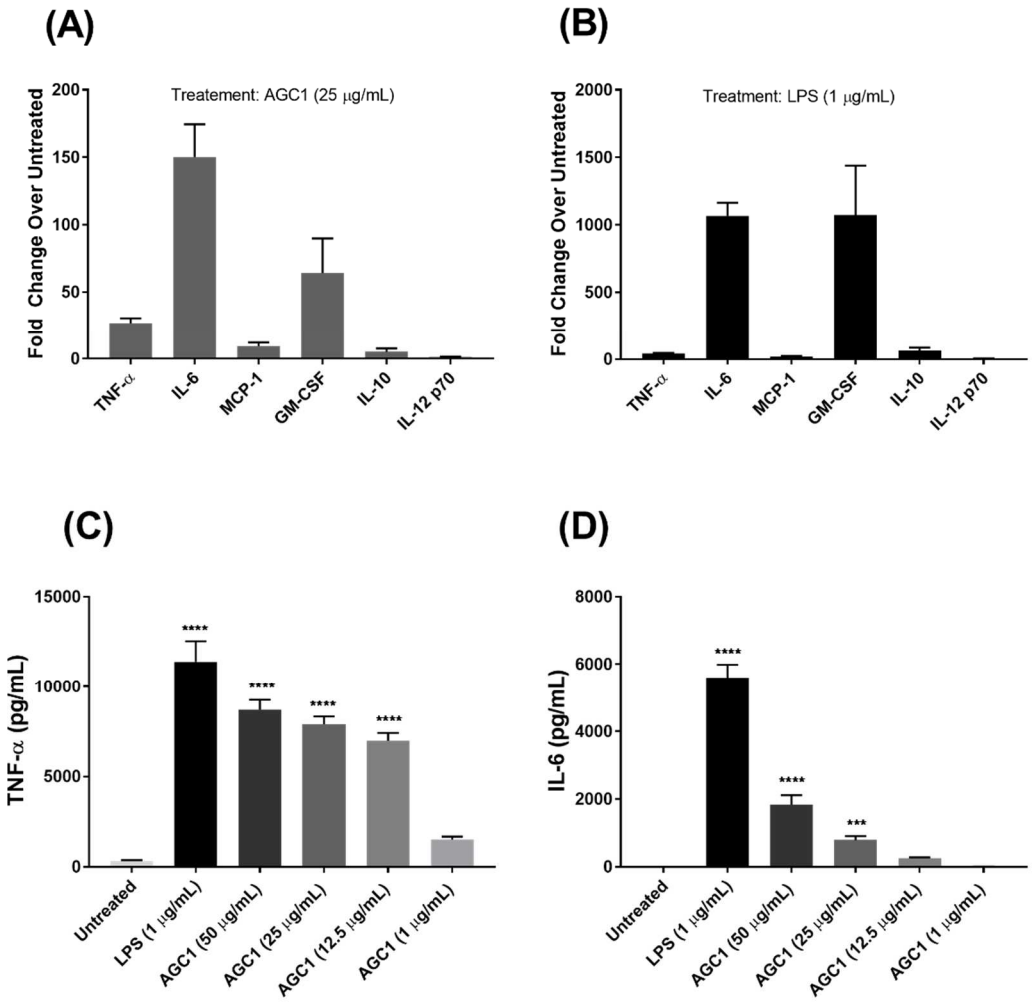

Figure 4.4. Cytokine, chemokine, and growth factor production in response to AGC1 and LPS treatments in RAW 264.7 cells. Cells were treated with the indicated concentrations of AGC1, LPS or culture medium for 24 h. Following 24 h treatment,

culture supernatants were collected and analyzed. (A) and (B) represent a panel of cytokines, chemokines, and growth factors (TNF-α, IL-6, MCP-1, GM-CSF, IL-10, and IL-12 p70) that were stimulated in response to AGC1 (25 μg/mL) and LPS (1 μg/mL), respectively. The panel of mediators was analyzed using a multiplex bead-based assay at Eve Technologies, Canada. (C) and (D) show the production of proinflammatory cytokines TNF-α and IL-6, respectively, in response to different doses of AGC1. TNF-α and IL-6 were analyzed by ELISA (R&D Systems, USA). Results are expressed as mean ± SEM for three independent experiments. Statistical significance was reported based on one-way ANOVA followed by Dunnett's multiple comparison test (****$p<0.0001$, ***$p<0.001$, **$p<0.01$ compared with untreated control group).

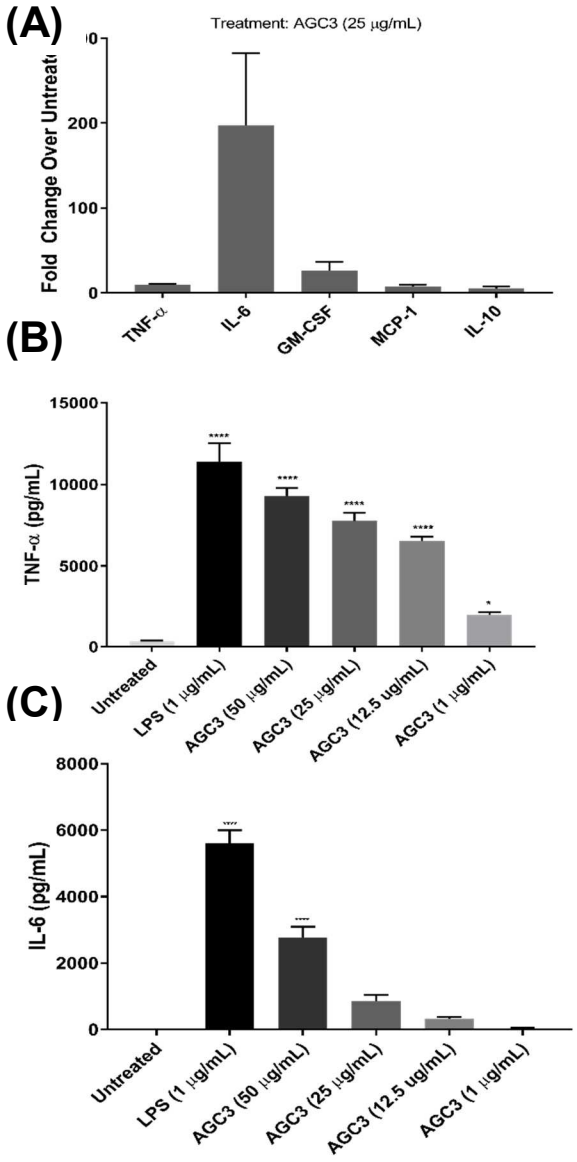

Figure 4.5. Cytokine, chemokine, and growth factor production in response to AGC3 and LPS treatments in RAW 264.7 cells. Cells were treated with AGC3 (25 µg/mL), LPS (1 µg/mL) or culture medium for 24h. Following treatments, culture supernatants were collected and analyzed for the presence of inflammatory mediators. (A) represents a panel of cytokines, chemokines, and growth factors (TNF-α, IL-6, MCP-1, GM-CSF, and IL-10) that were stimulated by AGC3. (B) and (C) represent the

production of TNF-α and IL-6, respectively, in response to various doses of AGC3. Cytokine panel was analyzed using a multiplex bead-based assay at Eve Technologies, Canada. Dose-dependent TNF-α and IL-6 production were analyzed by ELISA (R&D Systems, USA). All results are expressed as mean ± SEM for three independent experiments. Statistical significance was reported based on one-way ANOVA followed by Dunnett's multiple comparison test (****p<0.0001, ***p<0.001, **p<0.01 compared with untreated control group).

4.2.5 NO Production in RAW 264.7 cells

NO, another important mediator of classical macrophage (M1) activation, was analyzed in this study. The function of NO in the immune system is dynamic and it is partly responsible for the tumoricidal and microbicidal properties of M1 macrophages (Bogdan, 2001). NO is derived from the amino acid L-arginine by the catalytic activity of iNOS enzyme, which is encoded by the *NOS2* gene (Bogdan, 2001). In this study, a fluorescent *NOS2* reporter cell line (RAW264.7cells) was used to determine *NOS2* gene expression in response to AGC1 (25 µg/mL) and LPS (1 µg/mL) treatments. The mCherry fluorescence levels 24 h post-treatment was measured and quantified by confocal microscopy (Fig. 4.6A+B). The mCherry fluorescence indicated that both LPS and AGC1 strongly induced *NOS2* gene expression in RAW 264.7 cells. The kinetics of *NOS2* gene expression in the reporter cells was subsequently measured by live cell imaging. The reporter cells treated with AGC1 or LPS were imaged at 30 min intervals for 24 h. The mCherry fluorescence intensity of four representative reporter cells treated

with either LPS or AGC1 is shown in fig. 4.6C. The average mCherry fluorescence intensity in a population of cells (31 individual cells/condition) is shown (Fig. 4.6D). The mCherry expression is noticeable within 10 h after treatment with both compounds. However, the compounds followed different kinetics as the mCherry response diminished after 16 h in AGC1-treated cells. The mCherry fluorescence intensity in LPS-treated cells showed no signs of diminishing even after 24 h. These results indicated that AGC1 was a less potent immunostimulant compared to LPS.

Additionally, iNOS protein expression as well as downstream NO production was measured in response to 24 h AGC1 (25 μg/mL) and LPS (1 μg/mL) treatments in RAW 264.7 macrophages. Both compounds upregulated expression of iNOS after 24 h treatments (Fig. 4.6E). However, higher levels of iNOS was observed in LPS-treated cells, consistent with the results of our transcriptional reporter assays. Nitrite, which serves as an indirect marker of NO production, was measured in culture medium of cells treated with polysaccharides and LPS. AGC1 significantly (25-50 μg/mL) enhanced production of nitrite in a dose-dependent manner (Fig. 4.6F). Similar enhancement of nitrite production was observed due to AGC3 treatments (Fig. 4.7). Overall, the induction of *NOS2* gene, upregulation of iNOS, and NO production indicate M1 macrophage activation in RAW 264.7 cells.

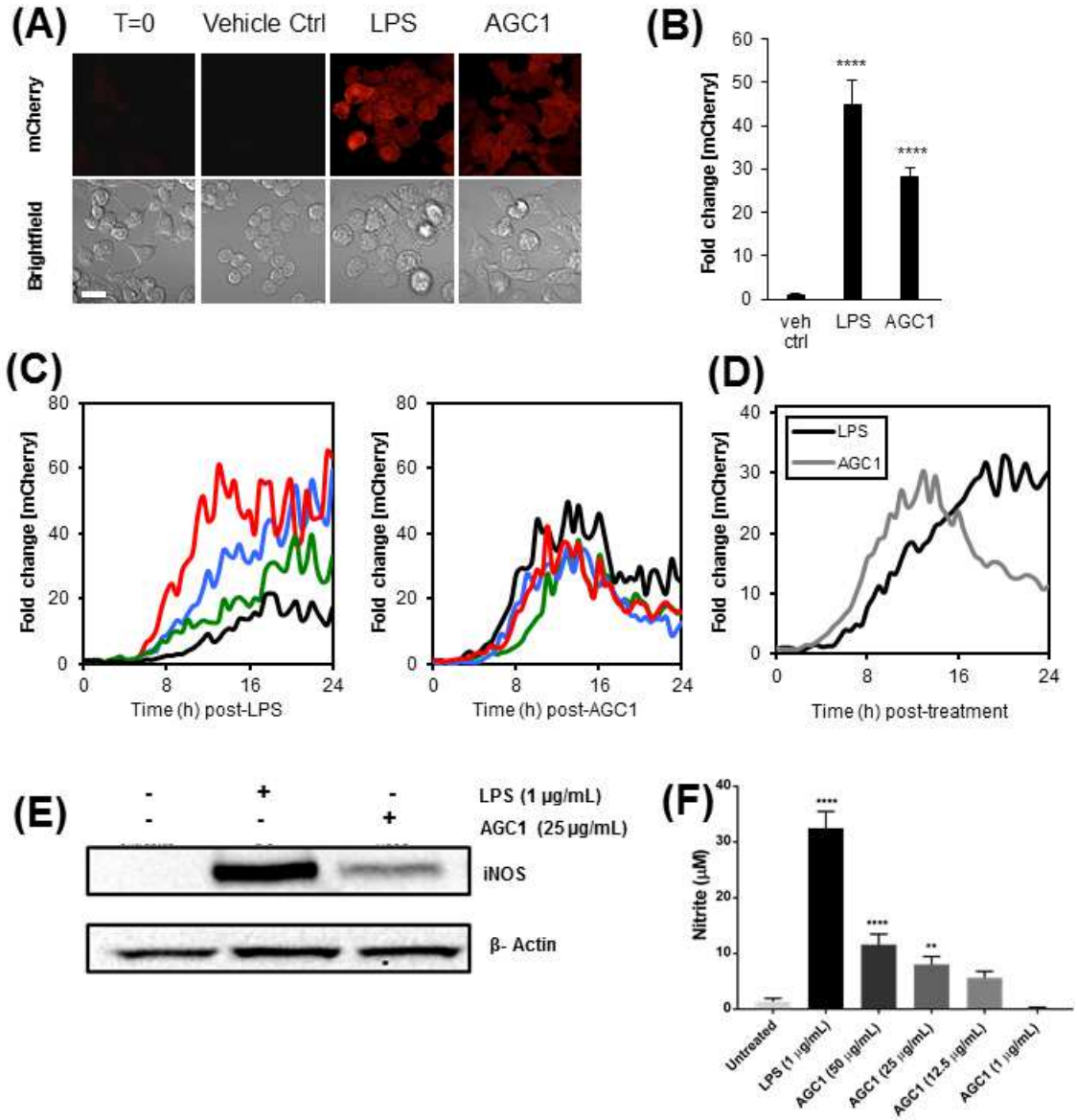

Figure. 4.6. *NOS2* gene expression, iNOS protein expression, and NO production in response to AGC1 treatments in RAW 264.7 murine macrophage cells. (A) shows confocal microscopy images of mCherry fluorescence in live RAW 264.7 *NOS2*-mCherry reporter cells treated with vehicle control, LPS (1 µg/mL), and AGC1 (25 µg/mL) for 24 h. Scale bar = 20 µM. (B) represents quantification of mCherry

fluorescence 24 h post-treatment with vehicle control, LPS, and AGC1. The data was acquired from a minimum of 153 cells across three biological replicates. Results are expressed as mean ± SEM. ****p<0.0001 compared with LPS-treated group as determined using the Kruskal-Wallis/Dunn's multiple comparison test. (C) shows quantification of mCherry fluorescence in four representative reporter cells treated with AGC1 or LPS and imaged at 30 min intervals. (D) represents the average of mCherry fluorescence intensity from a minimum of 31 cells per condition for the experiment depicted in (C). (E) shows the expression of iNOS protein in RAW 264.7 murine macrophages treated with LPS (1 µg/mL) or AGC1 (25 µg/mL) for 24 h. Protein expression was qualitatively measured by western blotting. (F) shows the dose-dependent production of nitrite in RAW 264.7 cells treated with LPS (1 µg/mL) or AGC1 (1, 12.5, 25, and 50 µg/mL) for 24 h. Nitrite production was measured by the modified Griess assay (Sigma Aldrich, USA). Results are expressed as mean ± SEM for three independent experiments. Statistical significance was reported based on one-way ANOVA followed by Dunnett's multiple comparison test (****p<0.0001, ***p<0.001, **p<0.01 compared with untreated control group).

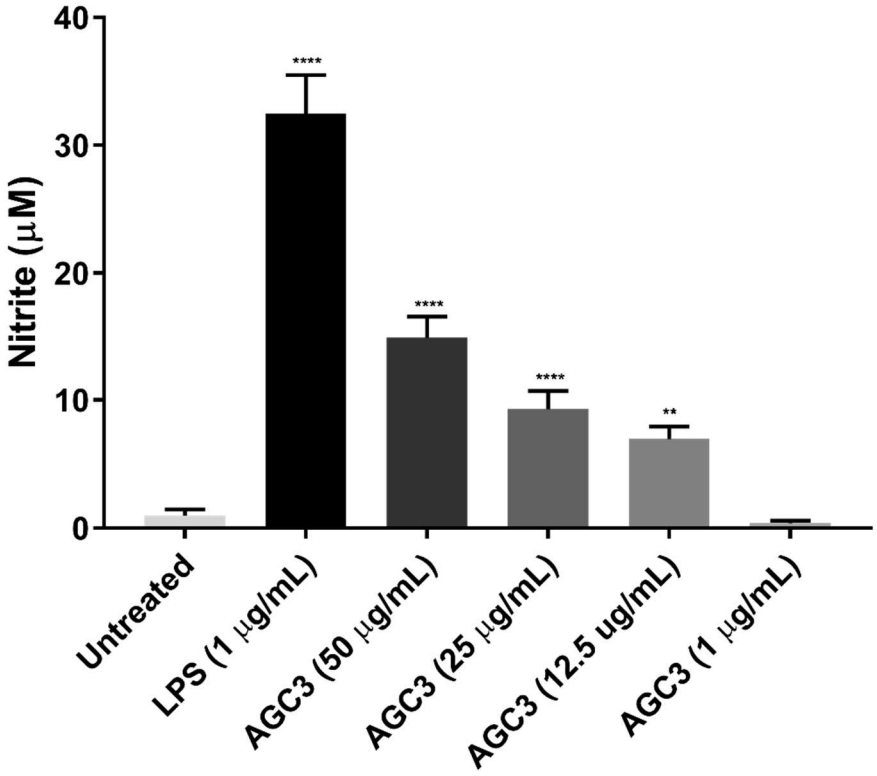

Figure 4.7. Nitrite production in response to AGC3 treatment in RAW 264.7 murine macrophage cells. Cells were treated with AGC3 (1, 12.5, 25, and 50 µg/mL), LPS (1 µg/mL) or culture medium for 24 h. Following treatment, culture supernatants were collected and analyzed for the presence of nitrite by the modified Griess assay (Sigma Aldrich, USA). Results are expressed as mean ± SEM for three independent biological replicates. Statistical significance was reported based on one-way ANOVA followed by Dunnett's multiple comparison test (****p<0.0001, ***p<0.001, **p<0.01 compared with untreated control group).

4.2.6 Production of Proinflammatory Mediators in Primary Murine Splenocytes

The immunostimulatory activity of AGC1 and AGC3 was also tested in primary murine splenocytes *ex vivo.* Splenocytes were harvested from male ICR mice and treated with polysaccharides and controls (LPS and culture medium) for 48 h. Following 48 h treatment, the culture supernatants were analyzed for the presence of a range of cytokine mediators (IFN-γ, IL-1β, GM-CSF, IL-2, IL-4, IL-6, IL-1β; IL-12 p70, MCP-1, and TNF-α). The analyses indicated that both AGC1 (25 μg/mL) and AGC3 (25 μg/mL) stimulated the production of six mediators including TNF-α, IL-6, GM-CSF, IL-10, IL-1β, and IFN-γ *ex vivo* (Fig. 4.8A+4.9A). The highest stimulation was seen in IL-1β production (27-fold over untreated by AGC1 and 20-fold over untreated by AGC3), followed by IL-6 (17-fold by AGC1 and 15-fold by AGC3), TNF-α (19-fold by AGC1 and 12-fold by AGC3), and IL-10 (11-fold by AGC1 and 9-fold by AGC3). Both GM-CSF and IFN-γ were stimulated 3-fold over untreated by AGC1 and AGC3. The stimulation of proinflammatory mediators by 1 μg/mL LPS was noticeably higher compared to both AGC1 and AGC3 (Fig. 4.8B). In LPS-treated splenocytes, the highest stimulation was seen in IFN-γ and IL-10 production (80-fold over untreated) followed by IL-1β (68-fold), IL-6 (54-fold), TNF-α (19-fold), and GM-CSF (8-fold). The degree of immunostimulation by AGC1 and AGC3 was also comparatively lower in primary murine splenocytes compared to the RAW 264.7 cell line. However, it should be noted that the primary splenocytes are a heterogeneous population of cells consisting of mostly macrophages and lymphocytes unlike the RAW 264.7 macrophages. Another interesting observation is the stimulation of IFN-γ by both polysaccharides *ex vivo.* IFN-γ is known

to be a mediator of the Th1 branch of the adaptive immunity (Duque and Descoteaux, 2014). However, further studies need to be carried out to evaluate the effects of AGC1 and AGC3 on adaptive immune response.

The production of two proinflammatory mediators, TNF-α and nitrite, was also measured in response to different doses (1, 12.5, 25, and 50 μg/mL) of AGC1 and AGC3. Both polysaccharides significantly (p<0.05, at doses of 12.5-50 μg/mL; Fig. 4.8C+4.9B). stimulated TNF-α after 48 h treatments. The production of nitrite was also significantly (p<0.05) enhanced by both fractions but only at a higher dose of 50 μg/mL (Fig. 4.8D+4.9C). Overall, the results of the *ex vivo* immunoassays support that AGC1 and AGC3 are potent immunostimulators.

4.2.7 Splenocyte Proliferation

Historically, several plant polysaccharides and glycoproteins (e.g. bupleuran 2IIc and phytohaemagglutanin) have shown proliferative and mitogenic properties (Yamada and Kiyohara, 2007; Nowell, 1960). Proliferation of immune cells is generally considered a hallmark of a mitogen or immunostimulant. Cell proliferation and differentiation of T-cells or B-cells can be trigerred either directly or indirectly in conjunction with cytokines (Schepetkin and Quinn, 2006). Hence, the effects of AGC1 and AGC3 on primary murine splecnocyte proliferation were analyzed *ex vivo.* Splenocyte proliferation was initially tested using the MTT assay that measures the net metabolic activity of cells. Following 48 h treatment with AGC1, AGC3, and ConA (positive control), the relative splenocyte proliferation was measured using the MTT cell proliferation assay kit (Cayman Chemical Company, USA). Both polysaccharides significantly (p<0.05; at doses 12.5-50 μg/mL for

AGC1 and 25-50 µg/mL for AGC3) stimulated proliferation of murine splenocytes *ex vivo* (Fig. 4.10+4.11A). A second method using the Click-iT™ Plus EdU Flow Cytometry Assay Kit (Invitrogen, USA) was used to determine the number of replicating splenocytes in response to AGC3 treatment. EdU is a nucleoside analog that binds to replicating DNA during DNA synthesis. The newly incorporated EdU is conjugated with Alexa Fluor™ 488 picolyl azide by click reaction and analyzed by flow cytometry. Following 48 h treatment, with polysaccharides and controls (LPS and ConA), the number of replicating splenocytes in 12.5 µg/mL AGC3-treated cells was significantly higher compared to untreated (Fig. 4.11B). The number of replicating splenocytes in AGC3-treated cells was not significantly different from ConA (0.5 µg/mL) treated cells. Both AGC3 and ConA treatments were significantly different from LPS (1 µg/mL) treatment. Overall, both MTT assay and the flow cytometry analyses indicate that the polysaccharides can induce proliferation of primary murine splenocytes.

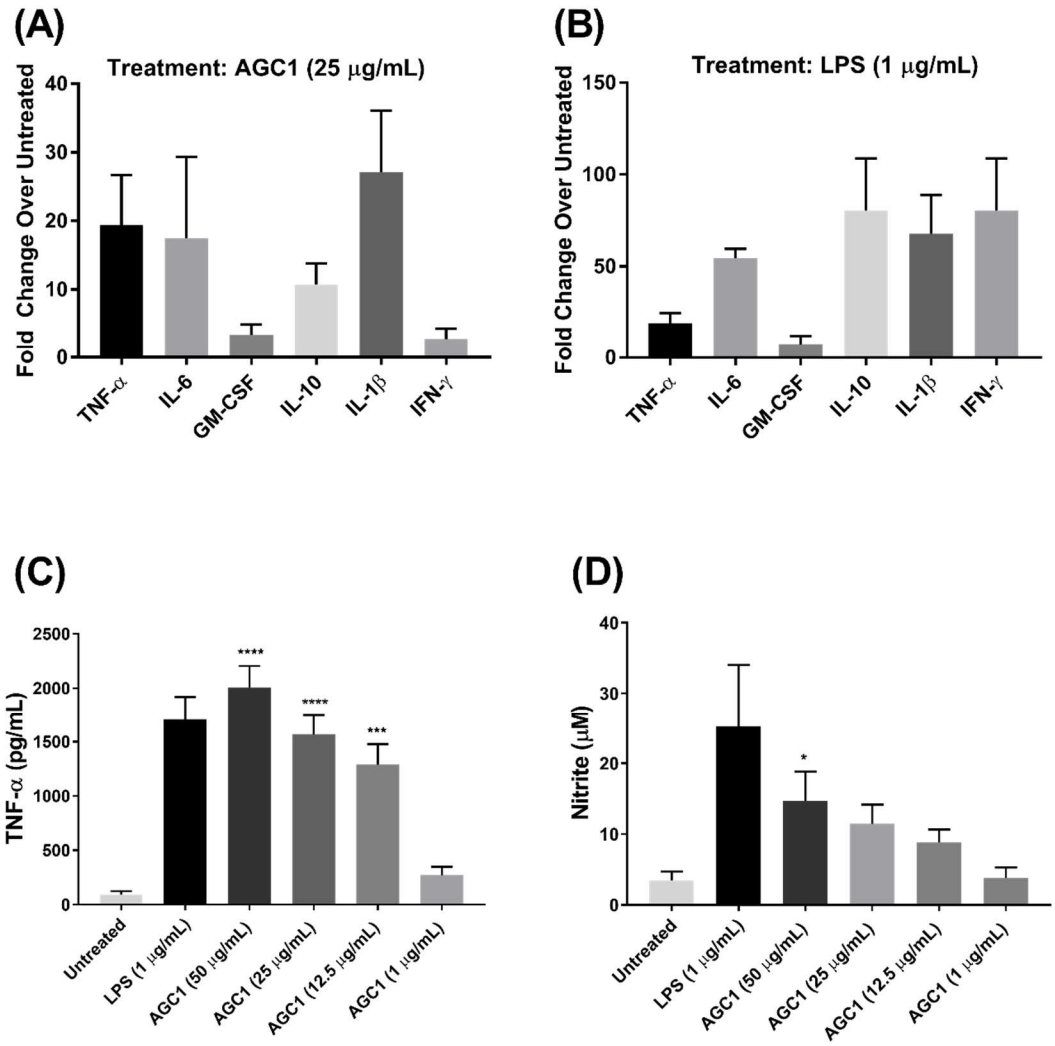

Figure 4.8. Production of inflammatory mediators in response to AGC1 treatments in primary murine splenocytes *ex vivo.* Splenocytes were harvested from male ICR mice, seeded onto 96-well plates and treated with AGC1 (1, 12.5, 25, and 50 μg/mL), LPS (1 μg/mL) or culture medium for 48 h. The culture supernatants were then collected, filtered and analyzed for the presence of inflammatory mediators (IFN-γ, IL-1β, GM-CSF, IL-2, IL-4, IL-6, IL-1β; IL-12 p70, MCP-1, and TNF-α). (A) shows the stimulation (fold change over untreated) of TNF-α, IL-6, GM-CSF, IL-10, IL-β, and IFN-γ in

response to 25 μg/mL AGC1 treatments. (B) shows the stimulation of IL-6, GM-CSF, IL-10, IL-β, and IFN-γ in response to 1 μg/mL LPS (positive control). (C) and (D) represent the dose-dependent stimulation of TNF-α and nitrite in response to AGC1 treatments, respectively. Results are expressed at mean ± SEM for three independent biological replicates. Statistical significance was reported based on one-way ANOVA followed by Dunnett's multiple comparison test (****p<0.0001, ***p<0.001, **p<0.01, *p<0.05 compared with untreated control group).

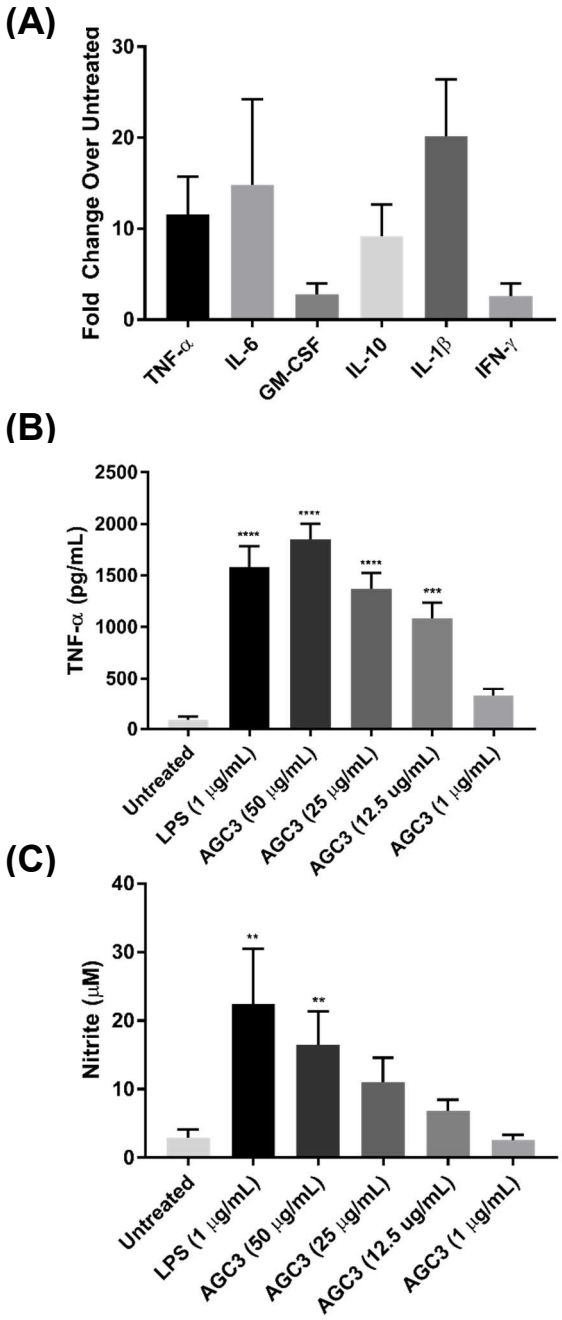

Figure 4.9. Production of inflammatory mediators in response to AGC3 treatments in primary murine splenocytes *ex vivo.* Primary murine splenocytes were treated with AGC3 (1, 12.5, 25, and 50 µg/mL), LPS (1 µg/mL) or culture medium for 48 h.

Following 48 h treatments, culture supernatants were collected, filtered and analyzed for the presence of inflammatory mediators (IFN-γ, IL-1β, GM-CSF, IL-2, IL-4, IL-6, IL-1β, IL-12 p70, MCP-1, and TNF-α). (A) shows the stimulation (fold change over untreated) of TNF-α, IL-6, GM-CSF, IL-10, IL-β, and IFN-γ in response to 25 μg/mL AGC3 treatments. (B) and (C) represent the stimulation of TNF-α and nitrite in response to different doses of AGC3, respectively. Results are expressed at mean ± SEM for three independent biological replicates. Statistical significance was reported based on one-way ANOVA followed by Dunnett's multiple comparison test (****p<0.0001, ***p<0.001, **p<0.01 compared with untreated control group).

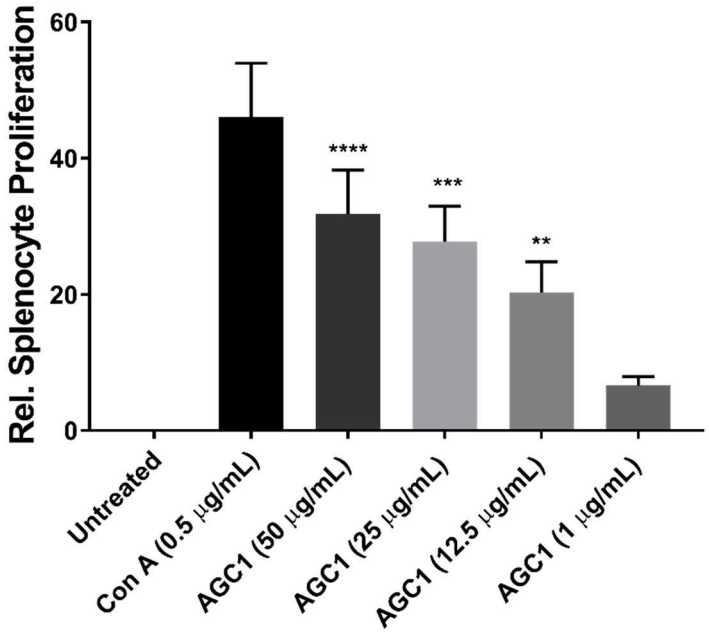

Figure 4.10. Proliferation of murine splenocytes in response to AGC1 treatments. Male ICR mice were sacrificed, splenocytes harvested, seeded onto 96-well plates and

treated with different concentrations (1, 12.5, 25, and 50 µg/mL) of AGC1, ConA (0.5 µg/mL) or culture medium for 48 h. Following treatment, splenocyte proliferation was determined by the MTT assay. The following equation was used to calculate relative splenocyte proliferation: RSP= $[(Abs_{sample}/Abs_{untreated\ control})\ X\ 100] - 100$. The results are expressed as mean ± SEM for three independent replicates. Statistical significance was reported based on one-way ANOVA followed by Dunnett's multiple comparison test (****$p<0.0001$, ***$p<0.001$, **$p < 0.01$ compared with untreated control group).

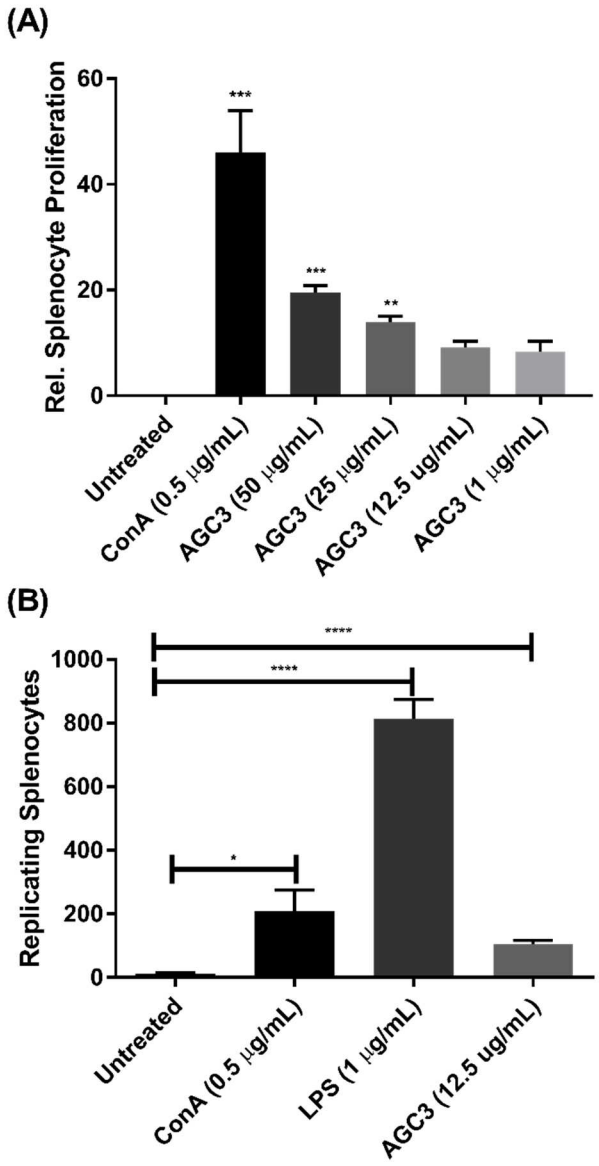

Figure 4.11. Proliferation of murine splenocytes in response to AGC3 treatments. Splenocytes were harvested from male ICR mice, seeded onto 96-well plates and treated with different concentrations (1, 12.5, 25, and 50 μg/mL) of AGC3, ConA (0.5 μg/mL), LPS (1 μg/mL) or culture medium for 48 h. Following 48 h treatment, splenocyte proliferation was analyzed by the MTT assay and the Click‑iT™ Plus EdU Flow

Cytometry Assay. (A) represents the dose-dependent relative splenocyte proliferation as determined by the MTT assay. Relative splenocyte proliferation was calculated based on the following equation: RSP= [(Abs_{sample}/$Abs_{untreated\ control}$) X 100] – 100. The results are expressed as mean ± SEM for three independent replicates. Statistical significance was reported based on one-way ANOVA followed by Dunnett's multiple comparison test (****p<0.0001, ***p<0.001, **p< 0.01 compared with untreated control group). (B) represents the number of replicating splenocytes as determined by the Click-iT™ Plus EdU Flow Cytometry Assay. The number of EdU positive cells was then determined using 488 nm laser of the Guava® easyCyte™ HCT flow cytometer. Results are expressed as mean ± SEM for three independent replicates. Statistical significance was reported based on unpaired Student's t-test (****p<0.0001, *p<0.05; Untreated versus ConA, Untreated versus LPS and Untreated versus AGC3).

4.2.8 Putative Mechanisms of Macrophage Activation by AGC1 and AGC3

Two major pathways that regulate the expression of proinflammatory cytokines, chemokines, and iNOS are MAPK (e.g. p38) and NF-κB (e.g. p65) signaling pathways (Schepetkin and Quinn, 2006). Plant polysaccharides are speculated to bind to TLR and C-type lectin receptors that can potentially lead to the activation of these intracellular signaling cascades. Since both AGC1 and AGC3 stimulated several proinflammatory mediators including TNF-α, IL-6, and iNOS/NO, it was decided to test the roles of canonical NF-κB (p65) and MAPK (p38) transcription factors following AGC1 or AGC3 treatment. To determine the roles of the two pathways in macrophage activation, RAW

264.7 cells were pre-treated with Bay11-7082, a known inhibitor of NF-κB pathway or SB202190, a known inhibitor of p38 MAPK pathway, prior to stimulation with AGC1 and AGC3. The resultant production of TNF-α was reduced by 21% ($p<0.05$) due to BAY11-7082 (5 μM) pre-treatment and 25% due to SB202190 (30 μM) pre-treatment in AGC1-treated cells (Fig. 4.12). The production of TNF-α was also reduced 11% due to BAY11-7082 (5 μM) pre-treatment and 22% ($p<0.05$) due to SB202190 (30 μM) pre-treatment in AGC3-treated cells (Fig. 4.12). The results indicate that both p65 NF-κB and p38 MAPK transcription factors are partially responsible for the murine macrophage activation and expression of proinflammatory mediators. There is a possibility of significant crosstalk between NF-κ B and MAPK pathways that lead to the immunostimulation. Future studies will focus on the mechanism by which the two polysaccharides activate NF-κB and MAPK pathways. The roles of other MAP kinases such as ERK, PI3K and c-Jun N-terminal kinase (JNK) in the immunostimulatory process will also provide information regarding putative mechanisms of action.

Several researchers have attempted to identify specific cell surface receptors on immunocompetent cells that bind to plant polysaccharides. Toll-like receptors and C-type lectin receptors have been identified as the most promising candidates thus far (Yamada and Kiyohara, 2007). Due to the presence of high percentage of galactose in the non-reducing terminals of side chains in both AGC1 and AGC3, there is a possibility that the β-D-galactose-recognizing mammalian lectin, galectin-3 can be a potential candidate receptor for these compounds. Interestingly, there are at least fourteen different galectins that are currently known to be β-galactoside-binding lectins in humans (Yamada and

Kiyohara, 2007). Our future studies will attempt to identify such carbohydrate-binding lectins in macrophages that can bind to AGC1 and AGC3.

4.2.9. Arabinogalactans and Pectins as Immunomodulators

Based on our structural analysis, AGC1 is predominantly composed of arabinogalactan type II polysaccharide. Arabinogalactan type II polysaccharides isolated from several plant species such as *Anadenanthera colubrine* (Moretao et al., 2004), *Artemisia tripartite* (Xie et al., 2008), *Entada africana* (Diallo et al., 2001), *Echinacea purpurea* (Luettig et al., 1989; Wagner et al., 1988) and *Euterpe olerácea* (Holderness et al., 2011) have previously shown complement fixing as well as macrophage activating properties. Classical type II arabino-3,6-galactans and not arabino-4-galactans (type I) have been suggested to be representative immunomodulatory polysaccharides of plant origin (Yamada and Kiyohara, 2007). It has been previously speculated that the galactan cores of arabinogalactan type II polysaccharides have complement fixation activity (Yamada and Kiyohara, 2007). Other studies on arabinogalactan type II have shown that the arabinosyl side-chains stimulate macrophages (Peng et al., 2016). However, these studies are still preliminary and future research focusing on enzymatic or mild acid hydrolysis of arabinogalactans such as AGC1 will help in the identification of specific bioactive glycan moieties.

The polysaccharide fraction AGC3 contains glycosyl linkages commonly found in a type of pectin called rhamnogalacturonan I. Immunomodulatory pectic (rhamnogalacturonan I) polysaccharides similar to AGC3 have also been isolated from *Avicennia marina* (Fang and Chen, 2013) and *Centella asiatica* (Wang et al., 2005).

Similar to the type II arabinogalactans mentioned earlier, pectins have also shown complement fixing, mitogenic, and macrophage activating properties. Interestingly, pectins are structurally related to arabinogalactans. The rhamnogalacturonan backbone of pectins are often substituted with neutral sugar-rich side chains such as arabinogalactans. There is a possibility of common active glycosyl moieties present in both the classes of polysaccharides. Additionally, the rhamified regions of pectins have been reported by Yamada and Kiyohara, (2007) to possess immunomodulatory properties. Similar to AGC1, future efforts will focus on the enzymatic breakdown and mild acid hydrolysis of AGC3 into oligosaccharides. The short chain oligosaccharides will be used to evaluate *in vitro* macrophage activating effects to identify active glycan moieties.

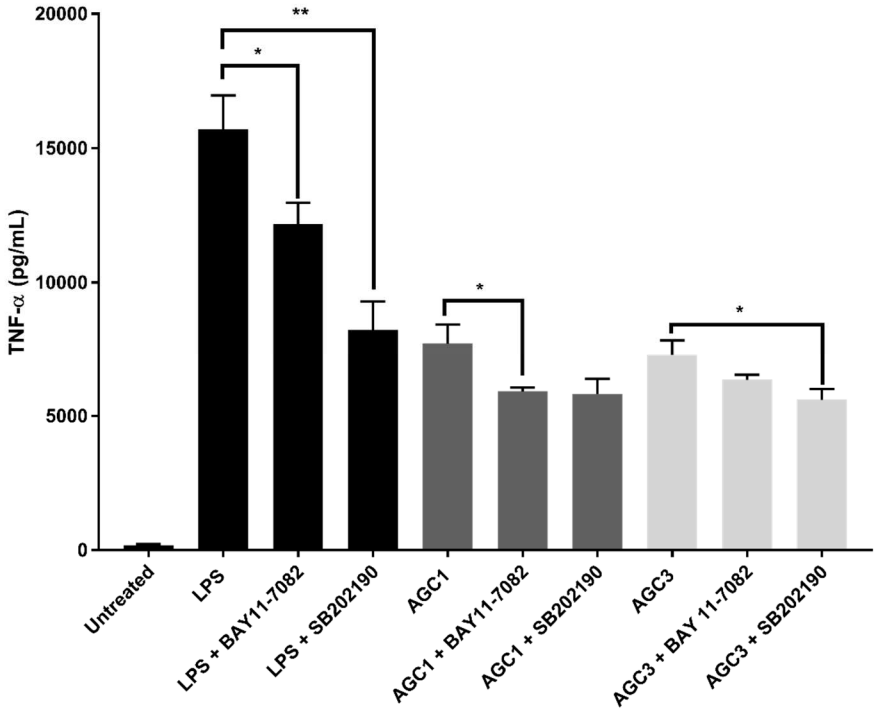

Figure 4.12. Activation of NF-κB (p65) and MAPK (p38) by AGC1 and AGC3 in RAW 264.7 cells. Cells were pre-treated with BAY11-7082 (5 μM) or SB202190 (30 μM) for 1 h prior to stimulation with 12.5 μg/mL of polysaccharides or 1 μg/mL of LPS for 4 h. Following treatment, culture supernatants were collected and analyzed for the production of TNF-α by ELISA. Results are expressed as mean ± SEM for three independent replicates. Statistical significance was (*p<0.05, **p<0.01) (LPS versus BAY11-7082+LPS; LPS versus SB202190+LPS; AGC1 versus BAY11-7082+AGC1; AGC1 versus SB202190+AGC1; AGC3 versus BAY11-7082+AGC3 and AGC3 versus SB202190+AGC3) was determined using a non-parametric Mann-Whitney's U- test.

4.3. Chapter Conclusions

The results of this chapter indicate that both AGC1 (predominantly composed of arabinogalactan type II polysaccharides) and AGC3 (predominantly composed of rhamnogalacturonan I polysaccharide) can activate murine macrophages and splenocytes *in vitro* and *ex vivo*. Both fractions stimulated several proinflammatory mediators including NO, TNF-α, IL-6, and GM-CSF in RAW 264.7 murine macrophage cell line and primary murine splenocytes. The kinetics of *NOS2* gene induction showed that AGC1 was a less potent immunostimulator compared to LPS. The polysaccharides also stimulated splenocyte proliferation indicating potential mitogenic properties. The results also indicate the potential roles of NF-κB (p65) and MAPK (p38) pathways in the immunostimulatory process. This study can serve as the foundation for more research on putative mechanisms of action. Although, the results suggest macrophage activation and

induction of innate immune response by AGC1 and AGC3, further research needs to be conducted on the polysaccharide's impact on the adaptive immune response. Overall, it can be concluded that NAG suspension cultures can be a source of bioactive polysaccharides with reduced endotoxin content. The production of polysaccharides using this approach might provide new avenues for commercial applications. It can be concluded that polysaccharide fractions AGC1 and AGC3 can be potentially used as an adjuvant or nutraceutical either by itself or in combination with other natural health products.

CHAPTER V

HPLC WITH CHARGED AEROSOL DETECTOR (CAD) AS A QUALITY CONTROL PLATFORM FOR ANALYSIS OF CARBOHYDRATE POLYMERS

Ghosh, R.; Kline, P. HPLC with charged aerosol detector (CAD) as a quality control platform for analysis of carbohydrate polymers. *BMC Res. Notes* 2019 *12*(1), 268.

doi: 10.1186/s13104-019-4296-y

5.1. Introduction

Carbohydrates have become increasingly important commercially not only as food or structural building blocks, but also as natural health products (Li et al., 2013). It is essential to have proper QC of carbohydrate-based therapeutics to ensure their efficacy and safety. Physicochemical properties such as homogeneity, size, and composition serve as important QC parameters for carbohydrates (Li et al., 2013). The QC process is often time-consuming and expensive due to the lack of a single platform capable of analyzing necessary parameters. Analysts rely on laborious derivatization procedures and complementary analytical instrumentation to test products. These problems underline the need for a simple multipurpose platform for rapid QC of carbohydrates.

Analysis of complex carbohydrates has been historically challenging due to their heterogeneity and diversity (Li et al., 2013). Additionally, monosaccharide composition analysis can be tricky due to the presence of epimers, formation of anomers, and lack of a chromophore (Ikegami et al., 2008). Common analytical techniques (GC-MS and reverse phase HPLC) for composition analysis require appropriate derivatization of monosaccharides (Ruiz-Matute et al., 2011; Yang et al., 2005) As a result analysis of

underivatized monosaccharides is becoming increasingly popular. High performance anion exchange chromatography with pulsed amphoteric detection (HPAEC-PAD) has proven to be an effective tool for direct analysis of monosaccharides in recent years (Zhang et al., 2012). However, the high pH of the eluent resulting in epimerization and degradation of carbohydrates, unstable baseline, loss of sensitivity, and requirement of a dedicated base-compatible HPLC are some of its disadvantages (Mariño et al., 2010). Hydrophilic interaction liquid chromatography (HILIC) coupled to evaporative light scattering detector (ELSD), mass spectrometer (MS), refractive index detector (RID), and charged aerosol detector (CAD) offer other alternate ways of analyzing underivatized carbohydrates (Godin et al., 2011; Ikegami et al., 2008; Karlsson et al., 2005; Lowenthal et al., 2015; Yan et al., 2016). The CAD, introduced by Dixon and Peterson, (2002), offers several advantages compared to other detectors used in the direct analysis of sugars. The response of CAD does not depend on the structural properties of the analyte and it offers greater sensitivity than ELSD (Hu et al., 2013). It is compatible with gradient elution and allows detection of all non-volatile and most semi-volatile analytes (Ligor et al., 2013). It is also relatively cheap and easy to use compared to MS. Hence, HILIC coupled with CAD can be an excellent tool for direct composition analysis and detection of impurities in samples. Although, neutral sugars have been previously separated using HILIC-CAD, there has not been any reports on the analysis of acidic and amino sugars.

In this study, a method has been developed to separate and detect amino sugars (GlcN, GalN, and GlcNAc) and acidic sugars (GlcA, GalA, Neu5Ac, and LIdoA) without derivatization using HILIC-CAD. Commonly found N-linked neutral sugar residues in

mammalian glycoproteins such as LFuc, Gal, and Man were also simultaneously separated. As an application of our proposed QC platform, we analyzed the monomer composition of commercially available hyaluronic acid (HA) products.

CAD has also been shown to be effective in size exclusion chromatography (SEC) with better impurity and polydispersity profiles compared to RID and ELSD (Kou et al., 2009). Therefore, SEC-CAD can be potentially employed for homogeneity and molecular weight analysis of carbohydrates. In this study, we demonstrated the homogeneity of commercially purchased HA products using a SEC-CAD method adapted from Chen et al., 2018.

5.2. Material and Methods

5.2.1. Material and Reagents

All standards, solvents, and buffer additives were of HPLC grade (Sigma Aldrich, Synthose Inc., and Fisher Scientific). HA supplements were purchased from local supermarkets.

5.2.2. Separation of Monosaccharides by HILIC-CAD

A Dionex Ultimate 3000 HPLC system coupled to a Corona charged aerosol detector was used for the chromatographic analysis. Separation was carried out using a Waters XBridge BEH Amide XP (3 X 150 mm; 2.5 µm) column. The mobile phase of the optimized method consisted of (A) 90% acetonitrile with 0.2% TEA and 25 mM ammonium acetate; and (B) water with 0.2% TEA and 25 mM ammonium acetate. The following gradient elution was used: 0% B at 0-15 min, 0-18% B at 15-40 min, 18% B at

40-45 min, 18-0% B at 45-47 min, and 0% B at 47-55 min. The flow rate was 0.5 mL/min. A column temperature of 50ºC and an injection volume of 10 µL (mixed standard monosaccharide solution at a concentration of 225 µg/mL) was used for the analysis. The effects of column temperature (50°C, 40°C, and 30°C) and buffers such as ammonium acetate (25 mM and 20 mM), ammonium formate (25 mM and 20 mM) and triethylamine (TEA) (0.2% and 0.1%) on chromatographic separation were evaluated. The following parameters were used for the CAD detector: i) nitrogen gas pressure: 35 psi; ii) detector response 100 pA; and iii) noise filter: high. Data processing was carried out using Chromeleon 6.8 software.

5.2.3. Validation

Seven different concentrations (15–1000 µg/mL) of the standards were injected in triplicate to construct a double logarithmic plot, which was used as a calibration curve (Li et al., 2014). The limit of detection (LOD) and limit of quantification (LOQ) was calculated based on previously reported methods (Khoomrung et al., 2013; Li et al., 2014). Intra-day precision (%RSD) was determined by repeating the analysis of a standard solution five times in a single day. Inter-day precision (%RSD) analysis was performed over 3 days.

5.2.4. Application of HPLC-CAD as a QC Platform

The monosaccharide composition of commercially purchased HA products were analyzed to demonstrate the application of the HILIC-CAD method. Samples (> 5 mg) were hydrolyzed using 2 mL of 2 M trifluoracetic acid (TFA) at 110°C for 2 h prior to composition analysis.

The homogeneity of HA was also analyzed by a separate high performance size exclusion chromatography (HPSEC) experiment. GPC grade HA standards and commercially purchased samples were analyzed on a TOSOH TSKgel G4000PW$_{xl}$ (7.8 X 300 mm; 10 μm) column for 35 min. Ammonium acetate (25 mM) at a flow rate of 0.5 mL/min was used as the eluent. A volume of 10 μL of sample was injected into the column. The CAD parameters were the same as before.

5.3. Results and Discussion

5.3.1. Separation of Monosaccharides by HILIC-CAD

The gradient method was able to separate uronic acids (GlcA, GalA, Neu5Ac, and LIdoA) and amino sugars (GlcN, GalN, and GlcNAc) as well as select neutral sugar residues (LRha, LFuc, Man, and Gal) (Fig. 5.1). The deoxy monosaccharides eluted first followed by acetylated amino sugars, aldohexoses, amino sugars, and uronic acids. This method can be potentially adapted for the monosaccharide composition analysis of other acidic/amino sugar-rich polysaccharides such as glycosaminoglycans and N-linked sugar residues found in mammalian glycoproteins.

A major problem in analyzing monosaccharides is the formation of α and β anomers resulting in split peaks. Addition of tertiary amines in the mobile phase, high temperature and high pH are common ways to increase the rate of the interconversion of anomers (Tanaka et al., 2003; Yan et al., 2016). During method development, different column temperatures (30°C, 40°C, and 50°C) (Appendix J) and concentrations of TEA in the mobile phase (0.1% and 0.2%) (Appendix K) were used to suppress split peaks. Although, temperatures below 30°C were able to separate most monosaccharides, it

produced anomeric peak doublets (data not shown). Column temperature of 50°C was able to adequately separate acidic and amino sugars along with select neutral sugars without formation of split peaks (Fig. 5.1). Addition of TEA in the mobile phase was also found to enhance mutarotation rates to yield single peaks (Appendix K). A concentration of 0.1% TEA was found to be sufficient to suppress peak doublets for most monosaccharides except mannose (Appendix K). Hence, a combination of 0.2% TEA and 50°C column temperature was chosen for the optimized method. Higher concentrations of TEA (> 0.2%) or high pH (>10) caused substantial detector noise and unstable baseline. Apart from tertiary amines, we also tested the effects of ammonium acetate (Appendix K) and ammonium formate (data not shown), on separation. Ammonium formate gave a slightly higher detector response compared to ammonium acetate (data not shown). However, ammonium acetate gave a more stable baseline and was subsequently chosen as the buffer of choice. Although, higher ammonium acetate concentrations increased retention times, it also resulted in better separations (Appendix L). Ammonium acetate concentrations above 25 mM led to high detector noise.

The optimized method was validated by evaluating linearity, LOD, LOQ and intra and inter-day precision of peak areas (Appendix I). After double logarithmic transformation, the calibration curves of 11 analytes showed good linearity (>0.99). The LOD and LOQ values were in the range of 50-83 ng/mL and 170-278 ng/mL respectively, which were higher compared to earlier studies involving neutral sugars (Li et al., 2014; Yan et al., 2016). The higher LOD and LOQs reported in this study might be due to the higher concentrations of ammonium acetate (25 mM) and TEA (0.2%) in the

mobile phase. The results indicated satisfactory intra and inter-day precision of peak areas (1-8 % RSD).

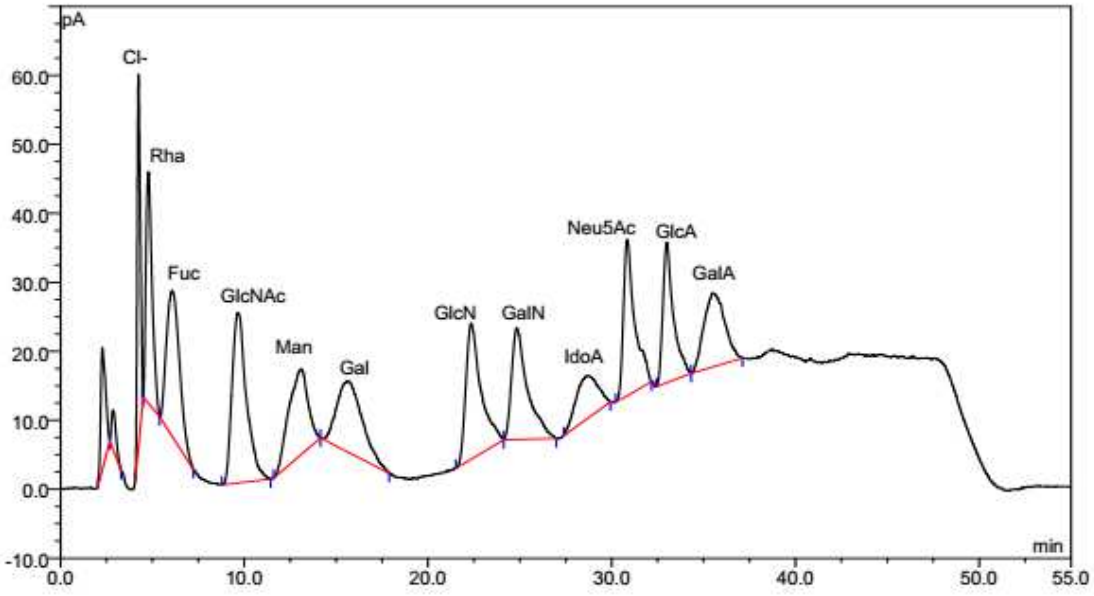

Figure 5.1. Separation of monosaccharides by HILIC-CAD. The HILIC-CAD gradient method was able to separate a mixture of 11 monosaccharide standards (225 µg/mL) (Rha, Fuc, GlcNAc, Man, Gal, GlcN, GalN, IdoA, Neu5Ac, GlcA, and GalA) in this study. Buffer additives of 25 mM ammonium acetate and 0.2% TEA and a column temperature of 50°C were used for the HPLC analysis.

5.3.2. HPLC-CAD as a QC Platform

5.3.2.1 Monomer Composition of Hyaluronic Acid

The glycosaminoglycan HA, a widely used dietary supplement, was used to demonstrate the utility of HPLC-CAD as a QC platform. HA is composed of a repeating

disaccharide unit made up of GlcNAc and GlcA (Necas et al., 2008). The HILIC-CAD gradient method was used to analyze the composition of a HA standard and a commercially available HA product (Fig. 5.2). Fig. 5.2A shows the chromatogram of GlcNAc and GlcA standards treated with 2 M TFA at 110°C for 2 h. The breakdown of GlcNAc into GlcN is evident from the chromatogram. Fig. 5.2B represents a chromatogram of NaCl solution treated under the same conditions as in fig. 5.2A. The HA standard used in our study was a sodium salt. Since CAD is a quasi-universal detector, it is likely that sodium and chloride ion peaks would show up in the chromatograms. The respective sodium and chloride ion peaks are visible in fig. 5.2B. Fig. 5.2C shows the chromatogram of an acid hydrolyzed HA standard. The chromatogram indicates the presence of GlcN, GlcA, sodium, chloride, and minor amounts of GlcNAc. The unknown peak is likely to be a disaccharide unit of GlcNAc and GlcA. Fig. 5.2D shows the chromatogram of an acid hydrolyzed HA serum sample. The contents of the sample in fig. 5.2D are identical to the HA standard indicating its authenticity. This HILIC-CAD method is easily adaptable to other similar carbohydrate-based therapeutics. The method is easy to execute and saves time compared to other laborious techniques involving derivatization. The entire monosaccharide composition analysis (hydrolysis of samples and HPLC analysis) using our method can be completed within 3 h. This is a significant improvement compared to other traditional methods involving derivatization which can take >24 h.

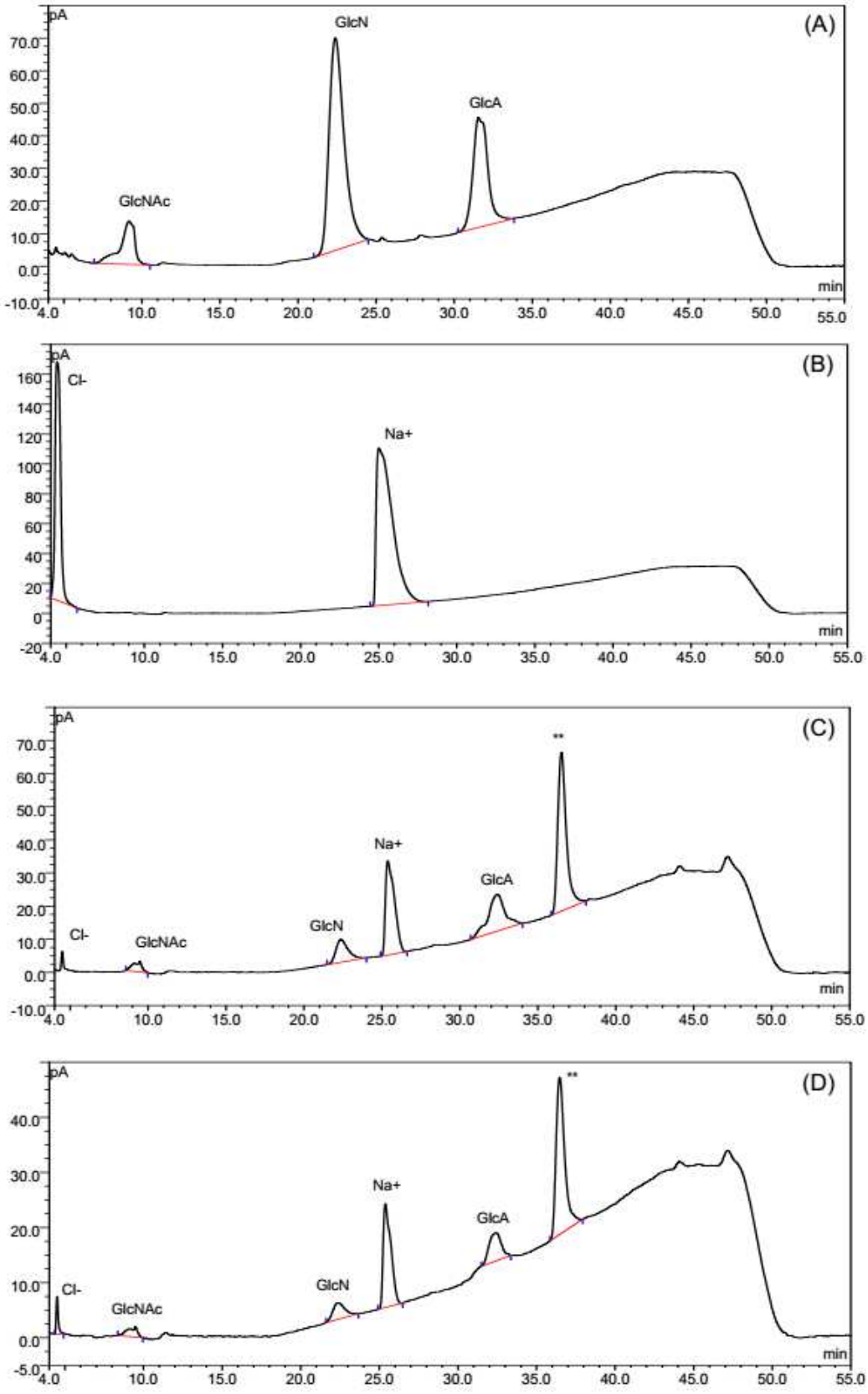
pA
GlcN
(A)
GlcA
GlcNAc
min
pA
Cl-
(B)
Na+
min
pA
**
(C)
Na+
GlcA
Cl-
GlcNAc
GlcN
min
pA
**
(D)
Na+
GlcA
Cl-
GlcNAc
GlcN
min

Figure 5.2. Monosaccharide composition of HA samples by HILIC-CAD. Authentic standards and commercially purchased HA samples were hydrolyzed by 2 M TFA for 2 h before composition analysis by the HILIC-CAD gradient method. (A) represents a chromatogram of GlcNAc and GlcA standards. The degradation of GlcNAc into GlcN is evident from the chromatogram. (B) is a representative chromatogram of NaCl solution. The sodium and chloride ion peaks are visible in the chromatogram. (C) shows a chromatogram of a hydrolyzed HA standard. The Cl^-, GlcNAc, GlcN, Na^+, and GlcA peaks can be seen along with an unknown peak (**). The unknown peak is speculated to be a disaccharide repeating unit of HA. (D) is a representative chromatogram of a hydrolyzed HA serum sample. The composition of (D) is identical to (C) indicating that it is an authentic product.

5.3.2.2. Homogeneity of Hyaluronic Acid Samples

The homogeneity of HA samples was also analyzed by HPSEC-CAD. Separation of HA standards of varying molecular weights is shown in fig. 5.3A. Fig. 5.3B and fig. 5.3C are representative HPSEC chromatograms of HA supplements. The sample in fig. 3B is a polymer predominantly composed of a single peak. The shape of the peak in HPSEC is often indicative of the homogeneity of the sample. The non-symmetrical peak shape in fig. 5.3B indicates the non-homogeneous nature of the sample. Fig. 5.3C contains two non-symmetrical peaks indicating a heterogeneous sample. The difference in molecular size and purity can have significant impact in terms of biological efficacy. HPSEC-CAD offers an easy way to check for homogeneity and size of polysaccharides.

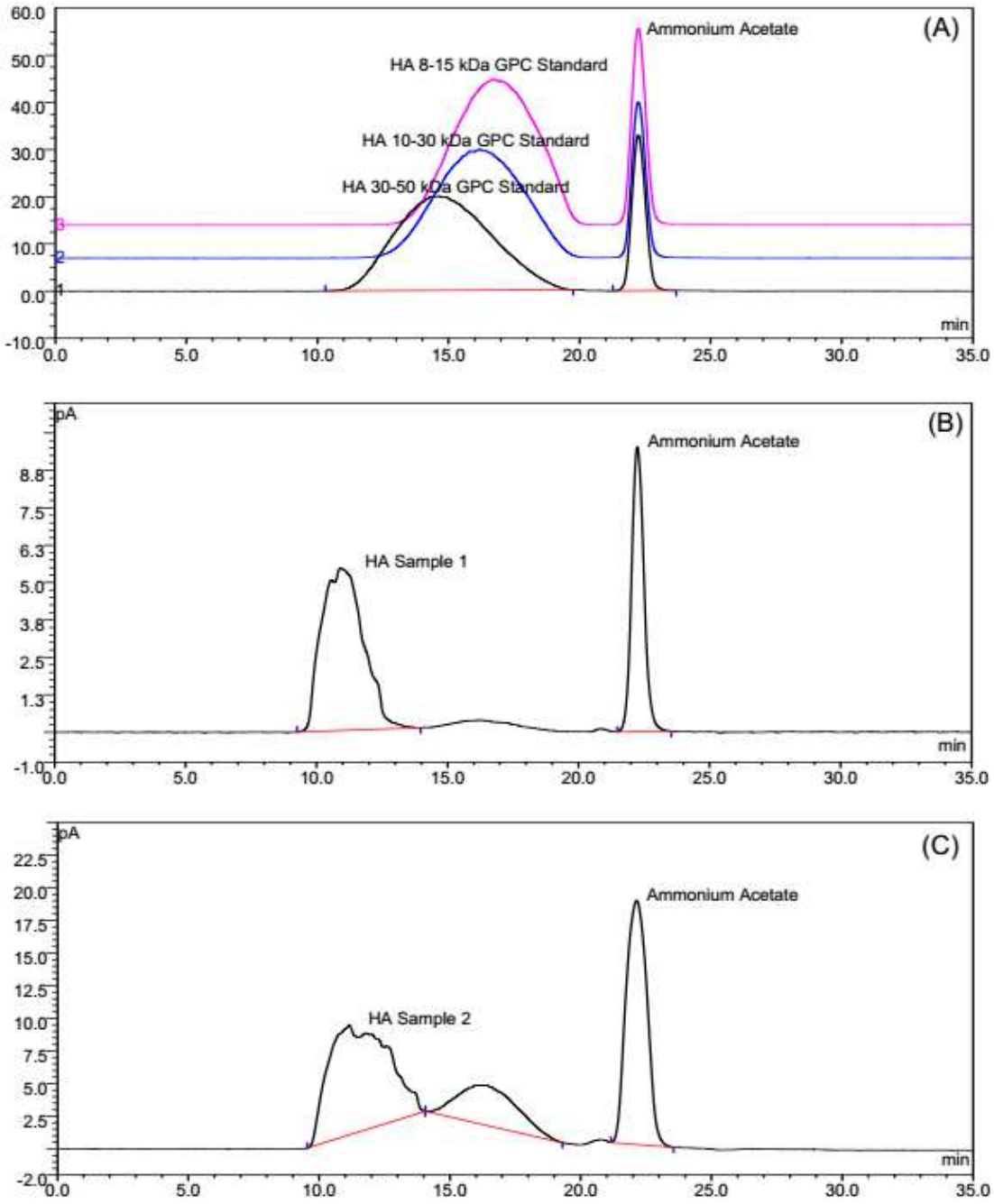

Figure 5.3. Purity and homogeneity analysis of HA samples by HPSEC-CAD. (A) shows the overlay of HPSEC chromatograms of HA GPC standards of varying molecular weights (pink: 8-15 kDa; blue: 10-30 kDa; black: 30-50 kDa). (B) and (C) represent

HPSEC chromatograms of commercially available HA products. Although (B) is predominantly composed of a single peak, the shape of the peak indicates that it might not be a homogeneous fraction. (C) contains two non-symmetrical peaks indicating that it is a heterogeneous sample.

5.4. Conclusions

This study demonstrated the utility of HPLC-CAD as a multipurpose analytical tool for QC analysis of carbohydrates. A HILIC-CAD method was developed for separation and detection of common uronic acids, amino sugars and select neutral sugars without derivatization. This method is an extension of other HILIC-CAD methods (Yan et al., 2016) for neutral sugar analysis. The HPLC-CAD platform can serve as a cheaper and simpler alternative to existing methods for composition analysis. Furthermore, the HPLC-CAD can be used to perform HPSEC experiments to analyze homogeneity and molecular weight of carbohydrate polymers.

5.5. Limitations

The platform can only be used as a QC tool for known carbohydrate samples. Analysis of unknown samples can be difficult. Since CAD is a semi-universal detector, unwanted impurities owing to hydrolysis conditions might interfere with composition analysis of unknown samples. Also, the HILIC-CAD method proposed in this study cannot separate all neutral sugar residues such as glucose and galactose. Our method, which separates most common acidic and amino sugars, must be used in complementation with other reported neutral sugar separation methods for complete composition analysis.

CHAPTER VI

OVERALL CONCLUSIONS

This study explored a novel approach using *Panax quinquefolius* tissue culture to produce bioactive polysaccharides. Since the tissues are grown in a sterile environment, this platform reduces the possibility of endotoxin contamination. Moreover, this format allows for the production of natural polysaccharides with consistent chemical characteristics since tissues are produced in an environmentally-controlled setting. The production of standardized bioactive polysaccharides is important for future commercial applications. In this study, we extracted and partially purified four polysaccharide fractions (AGC1, AGC2, AGC3, and AGC4) that demonstrated immunomodulatory properties. Although, the yield of polysaccharides was lower in the tissue culture system compared to mature plants, there is a possibility for further optimization of the cell culture medium to improve the yields for commercialization. Based on structural analyses, AGC1, AGC2, and AGC4 predominantly contain glycosyl linkages commonly found in type II arabinogalactans. AGC3 was found to be composed of rhamnogalacturonan I pectic polysaccharide. Future 2D NMR analysis will be necessary to completely characterize these polysaccharides. Dose-dependent *in vitro* and *ex vivo* immunostimulatory assays were performed with the type II arabinogalactan AGC1 and the rhamnogalacturonan I AGC3. A major focus of the study was fraction AGC1 as it was one of the most biologically active fractions that also demonstrated the highest purity. Both AGC1 and AGC3 stimulated several inflammatory mediators such as NO, TNF-α, IL-6, and GM-CSF in both RAW 264.7 murine macrophage cells and primary

murine splenocytes. The polysaccharides also demonstrated mitogenic properties by significantly stimulating proliferation of murine splenocytes. Different biochemical tests as well as kinetic studies (*NOS2* gene expression kinetics by AGC1) using live cell imaging showed that the polysaccharides were less potent immunostimulators compared to LPS. It is well known that an excessive proinflammatory response caused by LPS leads to life-threatening septic shock. Due to the immunostimulatory nature of immunomodulation by AGC1 or AGC3, these molecules can potentially be used as an adjuvant or nutraceutical either alone or in conjunction with other therapeutics. Preliminary studies on putative mechanisms of action demonstrated that both NF-κB (p65) and MAPK (p38) pathways are potentially involved in the immunostimulatory process. This study serves as the basis for further research on the mechanism of action for macrophage activation by the suspension culture polysaccharides. Future studies on the interaction between specific glycan moieties and macrophage cell surface receptors (TLRs, complement, scavenger, and lectin receptors) will be important for the development of carbohydrate-based therapeutics. This study highlighted an alternate avenue for the production of commercially important bioactive plant polysaccharides.

The second part of this study addressed the key issue of rapid QC of carbohydrate polymers. It is well-known that QC of carbohydrates is time consuming, laborious and requires complementary instrumentation. This study demonstrated the utility of HPLC-CAD as a QC analytical tool for homogeneity, molecular weight, and monosaccharide composition analysis of complex carbohydrates. An HILIC-CAD method was developed for simultaneous separation and detection of several acidic, amino, and neutral sugars without derivatization. A separate SEC-CAD method was also reported for homogeneity

and molecular weight analysis. Commercially purchased glycosaminoglycan (HA) samples were analyzed to demonstrate the application of the proposed platform. The platform has the potential to perform QC analysis of different types of complex carbohydrates including oligosaccharides, polysaccharides and glycoconjugates. QC of carbohydrate-based nutraceuticals using this platform can be beneficial for commercial purposes.

REFERENCES

Abrahamian, P.; Kantharajah, A. Effect of Vitamins on In Vitro Organogenesis of Plant. *Am. J. Plant Sci.* **2011**, *2*, 669-674.

Arango Duque, G.; Descoteaux, A. Macrophage Cytokines: Involvement in Immunity and Infectious Diseases. *Front. Immunol.* **2014,** *5*, 491.

Azike, C. G.; Charpentier, P. A.; Lui, E. M. K. Stimulation and Suppression of Innate Immune Function by American Ginseng Polysaccharides: Biological Relevance and Identification of Bioactives. *Pharm. Res.* **2015**, *32*, 876-897.

Bain, J.; Plater, L.; Elliott, M.; Shpiro, N.; Hastie, C. J.; McLauchlan, H.; Klevernic, I.; Arthur, J. S.; Alessi, D. R.; Cohen, P. The Selectivity of Protein Kinase Inhibitors: A Further Update. *Biochem. J.* **2007**, *408*, 297-315.

Biondo, P. D.; Goruk, S.; Ruth, M. R.; O'Connell, E.; Field, C. J., Effect of CVT-E002™ (COLD-fX®) Versus a Ginsenoside Extract on Systemic and Gut-Associated Immune Function. *Int. Immunopharmacol.* **2008**, *8*, 1134-1142.

Bogdan, C. Nitric Oxide and the Immune Response. *Nat. Immunol.* **2001,** *2*, 907-916.

Burkhart, E.; Jacobson, M.; Finley, J. A Case Study of Stakeholder Perspective and Experience with Wild American Ginseng (*Panax quinquefolius*) Conservation Efforts in Pennsylvania, U.S.A.: Limitations to a CITES Driven, Top-Down Regulatory Approach. *Biodivers Conserv*. **2012**, *21*, 3657-3679.

Chen, Q. L.; Chen, Y. J.; Zhou, S. S.; Yip, K. M.; Xu, J.; Chen, H. B.; Zhao, Z. Z. Laser Microdissection Hyphenated with High Performance Gel Permeation Chromatography-Charged Aerosol Detector and Ultra Performance Liquid Chromatography-Triple Quadrupole Mass Spectrometry for Histochemical Analysis of Polysaccharides in Herbal Medicine: Ginseng, a Case Study. *Int. J. Biol. Macromol.* **2018,** *107*, 332-342.

Clarke, A. E.; Anderson, R. L.; Stone, B. A. Form and Function of Arabinogalactans and Arabinogalactan-Proteins. *Phytochemistry* **1979**, *18*, 521-540.

Cui, G.; Zhang, W.; Wang, Q.; Zhang, A.; Mu, H.; Bai, H.; Duan, J. Extraction Optimization, Characterization and Immunity Activity of Polysaccharides from *Fructus Jujubae*. *Carbohydr. Polym.* **2014,** *111*, 245-255.

Diallo, D.; Paulsen, B. S.; Liljebäck, T. H.; Michaelsen, T. E. Polysaccharides from the Roots of *Entada africana* Guill. et Perr., Mimosaceae, with Complement Fixing Activity. *J. Ethnopharmacol.* **2001,** *74*, 159-171.

Dixon, R. W.; Peterson, D. S. Development and Testing of a Detection Method for Liquid Chromatography Based on Aerosol Charging. *Anal. Chem.* **2002,** *74*, 2930-2937.

DuBois, M.; Gilles, K. A.; Hamilton, J. K.; Rebers, P. A.; Smith, F. Colorimetric Method for Determination of Sugars and Related Substances. *Anal. Chem*. **1956**, *28*, 350-356.

Fang, X.; Chen, X. Structure Elucidation and Immunological Activity of a Novel Pectic Polysaccharide from the Stems of *Avicennia marina*. *Eur. Food Res. Technol*. **2013**, *236*, 243-248.

Ferreira, S. S.; Passos, C. P.; Madureira, P.; Vilanova, M.; Coimbra, M. A. Structure-Function Relationships of Immunostimulatory Polysaccharides: A Review. *Carbohydr. Polym.* **2015**, *132*, 378-396.

Gertsch, J.; Viveros-Paredes, J. M.; Taylor, P. Plant Immunostimulants-Scientific Paradigm or Myth? *J. Ethnopharmacol*. **2011**, *136*, 385-391.

Giavasis, I. Bioactive Fungal Polysaccharides as Potential Functional Ingredients in Food and Nutraceuticals. *Curr Opin. Biotechnol.* **2014**, *26*, 162-173.

Godin, B.; Agneessens, R.; Gerin, P. A.; Delcarte, J. Composition of Structural Carbohydrates in Biomass: Precision of a Liquid Chromatography Method Using a Neutral Detergent Extraction and a Charged Aerosol Detector. *Talanta* **2011,** *85*, 2014-2026.

Gunter, E. A.; Ovodov, Y. S. An Alternate Carbon Source for Enhancing Production of Polysaccharides by *Silene vulgaris* Callus. *Carbohydr. Res*. **2002**, *337*, 1641-1645.

Heiss, C.; Klutts, J. S.; Wang, Z.; Doering, T. L.; Azadi, P. The Structure of *Cryptococcus neoformans* Galactoxylomannan Contains β-D-Glucuronic Acid. *Carbohydr. Res.* **2009,** *344*, 915-920.

Holderness, J.; Schepetkin, I. A.; Freedman, B.; Kirpotina, L. N.; Quinn, M. T.; Hedges, J. F.; Jutila, M. A. Polysaccharides Isolated from Acai Fruit Induce Innate Immune Responses. *Plos One* **2011**, 6, e17301.

Hosain, N. A.; Ghosh, R.; Bryant, D. L.; Arivett, B. A.; Farone, A. L.; Kline, P. C. Isolation, Structure Elucidation, and Immunostimulatory Activity of Polysaccharide Fractions from *Boswellia carterii* Frankincense Resin. *Int. J. Biol. Macromol.* **2019,** *133*, 76-85.

Hu, D. J.; Cheong, K. L.; Zhao, J.; Li, S. P. Chromatography in Characterization of Polysaccharides from Medicinal Plants and Fungi. *J. Sep. Sci.* **2013,** *36*, 1-19.

Ikegami, T.; Horie, K.; Saad, N.; Hosoya, K.; Fiehn, O.; Tanaka, N., Highly Efficient Analysis of Underivatized Carbohydrates Using Monolithic-Silica-Based Capillary Hydrophilic Interaction (HILIC) HPLC. *Anal. Bioanal. Chem.* **2008,** *391*, 2533-2542.

Karlsson, G.; Winge, S.; Sandberg, H. Separation of Monosaccharides by Hydrophilic Interaction Chromatography with Evaporative Light Scattering Detection. *J. Chromatogr. A* **2005,** *1092*, 246-249.

Khajuria, A.; Gupta, A.; Malik, F.; Singh, S.; Singh, J.; Gupta, B. D.; Suri, K. A.; Suden, P.; Srinivas, V. K.; Ella, K; Qazi, G. N. A New Vaccine Adjuvant (BOS 2000) a Potent Enhancer Mixed Th1/Th2 Immune Responses in Mice Immunized with HBsAg. *Vaccine* **2007,** *25*, 4586-4594.

Khoomrung, S.; Chumnanpuen, P.; Jansa-Ard, S.; Ståhlman, M.; Nookaew, I.; Borén, J.; Nielsen, J. Rapid Quantification of Yeast Lipid Using Microwave-Assisted Total Lipid Extraction and HPLC-CAD. *Anal. Chem.* **2013,** *85*, 4912-4219.

Komalavilas, P.; Zhus, J. K.; Nothangel, E. A. Arabinogalactan-Proteins from the Suspension Culture Medium and Plasma Membrane of Rose Cells. *J. Biol. Chem.* **1991**, *266*, 15956-15965.

Kou, D.; Manius, G.; Zhan, S.; Chokshi, H. P. Size Exclusion Chromatography with Corona Charged Aerosol Detector for the Analysis of Polyethylene Glycol Polymer. *J. Chromatogr. A* **2009,** *1216*, 5424-5428.

Kumar, D.; Arya, V.; Kaur, R.; Bhat, Z. A.; Gupta, V. K.; Kumar, V. A Review of Immunomodulators in the Indian Traditional Health Care System. *J. Microbiol. Immunol. Infect.* **2012,** *45*, 165-84.

Lemmon, H. R.; Sham, J.; Chau, L. A.; Madrenas, J. High Molecular Weight Polysaccharides Are Key Immunomodulators in North American Ginseng Extracts: Characterization of the Ginseng Genetic Signature in Primary Human Immune Cells. *J. Ethnopharmacol.* **2012**, *142*, 1-13.

Li, J.; Hu, D.; Zong, W.; Lv, G.; Zhao, J.; Li, S., Determination of Inulin-Type Fructooligosaccharides in Edible Plants by High-Performance Liquid Chromatography with Charged Aerosol Detector. *J Agric. Food Chem.* **2014,** *62*, 7707-7713.

Li, S.; Wu, D.; Lv, G.; Zhao, J. Carbohydrate Analysis in Herbal Glycomics. *Trends Anal. Chem*. **2013**, *52*, 155-169.

Licciardi, P. V.; Underwood, J. R. Plant-Derived Medicines: A Novel Class of Immunological Adjuvants. *Int. Immunopharmacol.* **2011,** *11*, 390-398.

Ligor, M.; Studzinska, S.; Horna, A.; Buszewski, B. Corona-Charged Aerosol Detection: An Analytical Approach. *Crit. Rev. Anal. Chem*. **2013**, *43*, 64-78.

Loh, S. H.; Park, J. Y.; Cho, E. H.; Nah, S. Y.; Kang, Y. S. Animal Lectins: Potential Receptors for Ginseng Polysaccharides. *J. Ginseng Res.* **2017,** *41*, 1-9.

Lowenthal, M. S.; Kilpatrick, E. L.; Phinney, K. W. Separation of Monosaccharides Hydrolyzed from Glycoproteins Without the Need for Derivatization. *Anal. Bioanal. Chem.* **2015,** *407*, 5453-62.

Luettig, B.; Steinmüller, C.; Gifford, G. E.; Wagner, H.; Lohmann-Matthes, M. L. Macrophage Activation by the Polysaccharide Arabinogalactan Isolated from Plant Cell Cultures of *Echinacea purpurea*. *J. Natl. Cancer Inst.* **1989,** *81*, 669-675.

Luo, D.; Fang, B. Structural Identification of Ginseng Polysaccharides and Testing of Their Antioxidant Activities*. Carbohydr. Polym.* **2008**; *72*, 376-381.

Mariño, K.; Bones, J.; Kattla, J. J.; Rudd, P. M. A Systematic Approach to Protein Glycosylation Analysis: A Path Through the Maze. *Nat. Chem. Biol.* **2010,** *6*, 713-23.

McNeil, M.; Darvill, A. G.; Albersheim, P. Structure of Plant Cell Walls: X. Rhamnogalacturonan I, a Structurally Complex Pectic polysaccharide in the Walls of Suspension-Cultured Sycamore Cells. *Plant Physiol*. **1980**, 66, 1128-1134.

Mikami, T.; Nagase, T.; Matsumoto, T.; Suzuki, S.; Suzuki, M. Gelation of Limulus Amoebocyte Lysate by Simple Polysaccharides. *Microbiol. Immunol.* **1982,** *26*, 403-409.

Moretão, M. P.; Zampronio, A. R.; Gorin, P. A. J.; Iacomini, M.; Oliveira, M. B. M. Induction of Secretory and Tumoricidal Activities in Peritoneal Macrophages Activated by an Acidic Heteropolysaccharide (ARAGAL) from the Gum of *Anadenanthera colubrina* (Angico Branco). *Immunol. Lett*. **2004**, 93, 189-197.

Murashige, T.; Skoog, F. A Revised Medium for Rapid Growth and Bio Assays with Tobacco Tissue Cultures. *Physiol. Plant* **1962**, *15*, 473-497.

Murthy, H. N.; Lee, E.; Paek, K. Production of Secondary Metabolites from Cell and Organ Cultures: Strategies and Approaches for Biomass Improvement and Metabolite Accumulation. *Plant Cell Tissue Organ Cult.* **2014**, *118*, 1-16.

Necas, J.; Bartosikova, L.; Brauner, P.; Kolar, J. Hyaluronic Acid (Hyaluronan): A Review. *Vet. Med. (Praha)* **2008**, *53*, 397-411.

Newman, D. J.; Cragg, G. M. Natural Products as Sources of New Drugs from 1981 to 2014. *J. Nat. Prod.* **2016,** *79*, 629-661.

Nowell, P. C. Phytohemagglutinin: An Initiator of Mitosis in Cultures of Normal Human Leukocytes. *Cancer Res.* **1960,** *20*, 462-466.

Park, H. S.; Nelson, D. E.; Taylor, Z. E.; Hayes, J. B.; Cunningham, K. D.; Arivett B.A.; Ghosh, R.; Wolf, L.C.; Taylor, K.M.; Farone; M.B.; Handy, S.T.; Farone, A.L. Suppression of LPS-Induced NF-κB Activity in Macrophages by the Synthetic Aurone, (Z)-2-((5-(Hydroxymethyl) Furan-2-yl) Methylene) Benzofuran-3(2H)-one. *Int. Immunopharmacol*. **2017**, *43*, 116-128.

Pearson, F. C.; Bohon, J.; Lee, W.; Bruszer, G.; Sagona, M.; Dawe, R.; Jakubowski, G.; Morrison, D.; Dinarello, C. Comparison of Chemical Analyses of Hollow-Fiber Dialyzer Extracts. *Artif. Organs* **1984,** *8*, 291-298.

Peng, Q.; Liu, H.; Lei, H.; Wang, X. Relationship Between Structure and Immunological Activity of an Arabinogalactan from *Lycium ruthenicum*. *Food Chem.* **2016,** *194*, 595-600.

Pierce, J. W.; Schoenlebe, R.; Jesmok, G.; Best, J.; Moore, S. A.; Collins, T.; Gerritsen, M. E. Novel Inhibitors of Cytokine-Induced IκBα Phosphorylation and Endothelial Cell Adhesion Molecule Expression Show Anti-Inflammatory Effects *In Vivo*. *J. Biol. Chem*., **1997**, *272*, 21096-21103.

Popov, S. V.; Popova, G. Y.; Ovodova, R. G.; Bushneva, O. A.; Ovodov, Y. S. Effects of Polysaccharides from *Silene vulgaris* on Phagocytes. *Int. J. Immunopharmacol.* **1999,** *21*, 617-24.

Pugh, N. D.; Tamta, H.; Balachandran, P.; Wu, X.; Howell, J.; Dayan, F. E.; Pasco, D. S. The Majority of In Vitro Macrophage Activation Exhibited by Extracts of Some Immune Enhancing Botanicals Is Due to Bacterial Lipoproteins and Lipopolysaccharides. *Int. Immunopharmacol.* **2008,** *8*, 1023-1032.

Ruiz-Matute, A. I.; Hernández-Hernández, O.; Rodríguez-Sánchez, S.; Sanz, M. L.; Martínez-Castro, I. Derivatization of Carbohydrates for GC and GC-MS Analyses. *J. Chromatogr. B Analyt. Technol. Biomed. Life Sci.* **2011,** *879*, 1226-1240.

Schepetkin, I. A.; Quinn, M. T. Botanical Polysaccharides: Macrophage Immunomodulation and Therapeutic Potential. *Int. Immunopharmacol*. **2006**, *6*, 317-333.

Schindelin, J.; Arganda-Carreras, I.; Frise, E.; Kaynig, V.; Longair, M.; Pietzsch, T.; Preibisch, S.; Rueden, C.; Saalfeld, S.; Schmid, B.; Tinevez, J. Y.; White, D. J.; Hartenstein, V.; Eliceiri, K.; Tomancak, P.; Cardona, A. Fiji: An Open-Source Platform for Biological-Image Analysis. *Nat. Methods* **2012,** *9*, 676-682.

Sevag, M. G.; Lackman, D. B.; Smolens, J. The Isolation of the Components of Streptococcal Nucleoproteins in Serologically Active Form. *J. Biol. Chem*. **1938**, *124*, 425-436.

Smith, P. K.; Krohn, R. I.; Hermanson, G. T.; Mallia, A. K.; Gartner, F. H.; Provenzano, M. D.; Fujimoto, E. K.; Goeke, N. M.; Olson, B. J.; Klenk, D. C. Measurement of Protein Using Bicinchoninic Acid. *Anal. Biochem*. **1985**, 150, 76-85.

Species at Risk Public Registry Website. https://wildlife-species.canada.ca/species-risk-registry/species/speciesDetails_e.cfm?sid=217 (Accessed June 6, 2019).

Tanaka, H.; Zhou, X.; Masayoshi, O. Characterization of a Novel Diol Column for High-Performance Liquid Chromatography. *J. Chromatogr. A* **2003,** *987*, 119-125.

Thakur, M.; Weng, A.; Fuchs, H.; Sharma, V.; Bhargava, C. S.; Chauhan, N. S.; Dixit, V. K.; Bhargava, S. Rasayana Properties of Ayurvedic Herbs: Are Polysaccharides a Major Contributor. *Carbohydr. Polym*. **2012**, *87*, 3-15.

United States Fish and Wildlife Services Website. https://www.fws.gov/international/plants/american-ginseng.html (Accessed June 6, 2019)

Vanisree, M.; Lee, C.-Y.; Lo, S.-F.; Nalawade, S. M.; Lin, C. Y.; Tsay, H.S. Studies on the Production of Some Important Secondary Metabolites from Medicinal Plants by Plant Tissue Cultures. *Bot. Bull. Acad. Sin*. **2004**, *45*, 1-22.

Vetvicka, V. Glucan-Immunostimulant, Adjuvant, Potential drug. *World J Clin. Oncol.* **2011,** *2*, 115-119.

Vetvicka, V.; Vetvickova, J. β-Glucan – Is the Current Research Relevant? *Int. Clin. Pathol. J.* **2017**, *4*, 00089.

Wagner, H.; Stuppner, H.; Schäfer, W.; Zenk, M. Immunologically Active Polysaccharides of *Echinacea purpurea* Cell Cultures. *Phytochemistry* **1988**, *27*, 119-126.

Wang, A. S. Callus Induction and Plant Regeneration of American Ginseng. *HortScience* **1990**, *25*, 571-572.

Wang, X. S.; Liu, L.; Fang, J. N. Immunological Activities and Structure of Pectin from *Centella asiatica*. *Carbohydr. Polym.* **2005**, *60*, 95-101.

Wang, J.; Gao, W.-Y.; Zhang, J.; Zuo, B.-M.; Zhang, L.-M.; Huang, L.Q. Production of Ginsenoside and Polysaccharide by Two-Stage Cultivation of *Panax quinquefolium* L. Cells. *In vitro Cell. Dev. Biol. Plant* **2012**, 48, 107-112.

Wang, M.; Jiang, C.; Ma, L.; Zhang, Z.; Cao, L.; Liu, J.; Zeng, X. Preparation, Preliminary Characterization and Immunostimulatory Activity of Polysaccharide Fractions from the Peduncles of *Hovenia dulcis*. *Food Chem.* **2013,** *138*, 41-47.

Wang, L.; Yao, Y.; Sang, W.; Yang, X.; Ren, G. Structural Features and Immunostimulating Effects of Three Acidic Polysaccharides Isolated from *Panax quinquefolius*. *Int. J. Biol. Macromol.* **2015,** *80*, 77-86.

Wang, L.; Yu, X.; Yang, X.; Li, Y.; Yao, Y.; Lui, E. M. K.; Ren, G. Structural and Anti-Inflammatory Characterization of a Novel Neutral Polysaccharide from North American Ginseng (*Panax quinquefolius*). *Int. J. Biol. Macromol*. **2015**, *74*, 12-17.

Xie, G.; Schepetkin, I. A.; Siemsen, D. W.; Kirpotina, L. N.; Wiley, J. A.; Quinn, M. T. Fractionation and Characterization of Biologically-Active Polysaccharides from *Artemisia tripartita*. *Phytochemistry* **2008,** *69*, 1359-1371.

Yamada, H.; Kiyohara, H. Immunomodulating Activity of Plant Polysaccharide Structures. In: Comprehensive Glycoscience; Boons, G.J.; Lee, Y.C.; Suzuki, A.; Taniguchi, N.; Voragen, A.G.J., Eds.; Elsevier Ltd., Oxford, UK, 2007; Vol 4, pp. 663-693.

Yan, J.; Shi, S.; Wang, H.; Liu, R.; Li, N.; Chen, Y.; Wang, S. Neutral Monosaccharide Composition Analysis of Plant-Derived Oligo- and Polysaccharides by High Performance Liquid Chromatography. *Carbohydr. Polym.* **2016,** *136*, 1273-1280.

Yang, X.; Zhao, Y.; Wang, Q.; Wang, H.; Mei, Q. Analysis of the Monosaccharide Components in Angelica Polysaccharides by High Performance Liquid Chromatography. *Anal. Sci.* **2005,** *21*, 1177-1180.

Yoo, D. G.; Kim, M. C.; Park, M. K.; Park, K. M.; Quan, F. S.; Song, J. M.; Wee, J. J.; Wang, B. Z.; Cho, Y. K.; Compans, R. W.; Kang, S. M. Protective Effect of Ginseng Polysaccharides on Influenza Viral Infection. *PLoS One* **2012,** *7*, e33678.

Yu, X. H.; Liu, Y.; Wu, X. L.; Liu, L. Z.; Fu, W.; Song, D. D. Isolation, Purification, Characterization and Immunostimulatory Activity of Polysaccharides Derived from American Ginseng. *Carbohydr. Polym.* **2017,** *156*, 9-18.

Zhang, Z.; Khan, N. M.; Nunez, K. M.; Chess, E. K.; Szabo, C. M. Complete Monosaccharide Analysis by High-Performance Anion-Exchange Chromatography with Pulsed Amperometric Detection. *Anal. Chem.* **2012,** *84*, 4104-4110.

Zhu, W.; Han, B.; Sun, Y.; Wang, Z.; Yang, X. Immunoregulatory Effects of a Glucogalactan from the Root of *Panax quinquefolium* L. *Carbohydr. Polym*. **2012**, *87*, 2725-2729.

Zong, A.; Cao, H.; Wang, F. Anticancer Polysaccharides from Natural Resources: A Review of Recent Research. *Carbohydr. Polym.* **2012,** *90*, 1395-1410.

APPENDICES

APPENDIX A: Growth Rate of NAG Callus Tissues.

Callus tissues were induced from seeds, maintained and passaged for two years. Stable callus cell lines were used to inoculate liquid cell suspension cultures, which were scaled up to an adequate volume for extraction of polysaccharides. Panel (A) shows an example of callus tissue that was passaged every 30 days. Panel (B) shows the cellular mass of successive callus tissue/ passages. Each passage was initiated with 30 g of callus and tissue mass was measured before and after growth period. Passage 1 had 6-fold increase in mass, passage 2 had 8.33-fold increase in mass, passage 3 had 4.33-fold increase in mass and passage 4 had 6.83-fold increase in mass. A period of four passages has been shown in the figure.

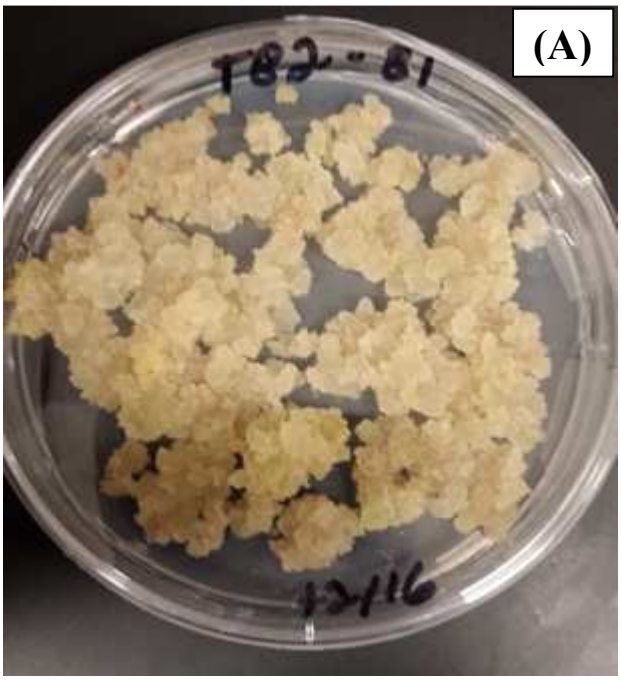

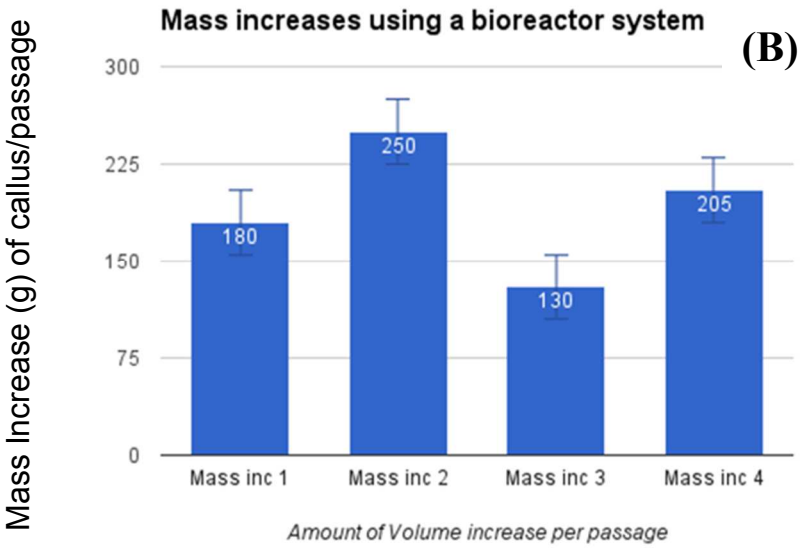
Mass increases using a bioreactor system
(B)
Mass Increase (g) of callus/passage
300
225
150
75
0
180
250
130
205
Mass inc 1
Mass inc 2
Mass inc 3
Mass inc 4
Amount of Volume increase per passage

APPENDIX B: IACUC Approval Letter

IACUC
INSTITUTIONAL ANIMAL CARE and USE COMMITEE
Office of Research Compliance,
010A Sam Ingram Building,
2269 Middle Tennessee Blvd
Murfreesboro, TN 37129

MIDDLE TENNESSEE STATE UNIVERSITY

IACUCN006: FCR PROTOCOL APPROVAL NOTICE

Tuesday, April 18, 2017

Principal Investigator	**Anthony Farone**
Co-Investigator(s):	Rajarshi Ghosh (MOBI Doctoral) and Brock Arivett (MOBI Doctoral)
Investigator Email(s):	*anthony.farone@mtsu.edu; rg3j@mtmail.mtsu.edu; baa2j@mtmail.mtsu.edu*
Department/Unit:	Biology, CBAS
Protocol ID:	**17-3010**
Protocol Title:	***Effect of botanical polysaccharides as potential immunomodulators in primary splenocytes and bone marrow-derived macrophages***

Dear Investigator(s),

The MTSU Institutional Animal Care and Use Committee has reviewed the animal use proposal identified above under the ***Full Committee Review (FCR) mechanism***. The IACUC met on 4/14/2017 to determine if your revised proposal meets the requirements for approval. The Committee determined through a unanimous vote that this revised protocol meets the guidelines for approval in accordance with PHS policy. A summary of the IACUC action(s) and other particulars of this this protocol is tabulated as below:

IACUC Action	**APPROVED for one year from the date of this notification**	
Date of Expiration	**4/30/2018**	
Number of Animals	12 (TWELVE)	
Approved Species	**Male ICR Mus musculus (less than 200g)**	
Category	☐ **Teaching**	☒ **Research**
Subclassifications	☐ Classroom ☐ Laboratory	☒ Laboratory ☐ Field Research ☐ Field Study ☒ Handling/Manipulation ☐ Observation
	Comment: NONE	
Approved Site(s)	MTSU vivarium – Rooms 1170C	
Restrictions	**1. Must comply with all FCR requirements and MTSU vivarium policy;** **2. Animal euthanasia must be performed in the procedure location away from other live mice**	
Comments	Initially reviewed by FCR on 03.10.2017	

This approval is effective for three (3) years from the date of this notice. This protocol **expires on 4/30/2020** The investigator(s) MUST file a Progress Report annually regarding the status of this study. Refer to the schedule for Continuing Review shown below; NO REMINDERS WILL BE SENT. A continuation request (progress report) must be approved by the IACUC prior to **4/30/2018** for this protocol to be active for its full term. Once a protocol has expired, it cannot be continued and the investigators must request a fresh protocol.

Continuing Review Schedule:

Reporting Period	Requisition Deadline	IACUC Comments
First year report	3/31/2018	Yet to be completed
Second year report	3/31/2019	Yet to be completed
Final report	3/31/2020	Yet to be completed

Post-approval Amendments:

Date	***Amendment***	***IACUC Notes***
NONE	NONE	NONE

MTSU Policy defines an investigator as someone who has contact with live or dead animals for research or teaching purposes. Anyone meeting this definition must be listed on your protocol and must complete appropriate training through the CITI program. Addition of investigators requires submission of an Addendum request to the Office of Research Compliance.

The IACUC must be notified of any proposed protocol changes prior to their implementation. Unanticipated harms to subjects or adverse events must be reported within 48 hours to the Office of Compliance at (615) 494-8918 and by email – compliance@mtsu.edu.

All records pertaining to the animal care be retained by the MTSU faculty in charge for at least three (3) years AFTER the study is completed. Be advised that all IACUC approved protocols are subject to audit at any time and all animal facilities are subject to inspections at least biannually. Furthermore, IACUC reserves the right to change, revoke or modify this approval without prior notice.

Sincerely,

Compliance Office
(On behalf of IACUC)
Middle Tennessee State University
Tel: 615 494 8918
Email: iacuc_information@mtsu.edu (for questions) and
iacuc_submissions@mtsu.edu (for sending documents)

APPENDIX C: Wavelength Scan of AGC1

Absence of peaks at 254 nm and 280 nm indicate that AGC1 does not contain proteins or nucleic acids.

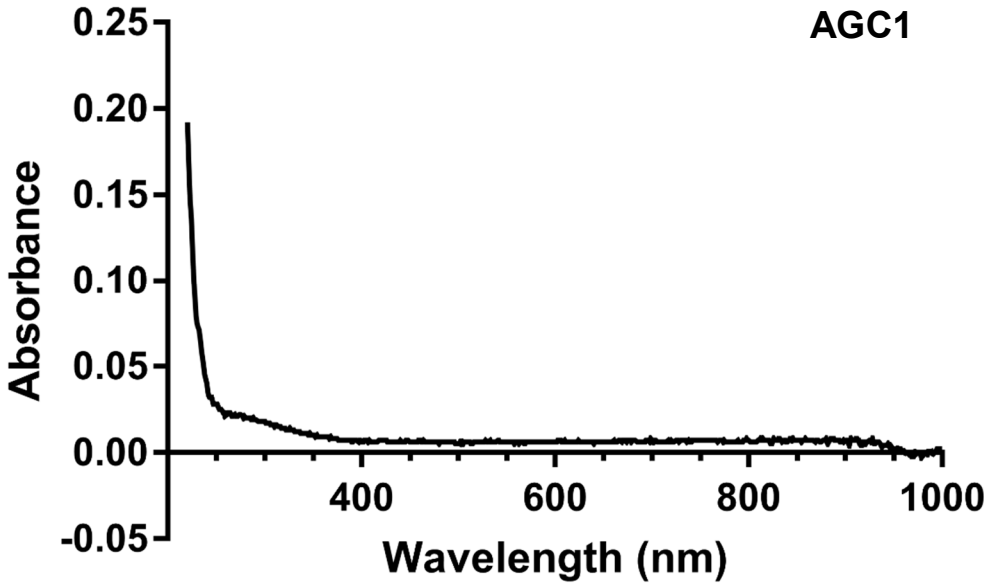

APPENDIX D: HPSEC-RID Chromatograms of NAG Suspension Culture Polysaccharide Fractions

The chromatograms indicate that AGC1, AGC2, and AGC3 are heterogeneous fractions due to the presence of multiple non-symmetrical peaks.

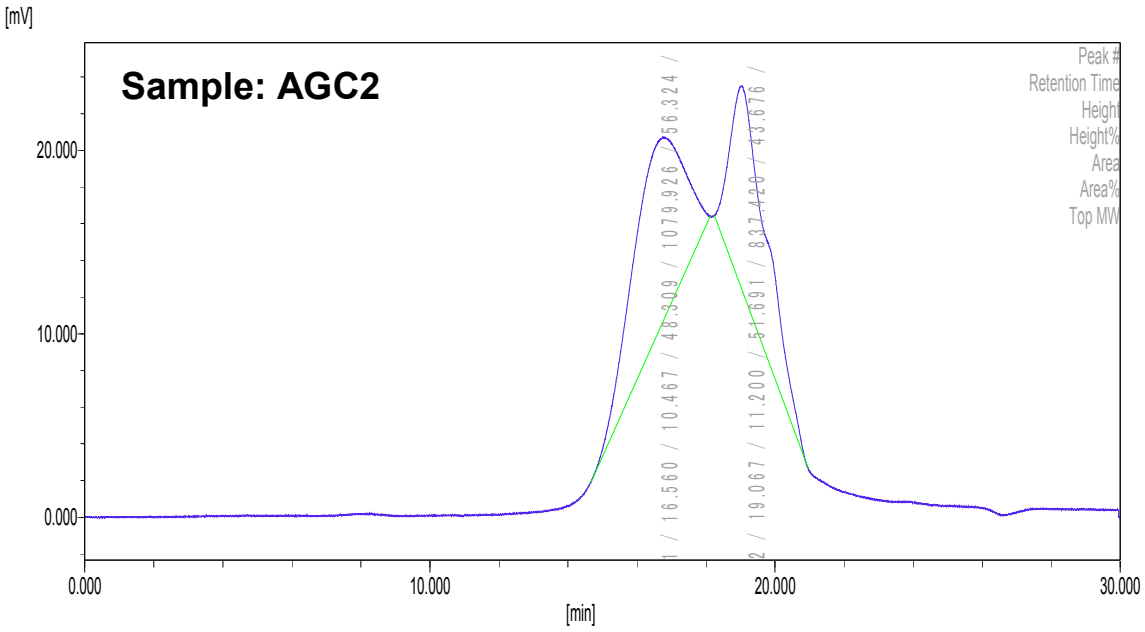

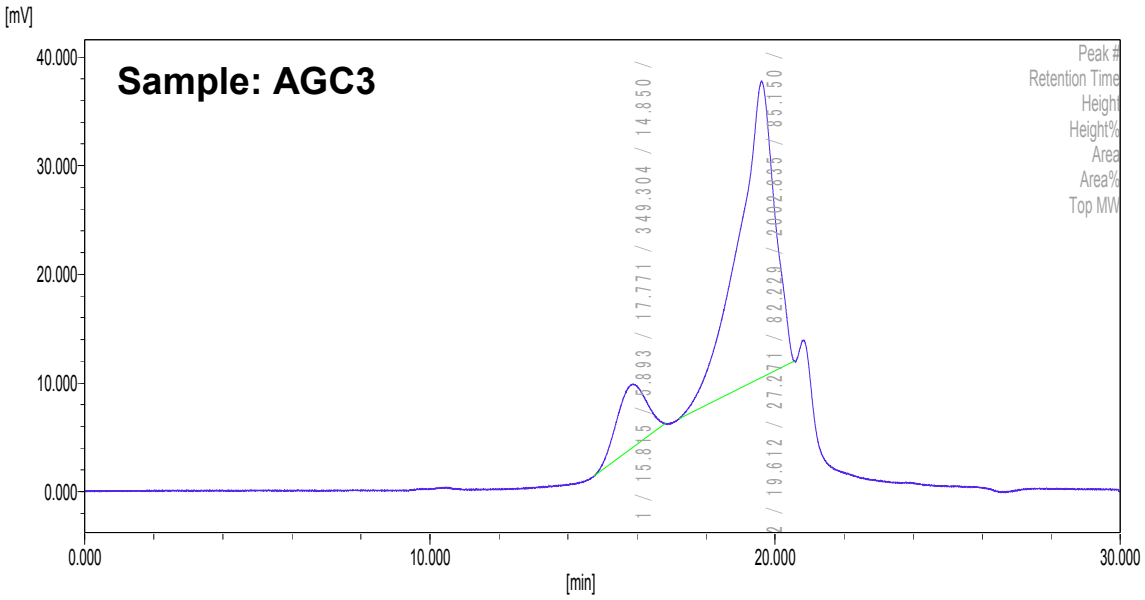
[mV]
Sample: AGC3
40.000
30.000
20.000
10.000
0.000
0.000
10.000
20.000
30.000
[min]
Peak #
Retention Time
Height
Height%
Area
Area%
Top MW
1 / 15.815 / 5.893 / 17.771 / 349.304 / 14.850 /
2 / 19.612 / 27.271 / 82.229 / 2002.835 / 85.150 /

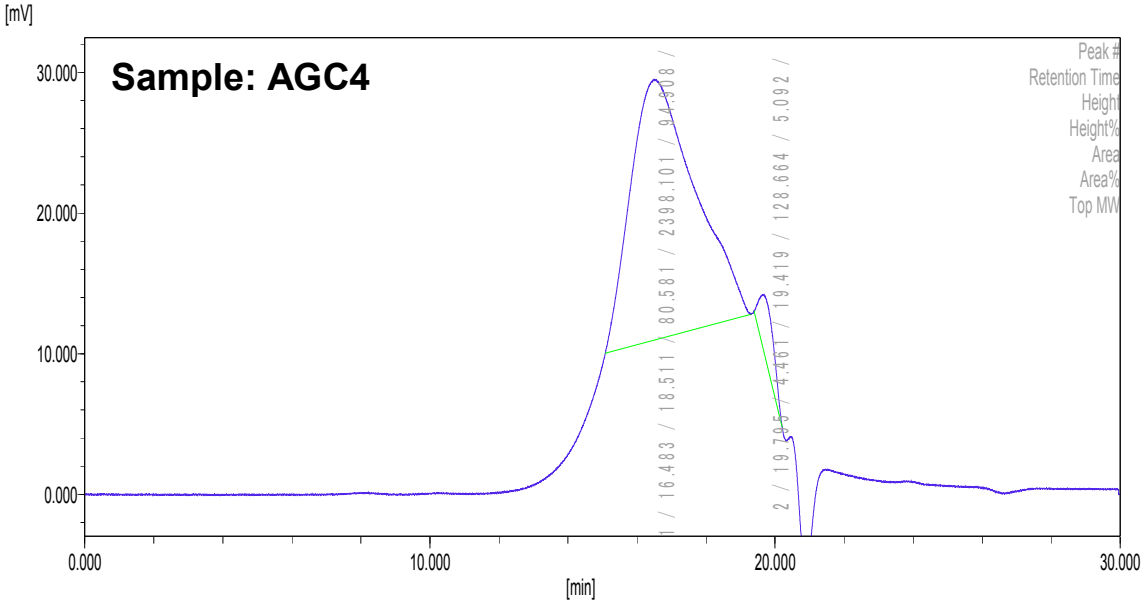
[mV]
Sample: AGC4
30.000
20.000
10.000
0.000
0.000
10.000
20.000
30.000
[min]
Peak #
Retention Time
Height
Height%
Area
Area%
Top MW
1 / 16.483 / 18.511 / 80.581 / 2398.101 / 94.908 /
2 / 19.705 / 4.461 / 19.419 / 128.664 / 5.092 /

APPENDIX E: Monosaccharide Composition Analysis of NAG Suspension Culture Polysaccharides by HPLC

The polysaccharide samples were acid hydrolyzed followed by PMP derivatization and HPLC analysis. The chromatograms indicate the presence of different monosaccharide residues in AGC2, AGC3, and AGC4.

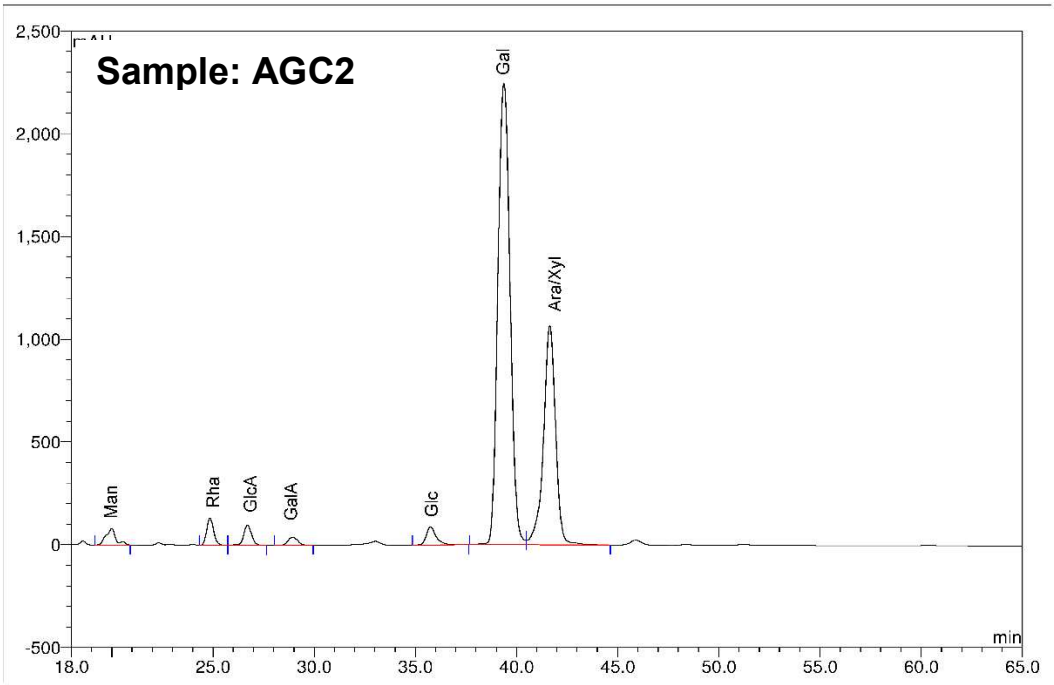

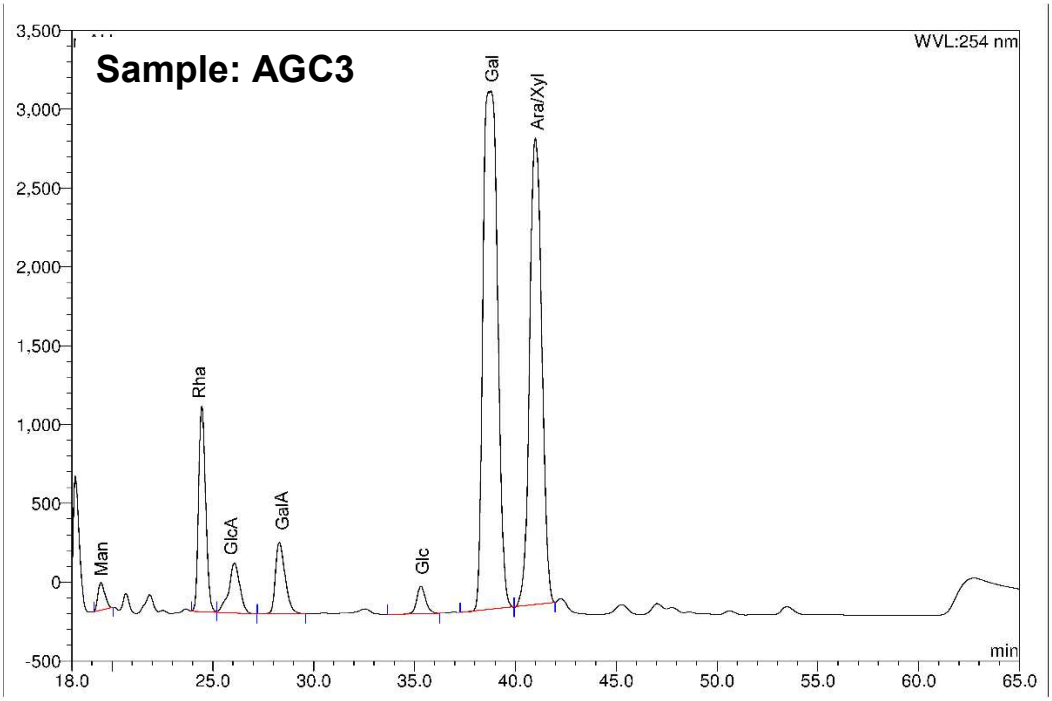
Sample: AGC3
WVL:254 nm
Man
Rha
GlcA
GalA
Glc
Gal
Ara/Xyl
min

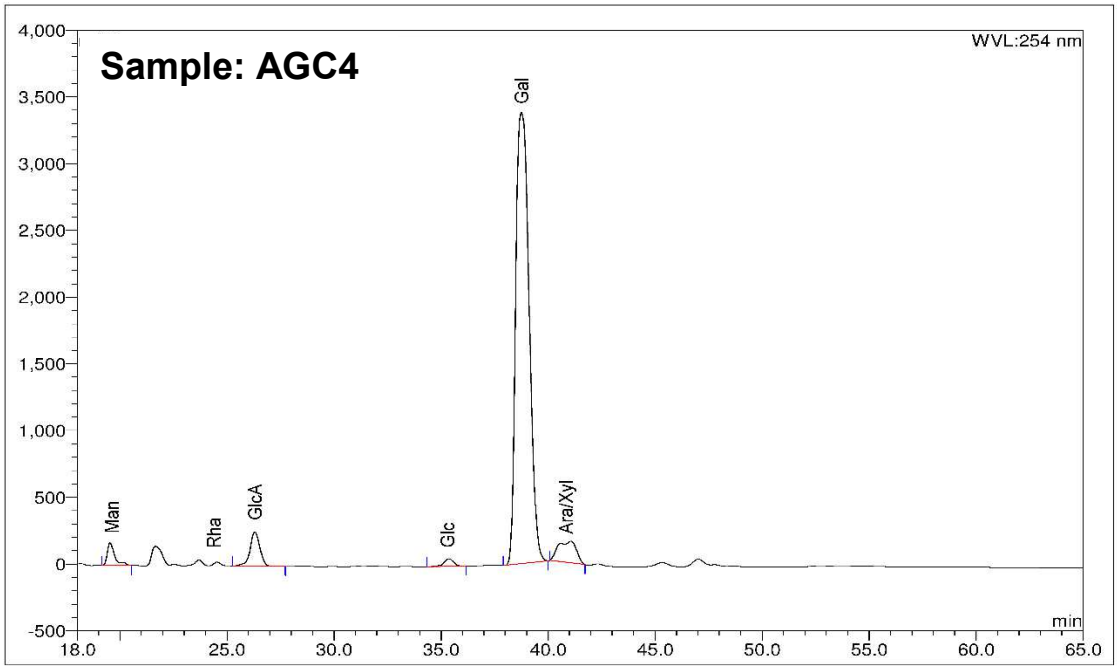
Sample: AGC4
WVL:254 nm
Man
Rha
GlcA
Glc
Gal
Ara/Xyl
min

APPENDIX F: GC-MS Total Ion Chromatograms of TMS Methyl Glycosides of Authentic Monosaccharide Standards

The total ion chromatograms of TMS methyl glycosides of eight different monosaccharide standards (Ara, Xyl, Glc, Gal, Man, Rha, GlcA, and GalA) are shown. Each labelled peak in the chromatograms corresponds to different isomers of a monosaccharide. The retention times were used for monosaccharide composition analysis of AGC1 by GC-MS.

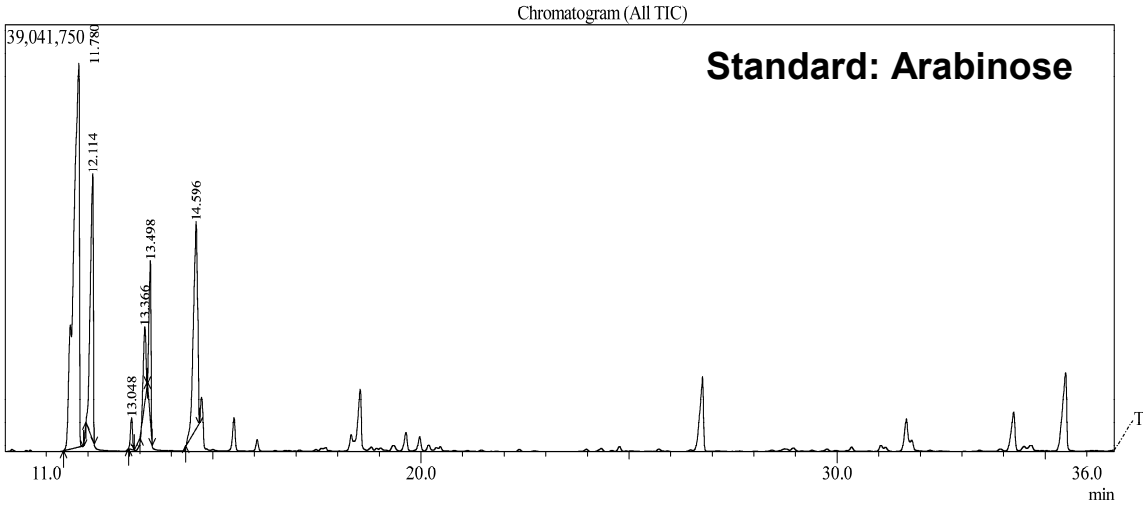

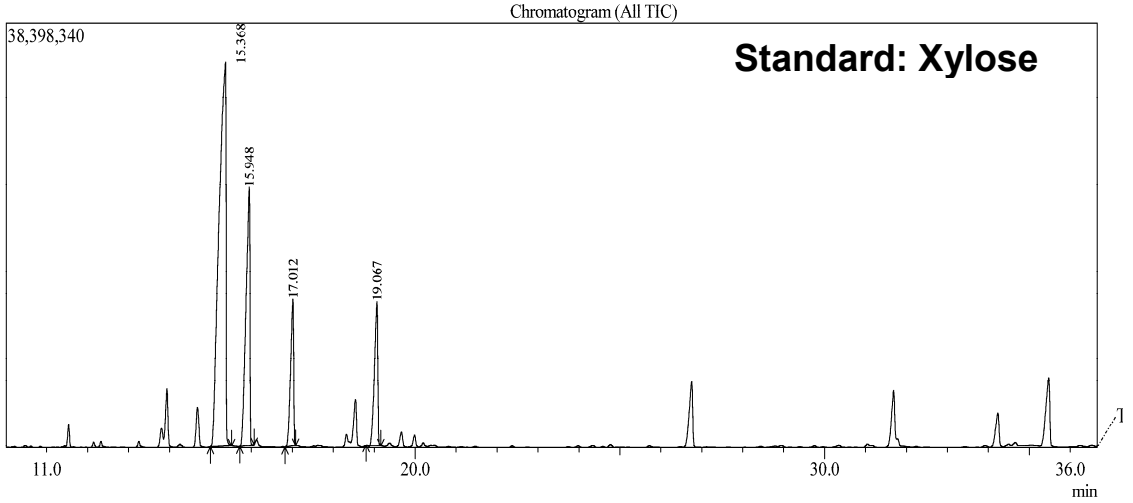
Chromatogram (All TIC)
38,398,340
Standard: Xylose
15.368
15.948
17.012
19.067
11.0
20.0
30.0
36.0
min

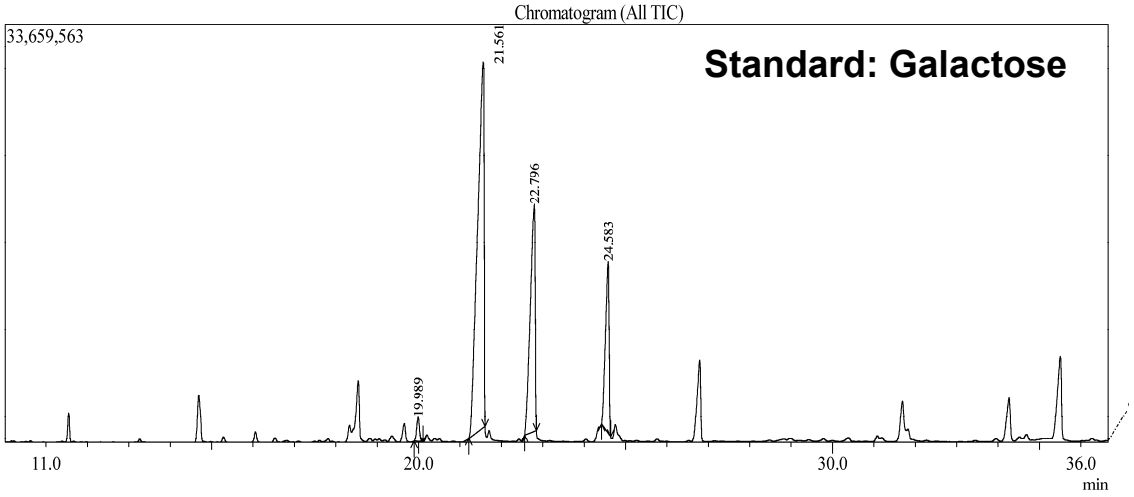
Chromatogram (All TIC)
33,659,563
Standard: Galactose
21.561
22.796
24.583
19.989
11.0
20.0
30.0
36.0
min

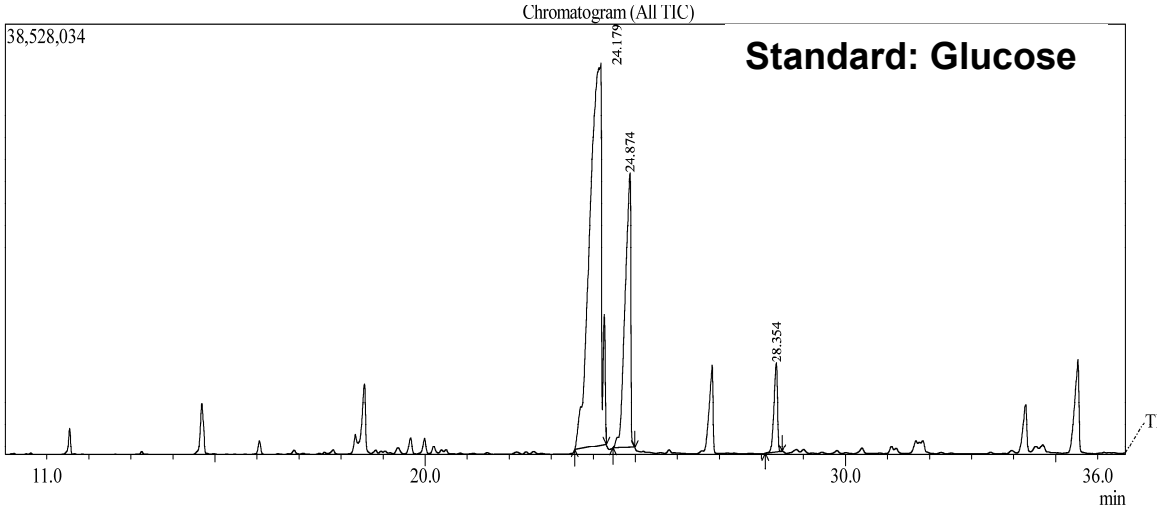
Chromatogram (All TIC)
38,528,034
Standard: Glucose
24.179
24.874
28.354
T
11.0
20.0
30.0
36.0
min

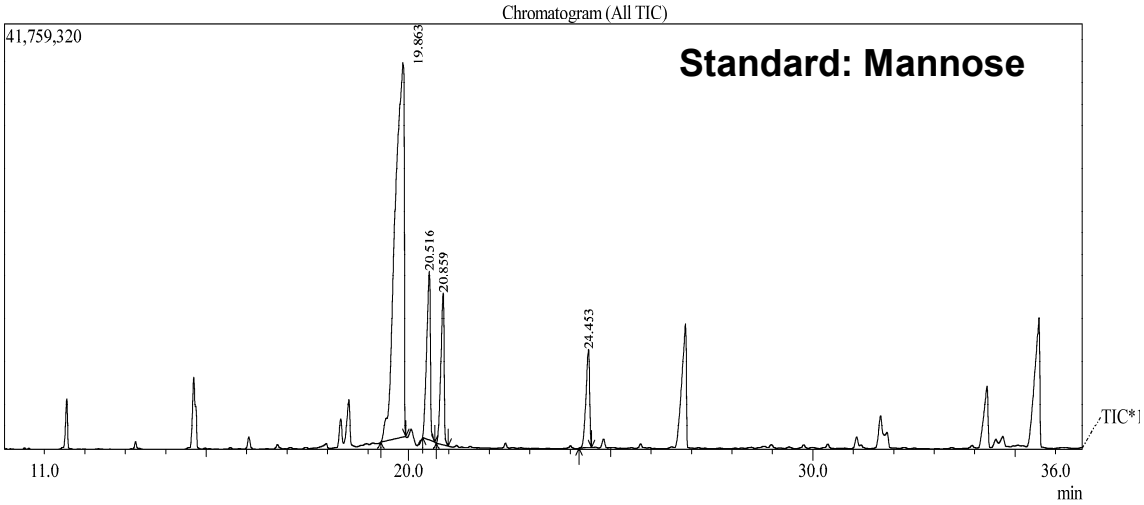
Chromatogram (All TIC)
41,759,320
Standard: Mannose
19.863
20.516
20.859
24.453
TIC*1
11.0
20.0
30.0
36.0
min

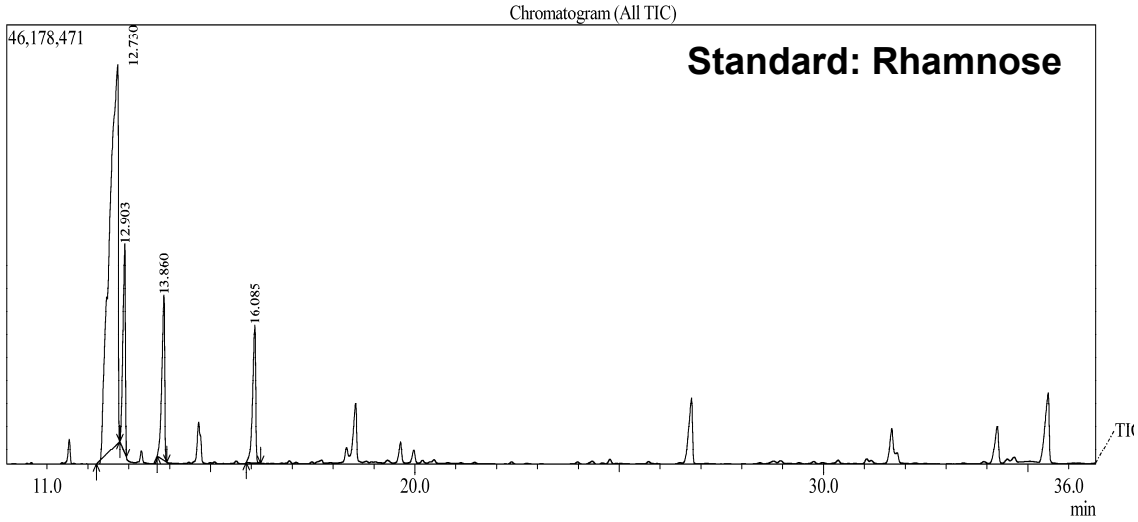
Chromatogram (All TIC)
46,178,471
Standard: Rhamnose
12.750
12.903
13.860
16.085
TIC
11.0
20.0
30.0
36.0
min

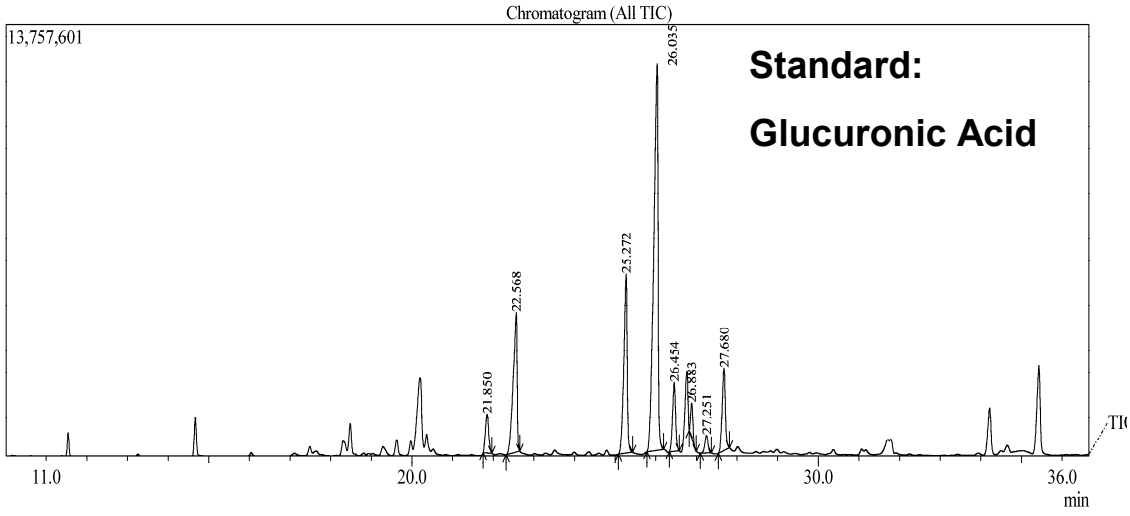
Chromatogram (All TIC)
13,757,601
Standard:
Glucuronic Acid
26.035
25.272
22.568
21.850
26.454
26.883
27.251
27.680
TIC
11.0
20.0
30.0
36.0
min

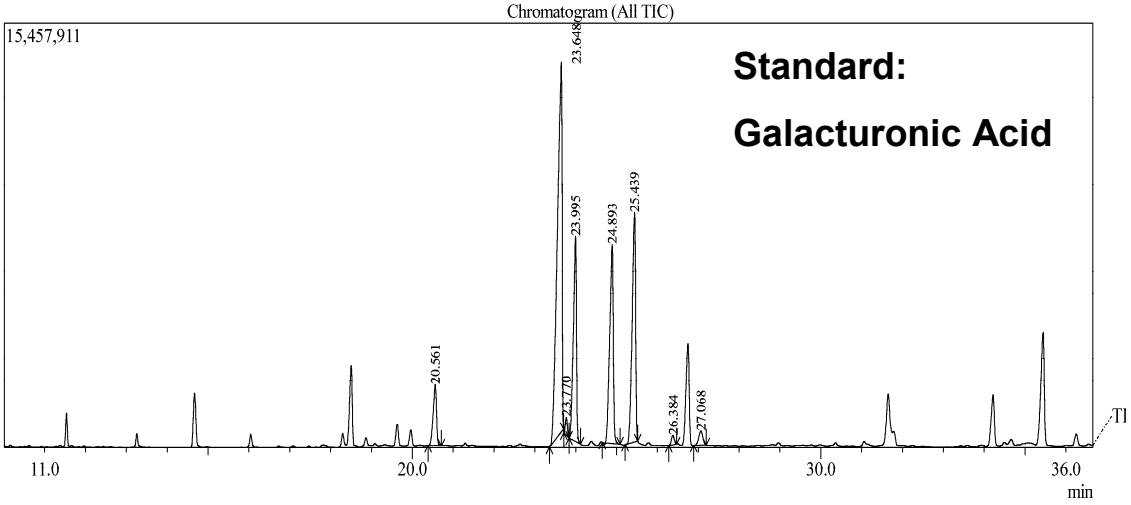
Chromatogram (All TIC)
15,457,911
Standard:
Galacturonic Acid
23.648
23.995
24.893
25.439
20.561
23.770
26.384
27.068
TI
11.0
20.0
30.0
36.0
min

APPENDIX G: GC-MS Total Ion Chromatograms of PMAA Derivatives of NAG Suspension Culture Polysaccharides

The annotated peaks indicate the different glycosyl linkages present in AGC2, AGC3, and AGC4.

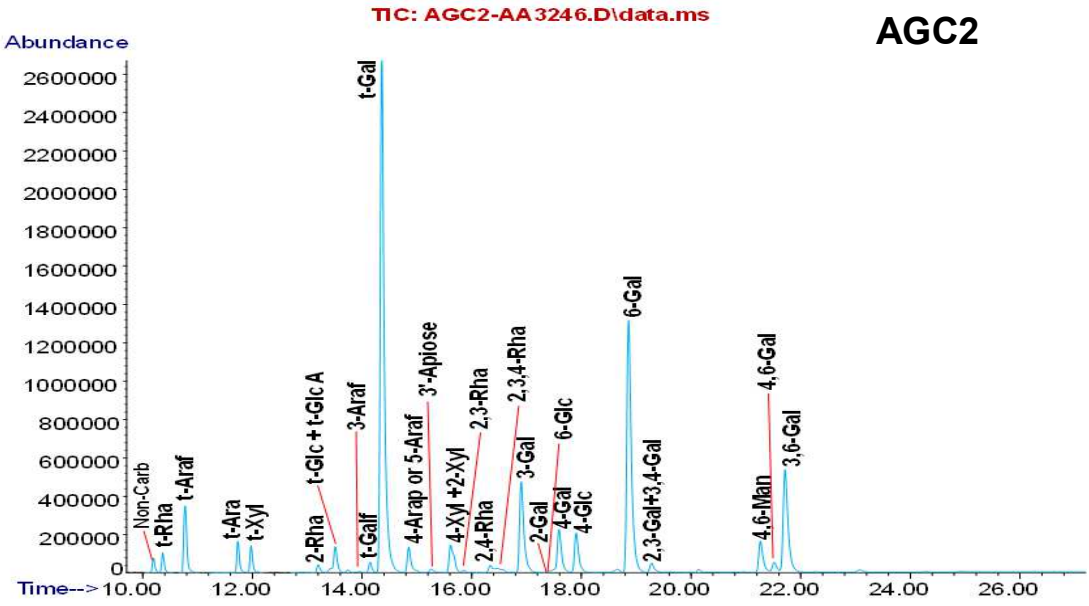

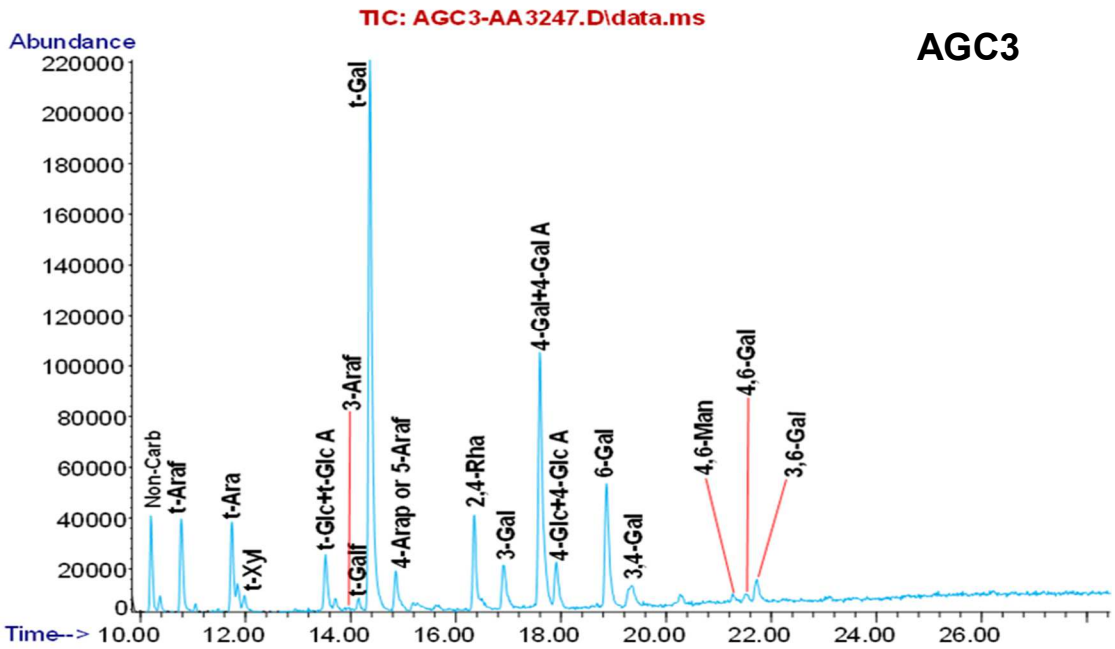
TIC: AGC3-AA3247.D\data.ms
Abundance
AGC3
Non-Carb
t-Araf
t-Ara
t-Xyl
t-Glc+t-Glc A
3-Araf
t-Galf
t-Gal
4-Arap or 5-Araf
2,4-Rha
3-Gal
4-Gal+4-Gal A
4-Glc+4-Glc A
6-Gal
3,4-Gal
4,6-Man
4,6-Gal
3,6-Gal
Time-->

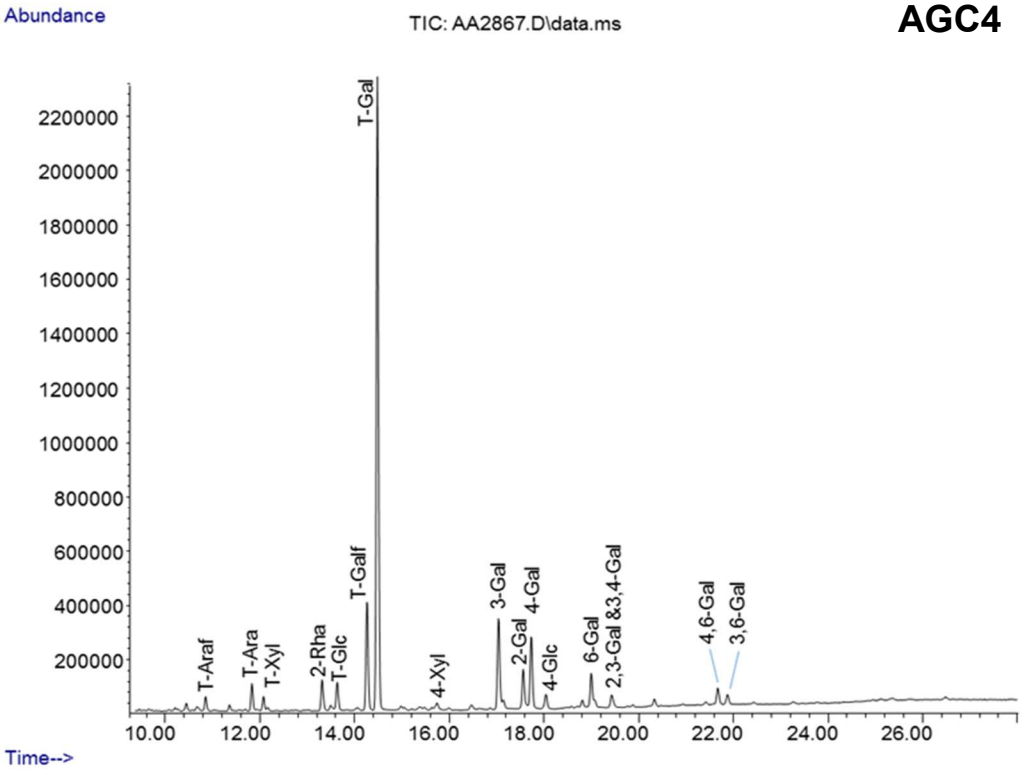
Abundance
TIC: AA2867.D\data.ms
AGC4
T-Araf
T-Ara
T-Xyl
2-Rha
T-Glc
T-Galf
T-Gal
4-Xyl
3-Gal
2-Gal
4-Gal
4-Glc
6-Gal
2,3-Gal &3,4-Gal
4,6-Gal
3,6-Gal
Time-->

APPENDIX H: Mass Spectra of Glycosyl Linkages Found in NAG Suspension Culture Polysaccharides

The mass spectra of t-Araf, t-Ara, t-Xyl, 2-Araf, 3-Rha, t-Glc, 3-Araf, t-Gal, 4-Ara or 5-Araf, 2-Xyl or 4-Xyl, 3-Glc, 3-Man, 3-Gal, 2-Gal, 6-Glc, 4-Gal, 6-Gal, 4-Glc, 2,3-Gal or 3,4-Gal, 4,6-Glc, and 3,6-Gal glycosyl linkages are provided.

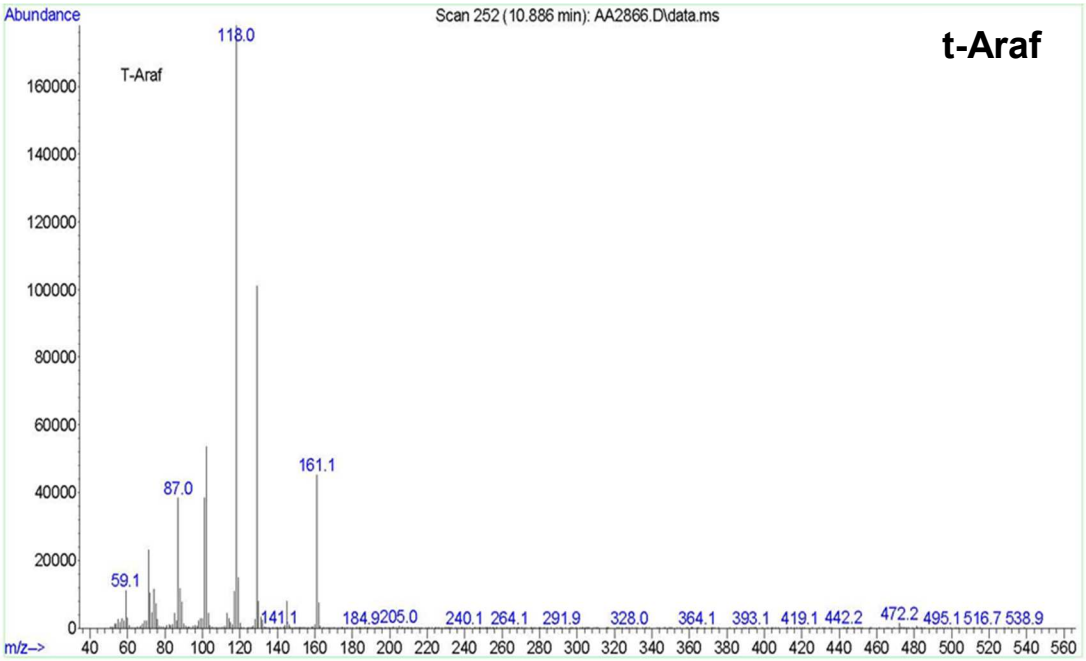

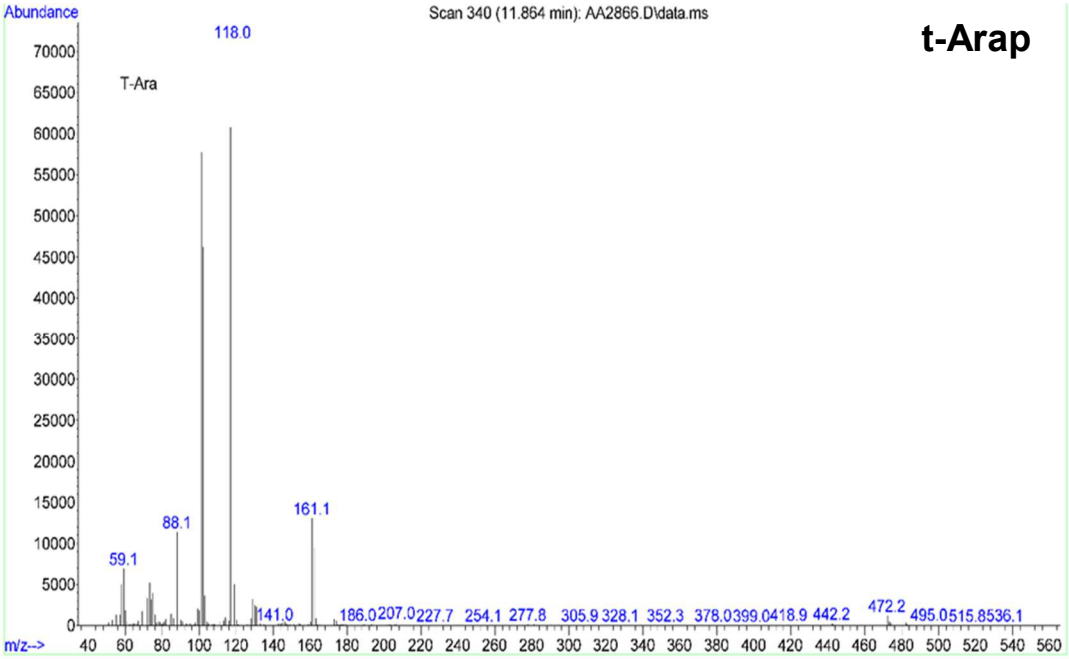
Abundance
Scan 340 (11.864 min): AA2866.D\data.ms
t-Arap
T-Ara
118.0
161.1
88.1
59.1
m/z-->

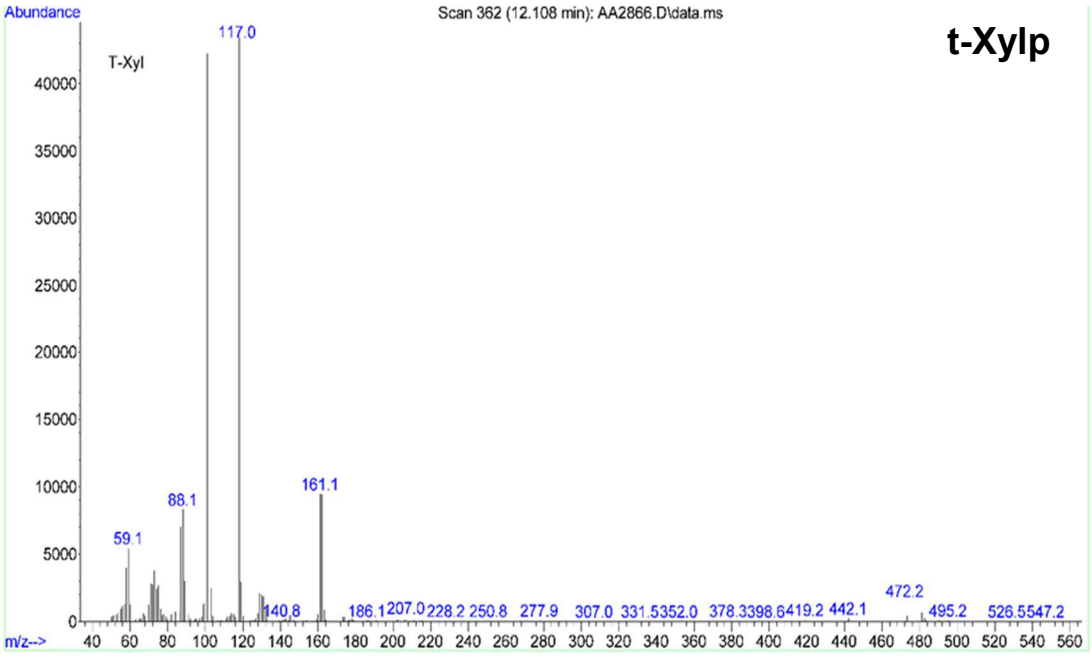
Abundance
Scan 362 (12.108 min): AA2866.D\data.ms
t-Xylp
T-Xyl
117.0
161.1
88.1
59.1
472.2
m/z-->

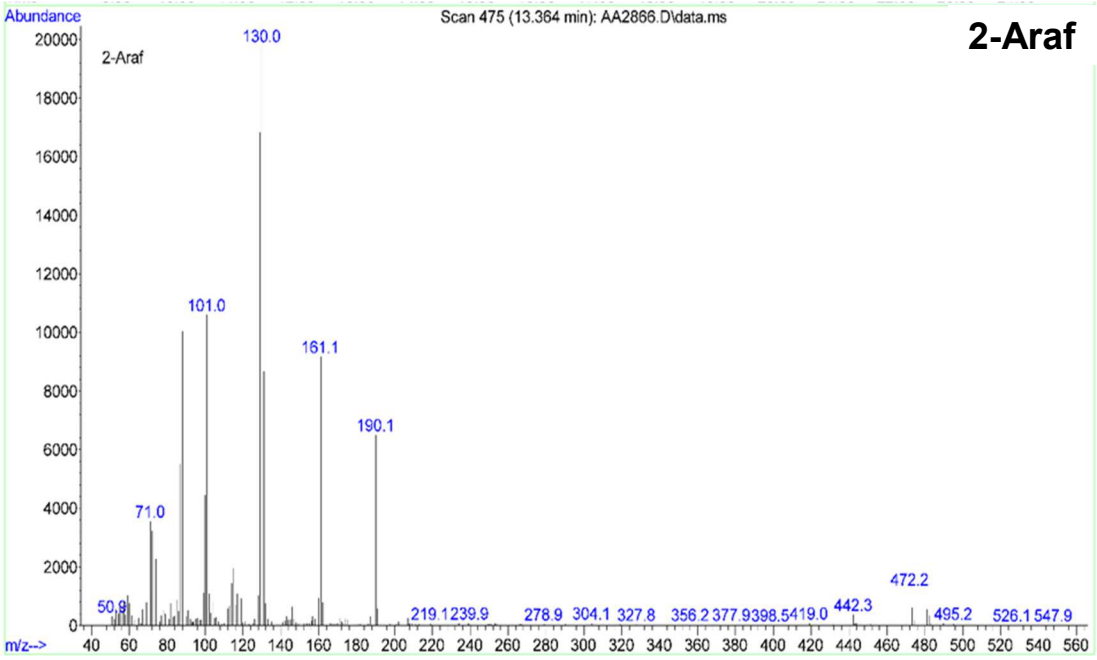
Abundance
Scan 475 (13.364 min): AA2866.D\data.ms
2-Araf
130.0
101.0
161.1
190.1
71.0
50.9
219.1
239.9
278.9
304.1
327.8
356.2
377.9
398.5
419.0
442.3
472.2
495.2
526.1
547.9
m/z-->

2-Araf

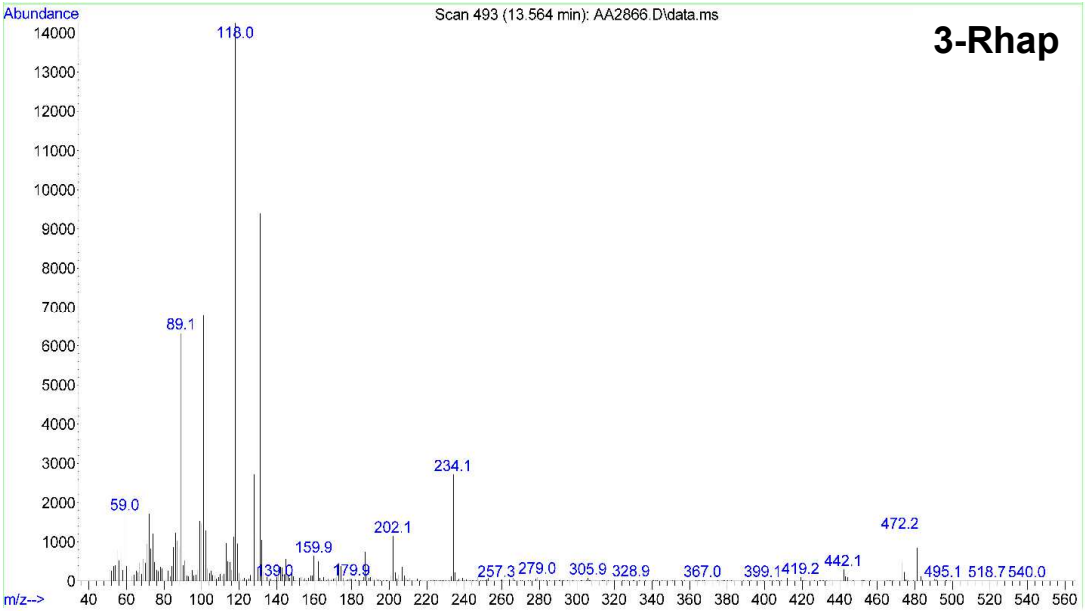
Abundance
Scan 493 (13.564 min): AA2866.D\data.ms
118.0
89.1
59.0
234.1
202.1
159.9
139.0
179.9
257.3
279.0
305.9
328.9
367.0
399.1
419.2
442.1
472.2
495.1
518.7
540.0
m/z-->

3-Rhap

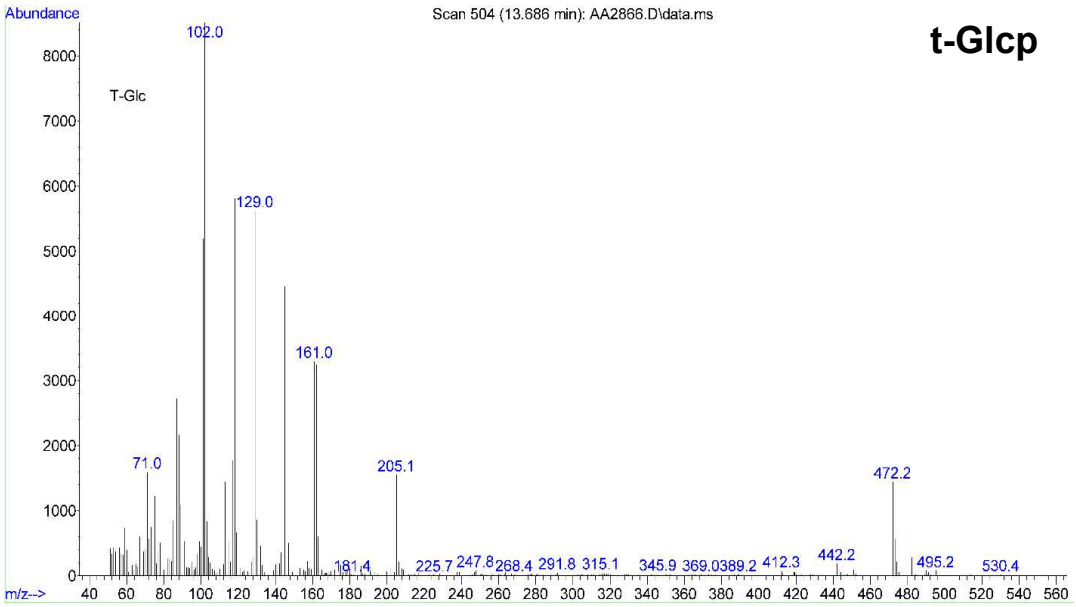
Abundance
Scan 504 (13.686 min): AA2866.D\data.ms
t-Glcp
T-Glc
102.0
129.0
161.0
71.0
205.1
472.2
181.4
225.7
247.8
268.4
291.8
315.1
345.9
369.0
389.2
412.3
442.2
495.2
530.4
m/z-->

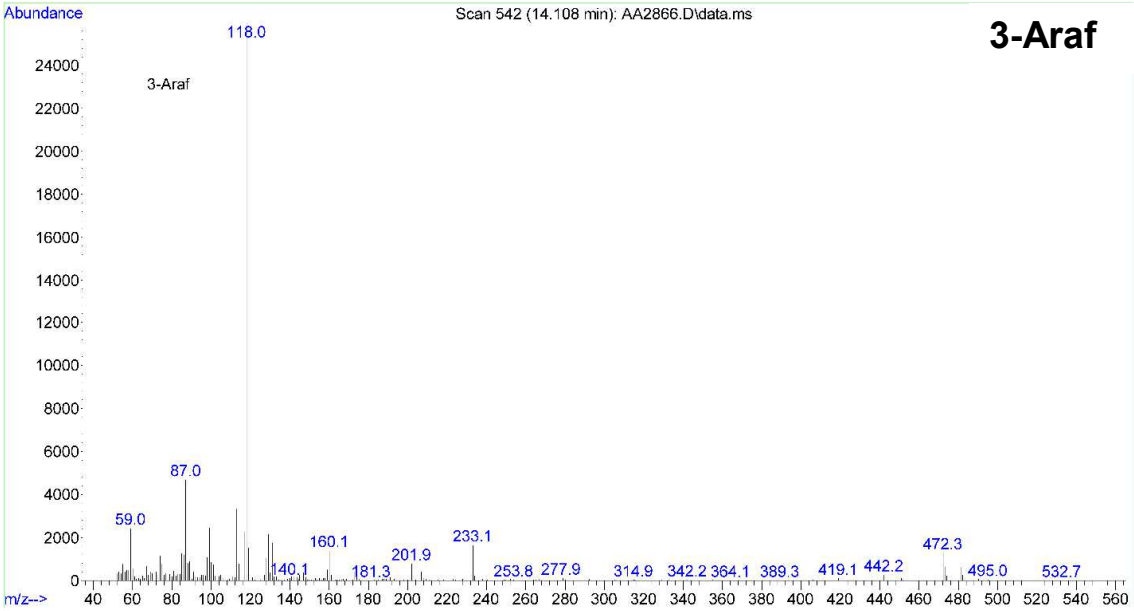
Abundance
Scan 542 (14.108 min): AA2866.D\data.ms
3-Araf
118.0
87.0
59.0
160.1
233.1
201.9
472.3
140.1
181.3
253.8
277.9
314.9
342.2
364.1
389.3
419.1
442.2
495.0
532.7
m/z-->

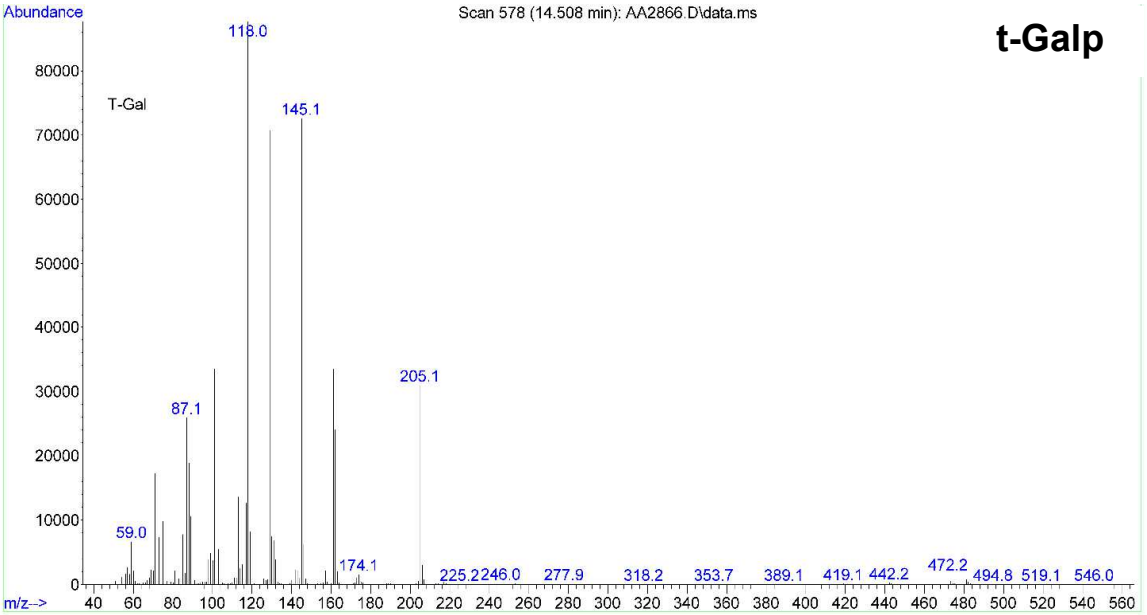
Abundance
Scan 578 (14.508 min): AA2866.D\data.ms
t-Galp
T-Gal
118.0
145.1
205.1
87.1
59.0
174.1
225.2246.0
277.9
318.2
353.7
389.1
419.1
442.2
472.2
494.8
519.1
546.0
m/z-->

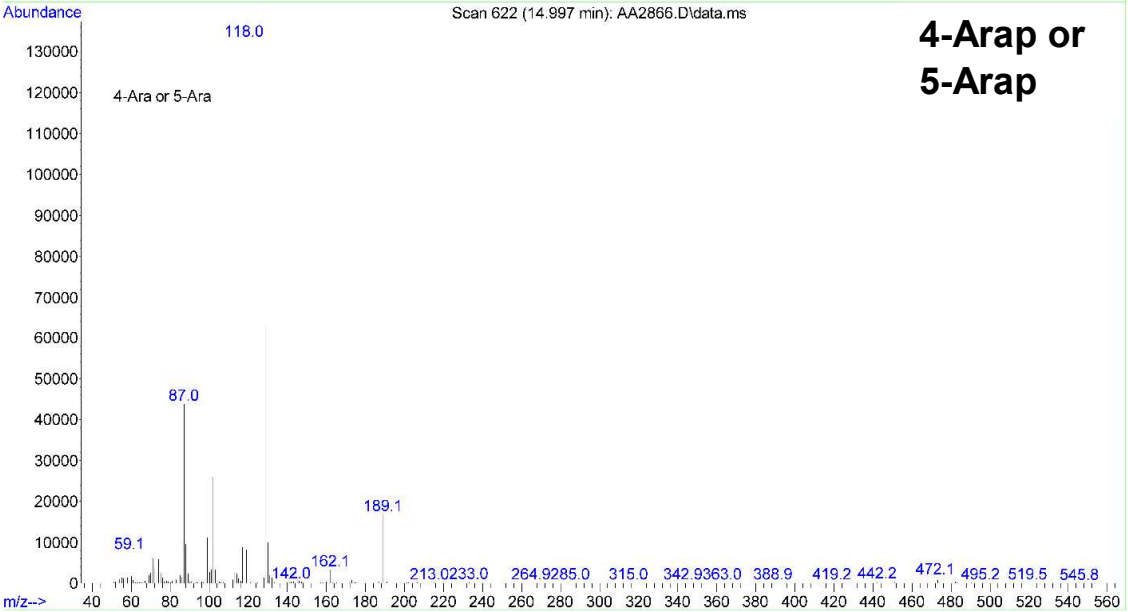
Abundance
Scan 622 (14.997 min): AA2866.D\data.ms
4-Arap or
5-Arap
118.0
4-Ara or 5-Ara
87.0
189.1
59.1
142.0
162.1
213.0233.0
264.9285.0
315.0
342.9363.0
388.9
419.2
442.2
472.1
495.2
519.5
545.8
m/z-->

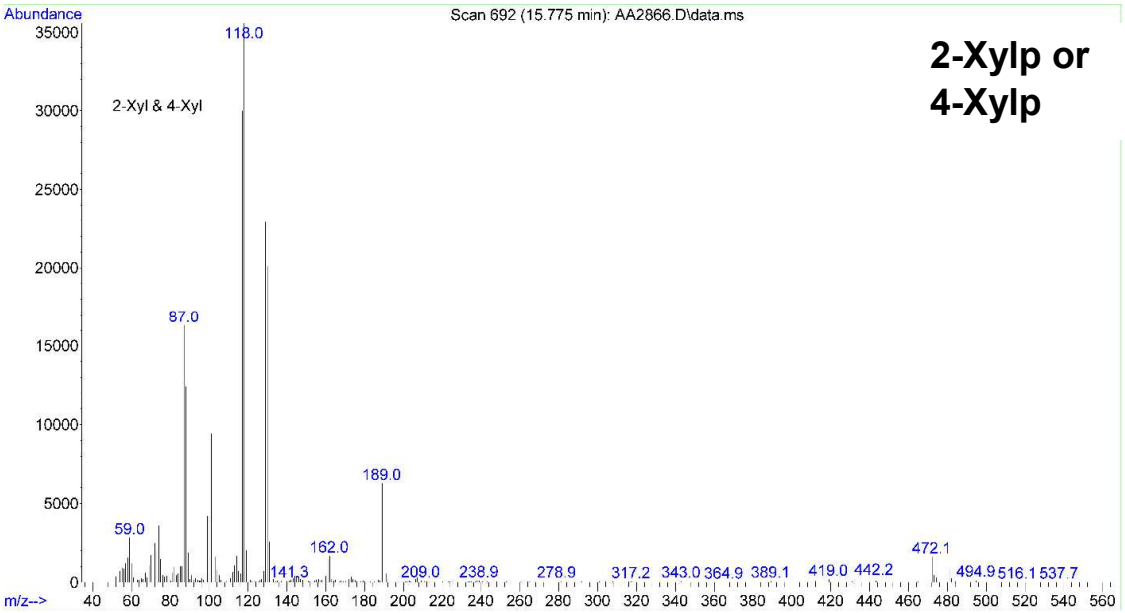
Abundance
Scan 692 (15.775 min): AA2866.D\data.ms
2-Xyl & 4-Xyl
2-Xylp or
4-Xylp
118.0
87.0
189.0
59.0
162.0
141.3
209.0
238.9
278.9
317.2
343.0
364.9
389.1
419.0
442.2
472.1
494.9
516.1
537.7
m/z-->

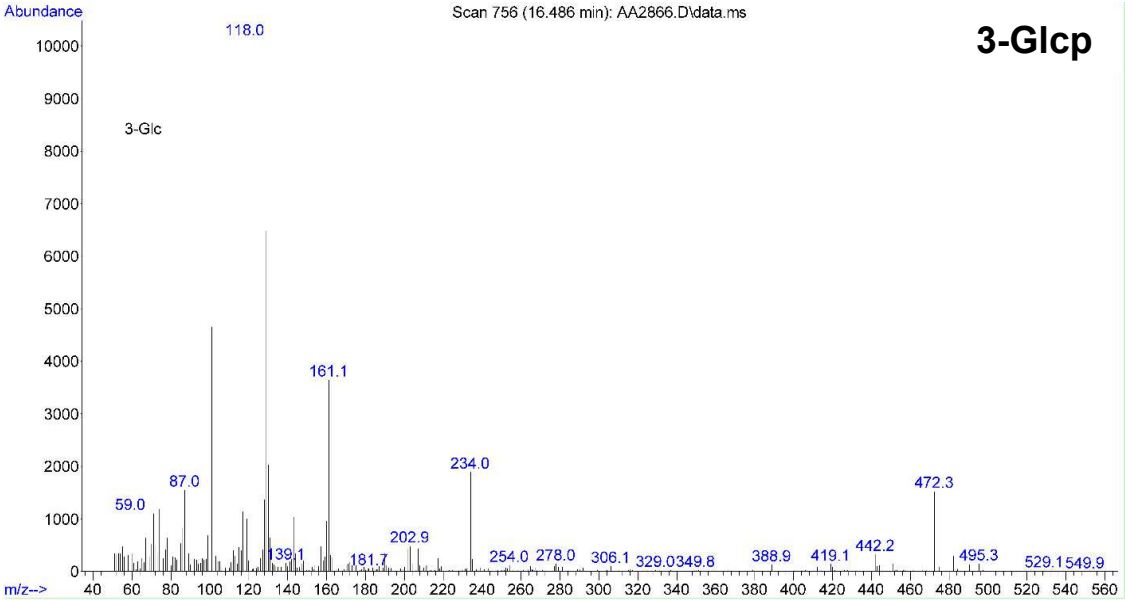
Abundance
Scan 756 (16.486 min): AA2866.D\data.ms
3-Glc
3-Glcp
118.0
161.1
234.0
87.0
59.0
472.3
202.9
139.1
181.7
254.0
278.0
306.1
329.0
349.8
388.9
419.1
442.2
495.3
529.1
549.9
m/z-->

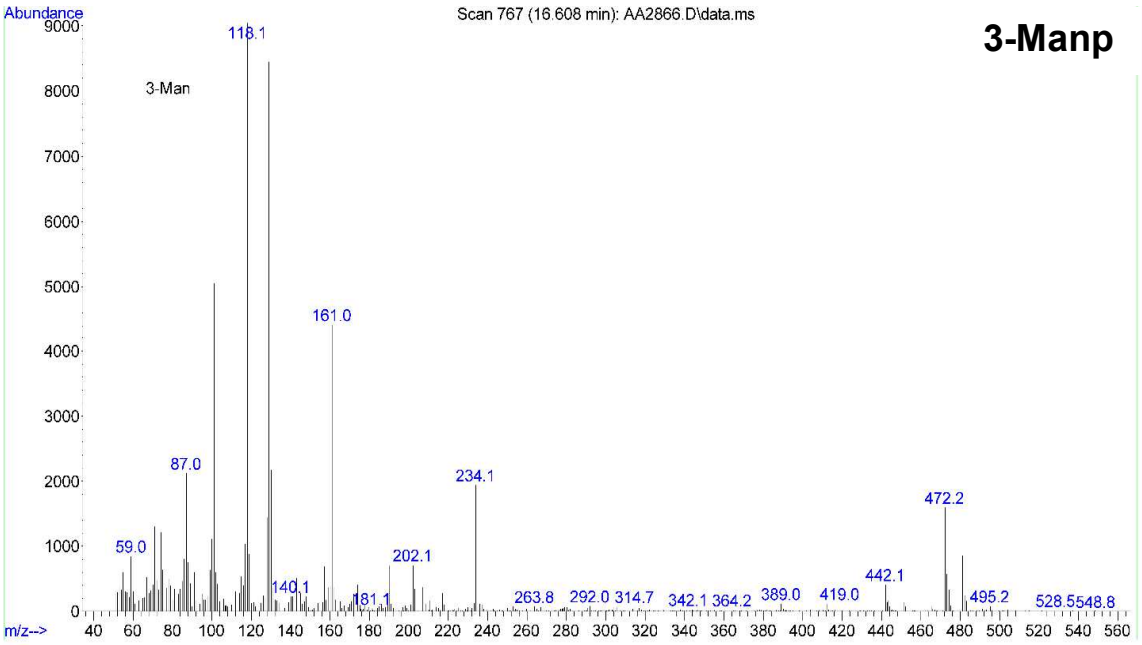
Abundance
Scan 767 (16.608 min): AA2866.D\data.ms
3-Manp
3-Man
118.1
161.0
87.0
234.1
472.2
59.0
202.1
140.1
181.1
263.8
292.0
314.7
342.1
364.2
389.0
419.0
442.1
495.2
528.5
548.8
m/z-->

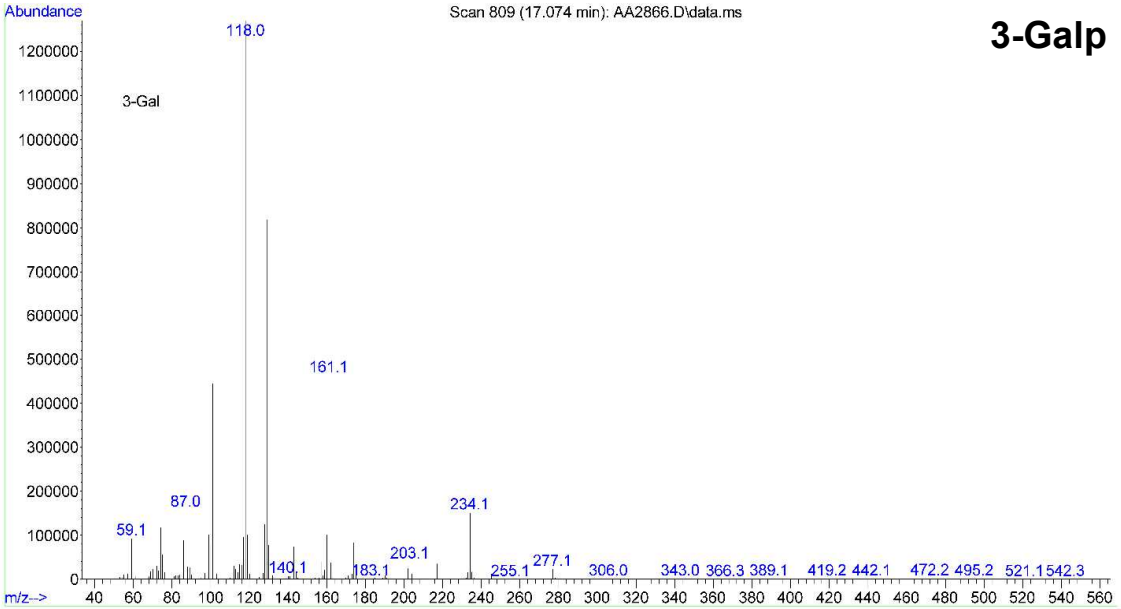
Abundance
Scan 809 (17.074 min): AA2866.D\data.ms
3-Galp
3-Gal
118.0
161.1
87.0
234.1
59.1
203.1
140.1
183.1
255.1
277.1
306.0
343.0
366.3
389.1
419.2
442.1
472.2
495.2
521.1
542.3
m/z-->

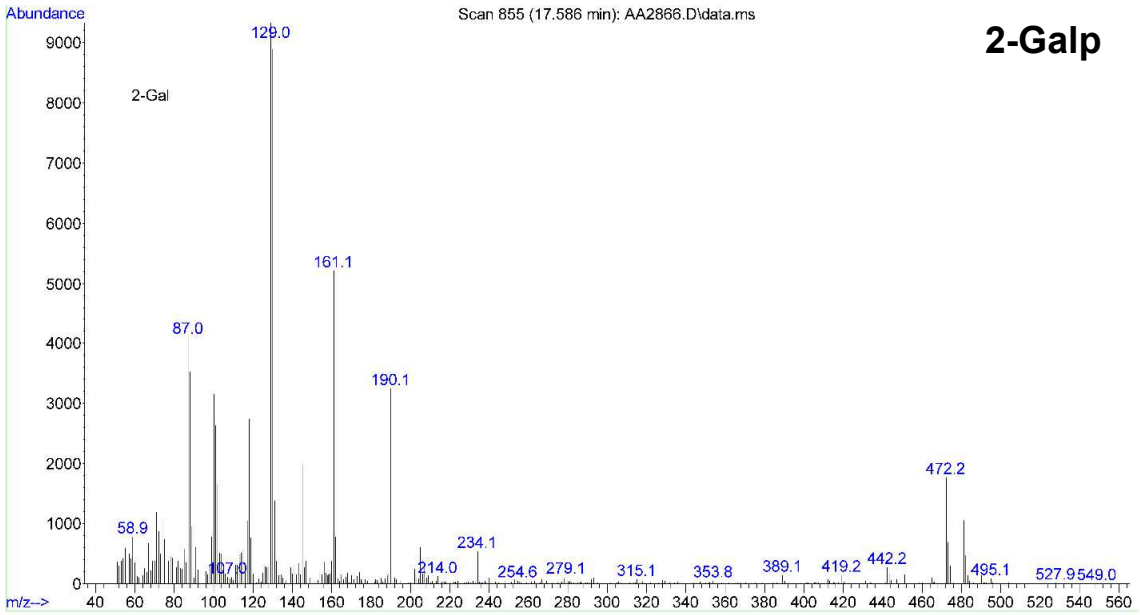
Abundance
Scan 855 (17.586 min): AA2866.D\data.ms
2-Galp
2-Gal
129.0
161.1
87.0
190.1
472.2
58.9
234.1
214.0
254.6
279.1
315.1
353.8
389.1
419.2
442.2
495.1
527.9
549.0
m/z-->

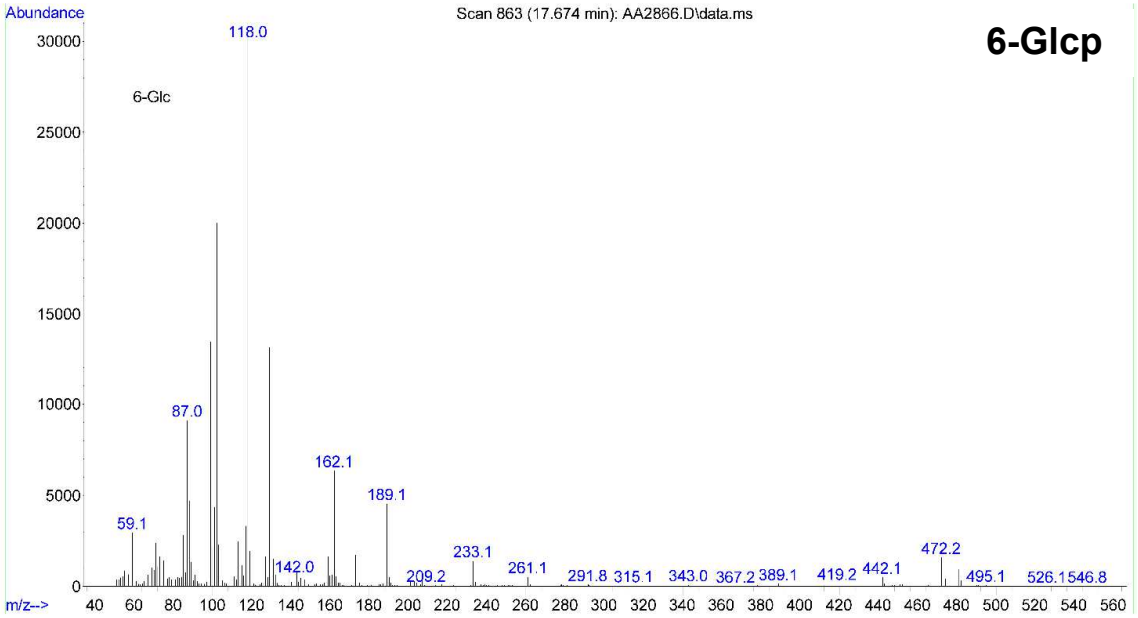
Abundance
Scan 863 (17.674 min): AA2866.D\data.ms
6-Glcp
6-Glc
118.0
87.0
162.1
189.1
59.1
233.1
142.0
209.2
261.1
291.8
315.1
343.0
367.2
389.1
419.2
442.1
472.2
495.1
526.1
546.8
m/z-->

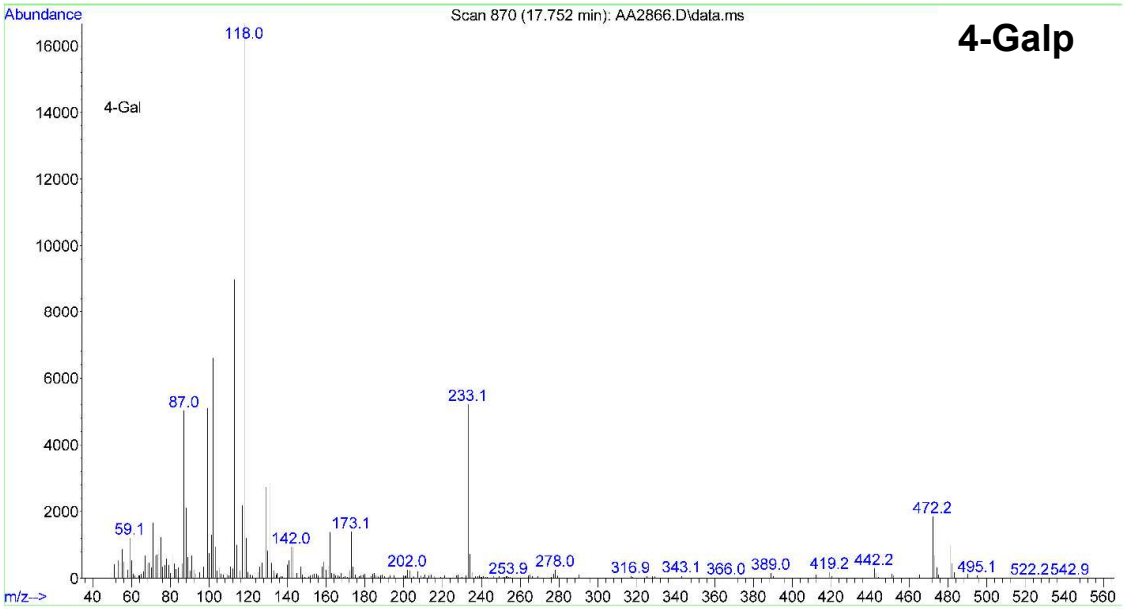
Abundance
Scan 870 (17.752 min): AA2866.D\data.ms
4-Galp
4-Gal
118.0
87.0
233.1
59.1
142.0
173.1
202.0
253.9
278.0
316.9
343.1
366.0
389.0
419.2
442.2
472.2
495.1
522.2
542.9
m/z-->

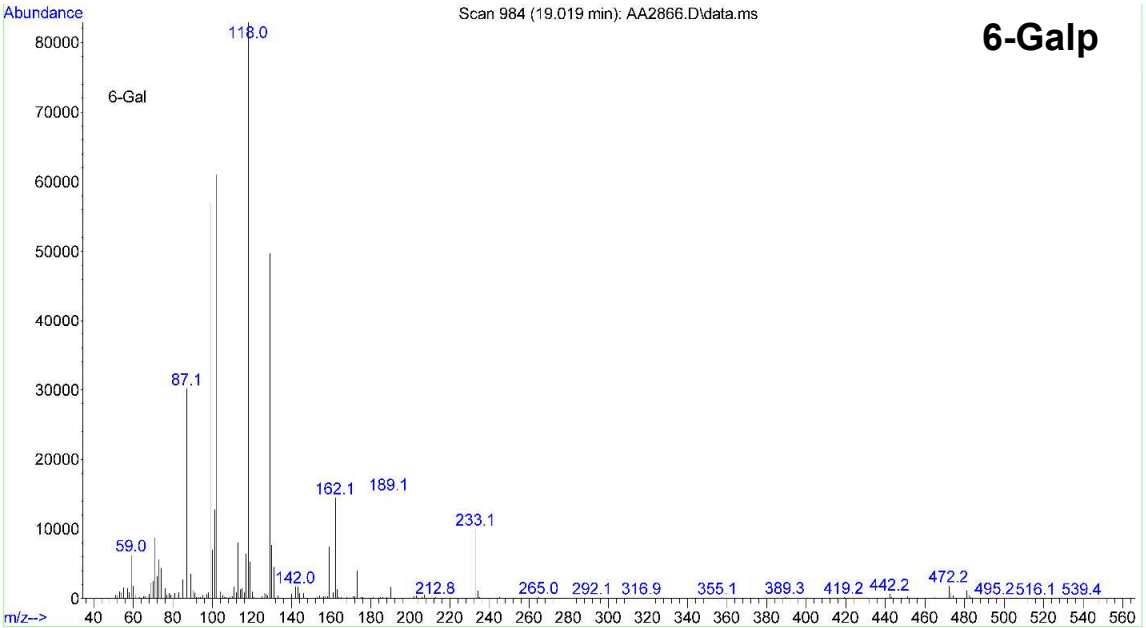
Abundance
Scan 984 (19.019 min): AA2866.D\data.ms
6-Galp
6-Gal
118.0
87.1
162.1
189.1
233.1
59.0
142.0
212.8
265.0
292.1
316.9
355.1
389.3
419.2
442.2
472.2
495.2
516.1
539.4
m/z-->

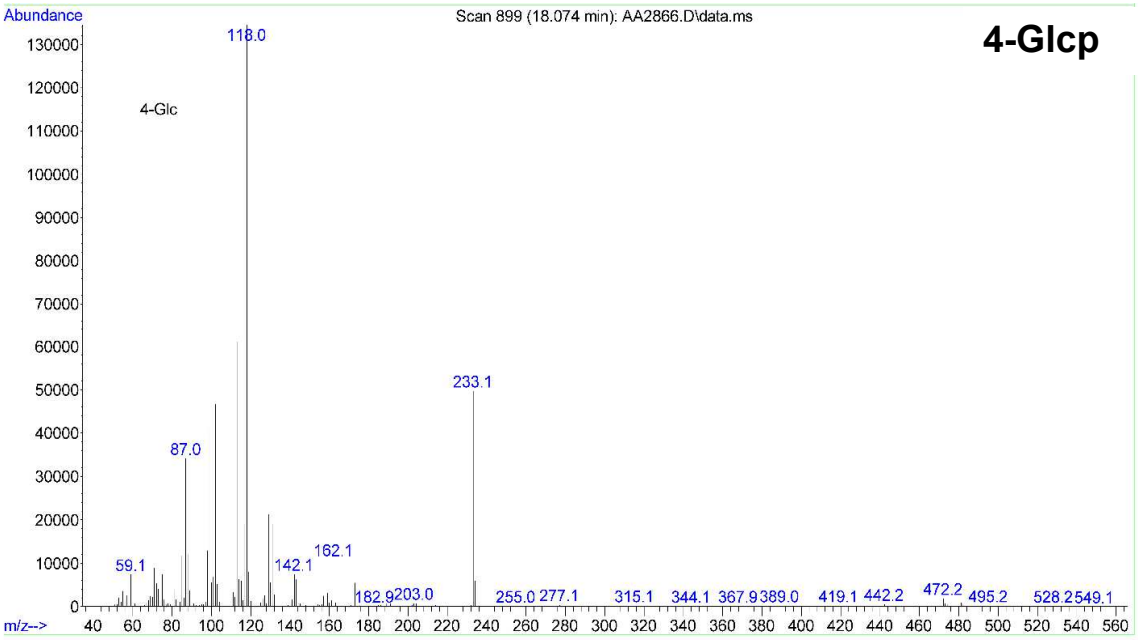
Abundance
Scan 899 (18.074 min): AA2866.D\data.ms
4-Glcp
4-Glc
118.0
233.1
87.0
59.1
142.1
162.1
182.9
203.0
255.0
277.1
315.1
344.1
367.9
389.0
419.1
442.2
472.2
495.2
528.2
549.1
m/z-->

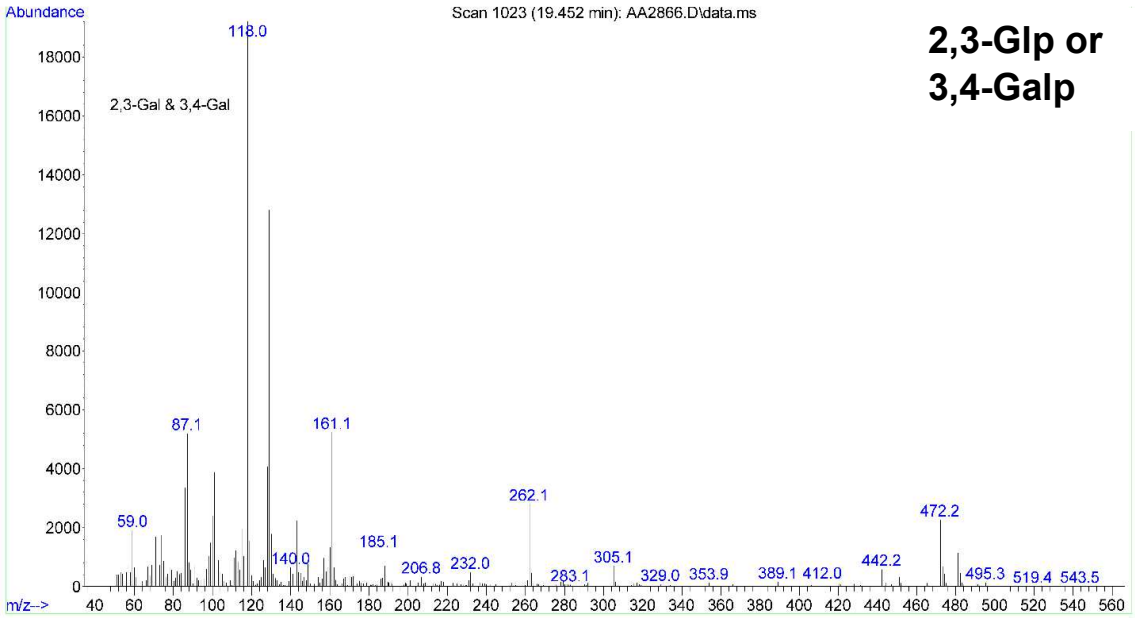
Abundance
Scan 1023 (19.452 min): AA2866.D\data.ms
2,3-Glp or
3,4-Galp
2,3-Gal & 3,4-Gal
118.0
87.1
161.1
59.0
262.1
472.2
185.1
140.0
206.8
232.0
305.1
283.1
329.0
353.9
389.1
412.0
442.2
495.3
519.4
543.5
m/z-->

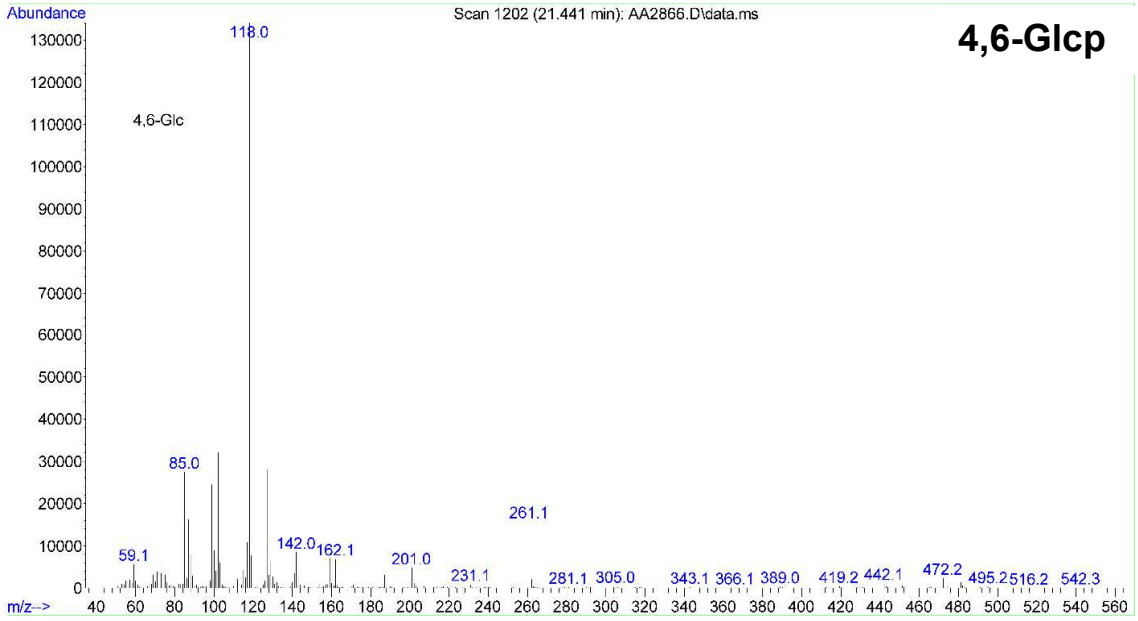
Abundance
Scan 1202 (21.441 min): AA2866.D\data.ms
4,6-Glcp
118.0
4,6-Glc
85.0
261.1
59.1
142.0
162.1
201.0
231.1
281.1
305.0
343.1
366.1
389.0
419.2
442.1
472.2
495.2
516.2
542.3
m/z-->

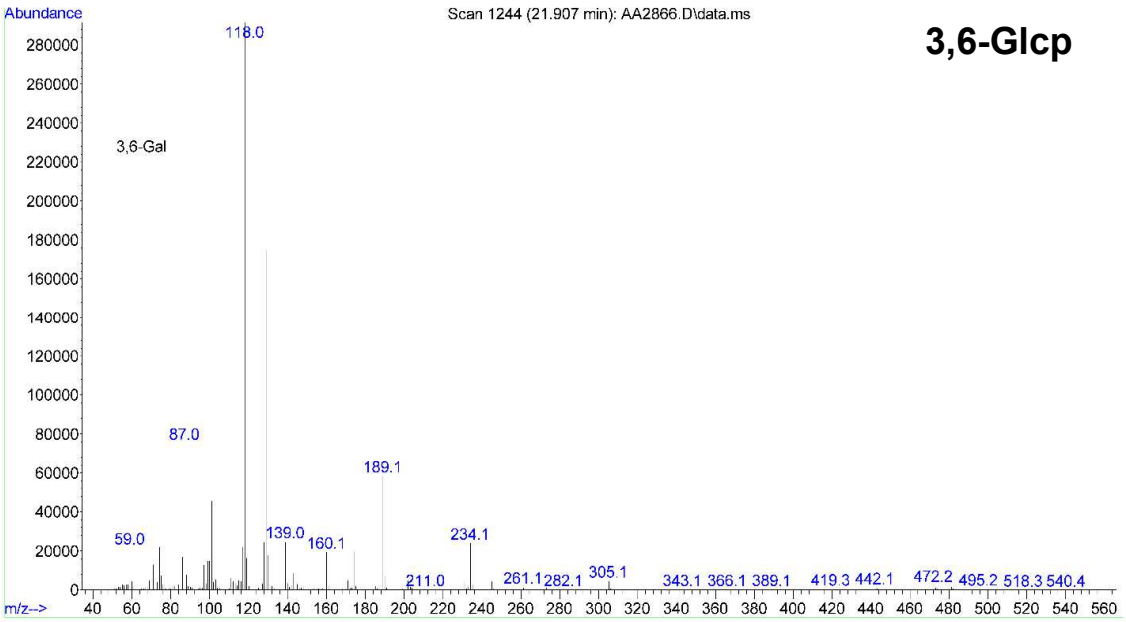
Abundance
Scan 1244 (21.907 min): AA2866.D\data.ms
3,6-Glcp
118.0
3,6-Gal
87.0
189.1
59.0
139.0
160.1
234.1
211.0
261.1
282.1
305.1
343.1
366.1
389.1
419.3
442.1
472.2
495.2
518.3
540.4
m/z-->

APPENDIX I: Linearity, LOD, LOQ and precision of the proposed HILIC-CAD method

Monosaccharide	Regression equation	R^2	LOD (ng/mL)	LOQ (ng/mL)	Precision (Peak Area)	
					Intra-day (%RSD)	Inter-day (%RSD)
LRha	y = 0.7226x – 1.3072	0.9965	68.82	232.35	3.99	2.49
LFuc	y = 0.8565x – 1.5429	0.9910	65.45	218.18	1.32	2.66
Man	y = 0.8879x – 1.8010	0.9993	50.51	169.09	4.86	2.01
Gal	y = 0.8975x – 1.7640	0.9946	55.42	184.75	2.50	0.92
GlcN	y = 0.9491x – 2.1228	0.9986	64.77	215.91	1.93	3.16
GalN	y = 0.9599x – 2.3001	0.9952	61.71	205.71	3.07	1.76
GlcNac	y = 0.8439x – 1.7494	0.9940	64.05	213.51	4.67	4.70
GluA	y = 0.7994x – 1.5368	0.9954	63.00	210.00	7.96	2.64
GalA	y = 0.9350x – 1.8938	0.9943	64.08	213.61	4.16	7.17
IdoA	y = 0.9070x – 1.8958	0.9979	83.40	278.00	5.96	4.61
Neu5Ac	y = 0.8129x – 1.4928	0.9977	53.08	176.92	5.14	2.43

APPENDIX J: Effects of column temperature on chromatographic separation

Mixtures of 11 monosaccharide standards (concentration: 225 μg/mL) were analyzed in A-C. Mobile phase additives and column temperature in: (A) 25 mM ammonium acetate/0.2% TEA/50°C; (B) 25 mM ammonium acetate/0.2% TEA/40°C; and (C) 25 mM ammonium acetate/0.2% TEA/30°C. The mobile phase gradient reported in the methods section was used for the separation. Although, lower temperatures lead to better separation of monosaccharides, they tend to form peak doublets below 30°C. An example of peak doublet (Man) can be seen in panel C. Higher temperatures of >30°C were found to adequately suppress doublets.

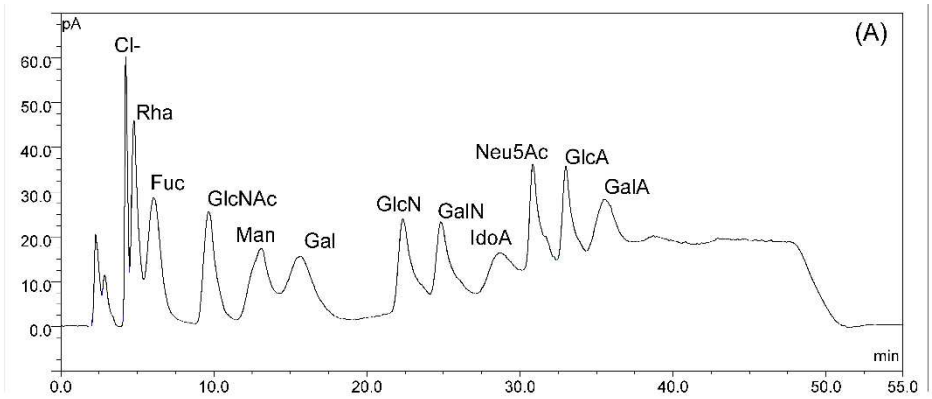
pA
(A)
Cl-
Rha
Fuc
GlcNAc
Man
Gal
GlcN
GalN
IdoA
Neu5Ac
GlcA
GalA
min
0.0
10.0
20.0
30.0
40.0
50.0
55.0
60.0

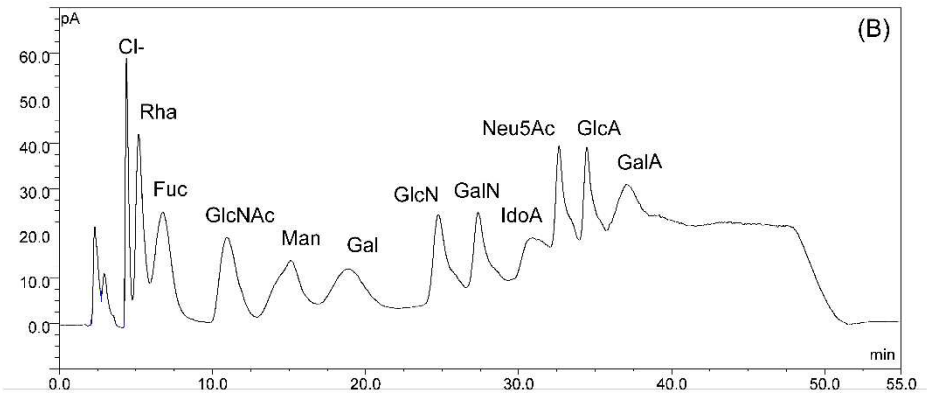
pA
(B)
Cl-
Rha
Fuc
GlcNAc
Man
Gal
GlcN
GalN
IdoA
Neu5Ac
GlcA
GalA
min
0.0
10.0
20.0
30.0
40.0
50.0
55.0
60.0

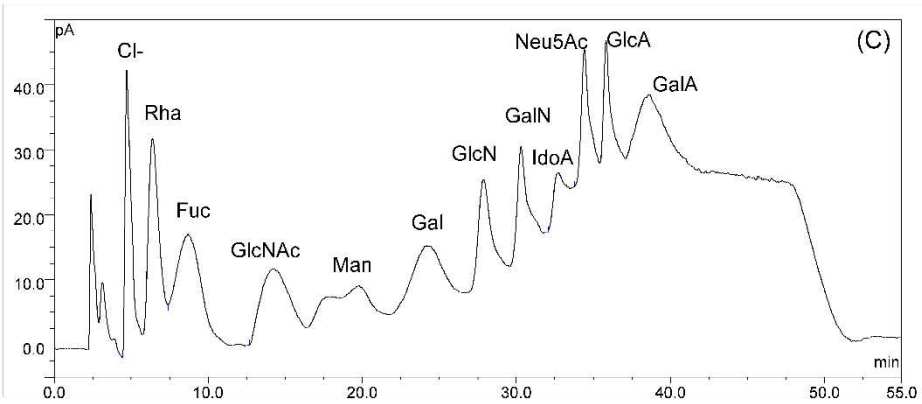
pA
(C)
Cl-
Rha
Fuc
GlcNAc
Man
Gal
GlcN
IdoA
GalN
Neu5Ac
GlcA
GalA
min
0.0
10.0
20.0
30.0
40.0
50.0
55.0

APPENDIX K: Effects of tertiary amine TEA on chromatographic separation

Mixtures of 11 monosaccharide standards (concentration: 225 µg/mL) were analyzed in A and B. Mobile phase additives and column temperature in: (A) 25 mM ammonium acetate/0.2% TEA/40°C; and (B) 25 mM ammonium acetate/0.1% TEA/40°C. The mobile phase gradient reported in the methods section with a flow rate of 0.3 mL/min was used for the analysis. A combination of 0.2% TEA and temperatures above 30°C were found to suppress split peaks.

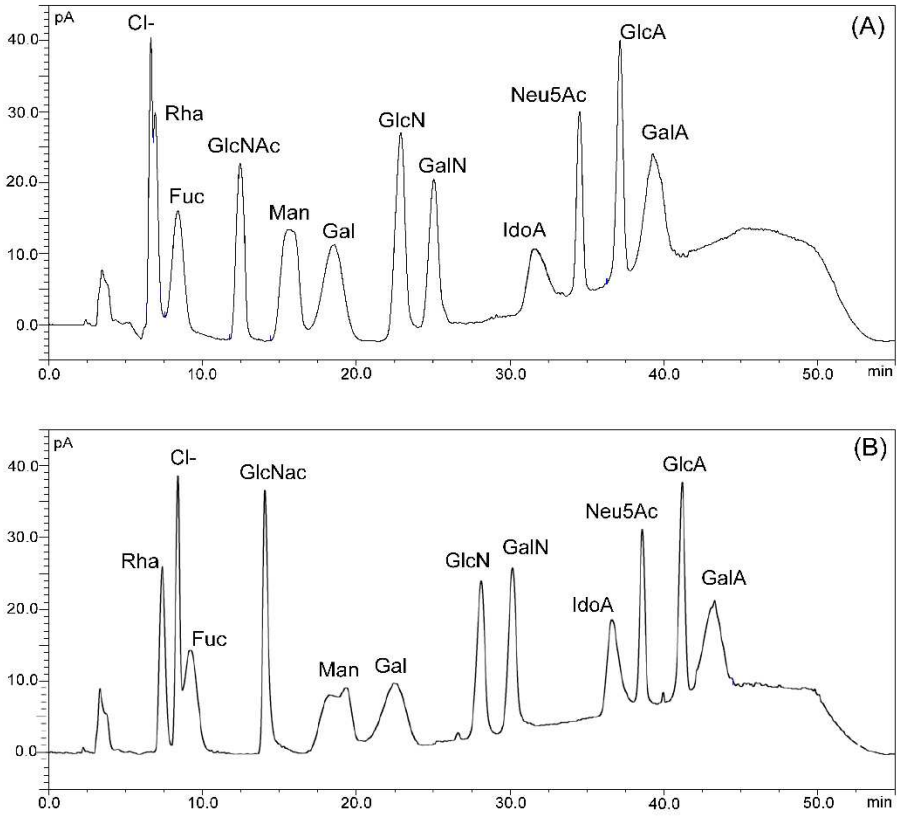

APPENDIX L: Effects of ammonium acetate on chromatographic separation

Mixtures of 11 monosaccharide standards (concentration: 225 µg/mL) were analyzed in A and B. Mobile phase additives and column temperature in: (A) 25 mM ammonium acetate/0.2% TEA/50°C; and (B) 20 mM ammonium acetate/0.2% TEA/50°C. The mobile phase gradient reported in the methods section with a flow rate of 0.3 mL/min was used for the analysis. Although, higher ammonium acetate buffer concentrations lead to increased retention times, it was generally found to produce better separations.